FINITE, INELASTIC DEFORMATIONS OF CLAMPED RECTANGULAR MEMBRANES SUBJECTED TO IMPULSIVE LOADINGS

By

CHARLES LINDBERGH

Bachelor of Science
The Citadel
Charleston, South Carolina
May, 1958

Master of Science
Oklahoma State University
Stillwater, Oklahoma
May, 1965

Submitted to the faculty of the Graduate College of the Oklahoma State University in partial fulfillment of the requirements for the degree of DOCTOR OF PHILOSOPHY
May, 1967

OKLAHOMA
STATE UNIVERSITY
LIBRARY
JAN 12 1968

FINITE, INELASTIC DEFORMATIONS OF CLAMPED RECTANGULAR MEMBRANES SUBJECTED TO IMPULSIVE LOADINGS

Thesis Approved:

Thesis Adviser

Robert L. James

Thomas Scott Dean

Dean of the Graduate College

659339

ACKNOWLEDGEMENT

The author wishes to take this opportunity to express his gratitude and sincere appreciation to the following individuals and organizations:

To Dr. Donald E. Boyd as his exemplary character, professional guidance and personal encouragement made the preparation of this dissertation possible;

To Professor J. J. Tuma, Dr. J. L. Chao, Dr. T. S. Dean, Dr. R. L. Janes, and Dr. A. E. Salama, the other members of his advisory committee, for their valuable counsel and encouragement;

To Dr. W. O. Carter, Dr. R. W. Little, and Dr. J. S. Kao, members of his former advisory committee, for their earlier guidance and inspiration. A special indebtedness to Drs. Carter and Little is acknowledged for their being instrumental in making his continued graduate education possible;

To Dr. T. A. Halliburton and the other faculty members of the Civil Engineering Department for their valuable instruction;

To Dr. D. D. Grosvenor and the staff of the Oklahoma

State University Computing Center;

To Mrs. Sara MacAlpine, Mrs. Lana Woods, and the staff of the Oklahoma State University Library;

To the United States Air Force for sponsoring his graduate studies;

To his parents, Mrs. Elise Saulisbury and the late Mr. Carl Lindbergh;

To Mr. E. L. Green for providing inspiration to commence graduate work;

To his wife, Russ, and children, Chuck and Stacey, for making his years of graduate study less burdensome through their love, understanding and sacrifices;

To Mrs. Peggy Harrison for her wonderful cooperation and careful typing of the manuscript;

To Mr. Eldon Hardy for dignifying this dissertation by preparing the final sketches and tables;

And finally, to his fellow graduate students who provided much through their friendship and professional association.

Charles Lindbergh

Charles Lindbergh

May, 1967
Stillwater, Oklahoma

TABLE OF CONTENTS

Chapter			Page
I.	INTRODUCTION		1
	1.1	Statement of the Problem	1
	1.2	Historical Note	2
II.	FORMULATION OF THE PROBLEM		7
	2.1	Introduction	7
	2.2	Interpretation of the Problem	7
	2.3	Governing Equations	10
III.	NUMERICAL SOLUTION OF PROBLEM		28
	3.1	Introduction	28
	3.2	Finite Difference Formulation	28
	3.3	Boundary Conditions	32
	3.4	Initial Conditions	35
	3.5	Numerical Method of Solution	36
	3.6	Selection of Space and Time Variables	44
	3.7	Displacement Function Approximation	48
IV.	NUMERICAL RESULTS		49
	4.1	General	49
	4.2	Variation of Initial Velocity Configuration	49
	4.3	Variation of Transient Pressure	51
	4.4	Variation of Aspect Ratio	53
	4.5	Variation of Initial Impulse and Stress-Strain Relation	54
V.	SUMMARY AND CONCLUSIONS		69
	5.1	Summary	69
	5.2	Discussion of Results	70
	5.3	General Conclusion and Possible Extensions	73
BIBLIOGRAPHY			76
APPENDIX A - PUCHER STRESS THEORY			81

APPENDIX B - FLÜGGE AND GEYLING DEFORMATION THEORY 89

APPENDIX C - SKEWED-ORTHOGONAL STRESS RESULTANT TRANSFORMATION 96

APPENDIX D - PLASTIC CONSTITUTIVE EQUATIONS 102

APPENDIX E - TAU VALUES 109

APPENDIX F - D COEFFICIENTS 112

APPENDIX G - DUi, DVj, and DWk COEFFICIENTS 114

APPENDIX H - INITIAL CONDITIONS 120

APPENDIX I - COMPUTER FLOW DIAGRAM 128

LIST OF TABLES

Table		Page
4-1.	Aspect Ratio Data	54
D-1.	Universal Stress Strain Relationship Parameters	108
H-1.	Explosive Material Properties	120

LIST OF FIGURES

Figure		Page
1.	Typical Deformation Pattern of Membrane	8
2.	Progressive Incremental Deformation of Membrane Element	9
3.	State of Dynamic Equilibrium	11
4.	Geometry of Pseudo-Shell Element	16
5.	Skewed-Orthogonal Strain Relations	19
6.	Typical Dynamic and Static Stress-Strain Relations	24
7.	Finite Difference Representation	30
8.	Dependency of Numerical Stability upon Time and Spacial Interval Magnitudes	45
9.	Evidence of Numerical Instability	47
10.	Representative Finite Difference Grid System .	50
11.	Variation of Terminal Transverse Displacements with Initial Velocity Configuration	56
12.	Effect of Initial Velocity Distribution on U Displacement Field	57
13.	Variation of Transient Transverse Displacements with Initial Velocity Configuration	58
14.	Terminal Transverse Displacements for Square Membrane	59
15.	Transient Pressure Profile	60
16.	Effect of Pressure Distribution on Transient Transverse Displacements	61
17.	Effect of Pressure Distribution on U Displacement Response	62

Figure		Page
18.	Typical Deformation Response of Square Membrane to Impulsive Pressure	63
19.	Effect of Aspect Ratio on the Transverse Displacement Field	64
20.	Effect of Aspect Ratio on the Horizontal U Displacement Field	65
21.	Effect of Aspect Ratio on the Horizontal V Displacement Field	66
22.	Variation of Permanent Center Displacement with Applied Impulse	67
23.	Influence of the Effective Stress-Strain Relationship on the Total Transverse Displacements	68
A-1.	Projection of Element of Double Curvature . . .	82
A-2.	State of Static Equilibrium	83
B-1.	Deformation of Curvilinear Element	91
B-2.	Orthogonal-Skewed Strain Relations	95
C-1.	Orthogonal-Skewed Force System	96
C-2.	Orthogonal-Skewed Stress System	98
H-1.	Development of Impulse for Deformation Process	121
H-2.	Effect of Explosive Material Constants on Total Impulse	127

NOMENCLATURE

x, y, z	Coordinate axes, basic reference system;
ω	Angle of skew;
dS_1, dS_2	Differential curvilinear line segments;
α, β	Angle between horizontal plane and curvilinear line segments;
U, V, W	Orthogonal incremental displacements;
R	Reference configuration of pseudo-shell;
Z	Current configuration of pseudo-shell;
N_x, N_y, N_{xy}	Skewed stress resultants
$\overline{N}_x, \overline{N}_y, \overline{N}_{xy}$	Equivalent projected stress resultants;
$S_x, N_{\bar{y}}, T_1$	Orthogonal stress resultants;
I_x, I_y, I_z	Moment of inertias;
$\overline{I}_x, \overline{I}_y, \overline{I}_z$	Projected equivalents of I_x, I_y, I_z;
P_x, P_y, P_z	External loads per unit area of shell;
$\overline{P}_x, \overline{P}_y, \overline{P}_z$	Projected equivalents of P_x, P_y, P_z;
$\delta e_x, \delta e_y, \delta \gamma_{xy}$	Incremental skewed strains
$\delta e_{\bar{x}}, \delta e_{\bar{y}}, \delta \gamma_{\overline{xy}}$	Equivalent incremental orthogonal strains;
$\Delta\lambda$	Plasticity parameter;
a, b, c	Membrane material constants;

ρ	Mass per unit volume;
tau_i	Kinematic equations' coefficients;
i, j	Indices designating node locations;
$D1_{i,j}$, $D2_{i,j}$, etc.	Coefficients of governing pivotal equations;
L_x, L_y	Planform side lengths;
$DU1_{i,j}$, $DU2_{i,j}$, etc.	Coefficients of displacement pivotal equations;
$DV1_{i,j}$, $DV2_{i,j}$, etc.	Coefficients of displacement pivotal equations;
$DW1_{i,j}$, $DW2_{i,j}$, etc.	Coefficients of displacement pivotal equations;
h_x, h_y	Node spacings;
Δt	Time increment;
M_x, M_y	Number interior node intervals;
[C], [D], [E]	Coefficient matrices for U displacement equation;
[F], [G], [H]	Coefficient matrices for V displacement equation;
k, θ, ϕ	Explosive material constants;
p, q	Spatial pressure shape parameters;
V_o	Principal velocity ordinate;
$\bar{\sigma}$	Effective stress;
$\overline{\delta\epsilon}$	Effective strain increment;
H	Universal stress-strain function;
Σ	Summation;
[ ]	Square matrix;
{ }	Column matrix, and
$[\ ^{-1}]$	Matrix inversion.

CHAPTER I

INTRODUCTION

1.1 Statement of the Problem

A method of analysis is developed for determining the finite, inelastic deformation of a clamped rectangular membrane subjected to either large transient pressures or high initial velocities. Bending effects are neglected. The material is assumed to be rigidly plastic-strain hardening in response to deformation. The incremental theory of plasticity is used and the total displacement of the membrane is mathematically described as the accumulated effects of numerous increments of deformations. Each increment of deformation is approached in a manner similar to the Flügge-Geyling formulation for analyzing the static deformations of membrane shells of rectangular planform. Each displacement increment is assumed to be small even though the total displacements are finite.

A dynamic equilibrium formulation leads to three coupled, nonlinear, partial differential equations. The constitutive equations are used to obtain these equations in terms of three rectangular displacement components.

An IBM 7040 digital computer is used to solve numerically the governing differential equations for the

transient and final displacements.

1.2 Historical Note

The dynamic deformations of structural members have long been of interest to the technical community. The primary related areas of application today include high-energy-rate metal forming processes and studies of structures responding to sudden energy releases of high intensity (as in bomb blasts).

In forming metal components using high-energy-rate processes, velocity overshadows mass as the principal parameter affecting the transfer of energy to the membrane to be shaped. This substitute becomes especially desirable when the size, shape or number of the formed parts cannot justify economically the expenditure for suitable metal pressing equipment. There is much variation in the component shapes and sizes which are required. The recent accelerated growth of this industry is due principally to the complexity in shapes of aerospace structures.

There is also the need to analyze the deformation of structures subjected to sudden energy releases of high intensity. One such demand is that to provide public shelters for protection against nuclear bomb attacks. Some of the other examples are not so apparent. One such item would be the explosion of aircraft compartment bulkheads due to depressurization in an adjacent compartment. Such a case would arise if a foreign object breeched the

fuselage while the aircraft was at a high altitude. Another possible application would be the response of submarine hulls to large underwater explosions. Still another is the structural reaction to impulsive forces acting on the pontoons of seaplanes during landing or takeoff as well as to those acting on the hulls of hydrofoil ships. There are certainly many other areas of direct interest; more than enough to substantiate the need for satisfactory analytical methods to determine the structural response of membranes to representative impulsive loads.

Of the basic configurations of membranes, the circular membrane has attracted most analytical investigators. From independent analyses for static loading by Mostow and Gleyzal (13) in 1948 up to a recent investigation of dynamic loading by Boyd (1) the deformation response of a circular membrane has been very thoroughly considered and analytically described. Mostow obtained an analytical solution for static loading using the stationary energy principle. Gleyzal's analysis differed in that the conditions of static equilibrium were used to obtain governing differential equations which were then solved numerically. Both investigators employed the deformation theory of plasticity. Hudson (11) in 1951 and Frederick (7) in 1959 formulated their problems using a mechanism analogous to a circular hinge moving inward from the perimeter. Hudson used the deformation theory of plasticity and the principle of the conservation of energy in formulating his governing

differential equations. Frederick included the "incremental theory" of plasticity as well while using the impulse-momentum and work-energy principles. Wang (24) in 1955 adopted a limit analysis approach with which he considered only bending stresses. As in all dynamic analyses before his, Wang applied a uniform initial starting velocity. Witmer, Balmer, Leech and Pian (27) published their work regarding the large dynamic deformation of plates and shells during 1963. Their analysis was most general; including such features as bending and membrane stresses, elastic-plastic deformation responses, and the incremental theory of plasticity. While the results are certainly very accurate, the extensive computer time required for each problem is a serious deficiency and is not, as admitted by the authors, suitable for parametric investigations. In 1966, Boyd (1) published his analysis which, even though less general than the preceding study, provided an effective and very efficient means of performing parametric investigations for circular membranes. Comparisons with the work by Witmer et al and with experimental results verified the simplifing assumptions used in his study.

Corresponding technical investigations of the dynamic deformation response of rectangular membranes are practically nonexistent. In fact, the only dynamic analysis found during the present investigation is that given by Timoshenko (23) for a vibrating elastic membrane which is

uniformly prestretched to the extent that in-plane variations of tensile stress are negligible. Thus, only a constant tension is considered. Furthermore, only transverse motion is allowed. The problem, thus, is linear. Timoshenko formed expressions for the change in the potential and kinetic energies in terms of the transverse displacements. By representing the displacements with a double sine series with time-dependent coefficients and applying a form of the Principle of Virtual Displacements, the individual modes of vibrations were obtained. The Rayleigh-Ritz method also was used in conjunction with a polynomial series to yield another form of the solution. Such a solution applies to a rigid, perfectly plastic membrane if no elastic unloading is allowed. Of course, the small displacement theory used is also a very restrictive assumption.

All other analytical and numerical investigations of rectangular membranes are related to static load conditions only. In 1921, Henky (41) derived a comprehensive numerical finite difference solution but applied it only to square membranes. Three years later Föppl (36) assumed trigonometric functions for displacements which satisfied boundary and symmetry conditions. The unknown constant coefficients were solved using a variational principle. In this manner Föppl obtained stresses and deflections for square membranes only, but suggested an extension to the rectangular case. Neubert and Sommer (45) extended Föppl's

development to rectangular membranes in 1940. Approximately eight years later, Mostow (13) determined the lateral displacement fields which were compatible with a given transverse displacement field and the stable equilibrium of the membrane and loading system. He assumed both parabolic and membrane formulations of the distributions of transverse displacements which required that the center displacement be known. A truncated power series representation of the in-plane displacements was assumed which satisfied all boundary conditions. The Principle of Stationary Potential Energy was used to evaluate the unknown coefficients in each series. During 1966, Pope (17) published a paper on the application of finite element analysis to the rectangular membrane problem using an elastic-plastic material. His development, however, was restricted to small deformations. Also, during 1966, Oden and Sato (16) developed a finite element formulation for the finite strain and displacements of elastic membranes of general shape.

Several experimental investigations have been reported [e.g. Day (4), Neubert and Sommer (46), and Head and Sechler (40)]. Neubert and Sommer experimentally verified the solutions of Föppl and Henky for a square membrane. Head and Sechler obtained data for square and rectangular membranes. The results confirmed the Föppl and Henky solutions for square membranes but disagreed with Föppl's solution for high width to length ratios of rectangular members.

CHAPTER II

FORMULATION OF THE PROBLEM

2.1 Introduction

This chapter includes the mathematical statement of the problem and the derivation of the equations which govern the motion of the membrane. More specifically, the fundamental approach of considering the dynamic equilibrium of a differential element of the membrane is employed. This leads to three governing partial differential equations in terms of stress resultants. The incorporation of the appropriate constitutive and kinematic equations result in the desired restatement of the equilibrium equations in terms of orthogonal displacements.

2.2 Interpretation of the Problem

This problem is viewed as one in which the total deformation must be provided by accumulated increments with the process continuing until the motion ceases. For some problems of finite deformations, this segmentation of the solution process can be most advantageous. That is, the nonlinearity due to the kinematic relations can be avoided by using small deformation theory. Such, fortunately, is true in the case of this development. A set of linear

kinematic expressions is formed with which the strains occurring during each increment of deformation are referenced to the configuration of the membrane surface at the start of the current increment. In this manner, the recording of the strain history and thus the proportionality parameter relating stress to strain increment are kept current and valid. Figures 1 and 2 illustrate the accumulation of the strains and displacements occurring during each of these steps. The magnitudes of these values depend upon the chosen time interval.

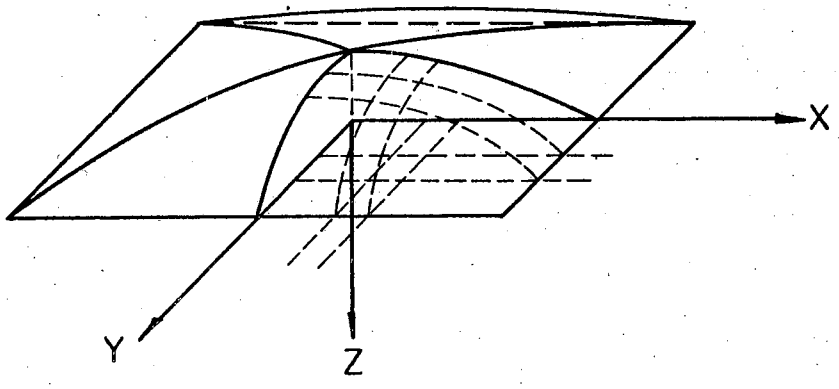

Figure 1. Typical Deformation Pattern of Membrane

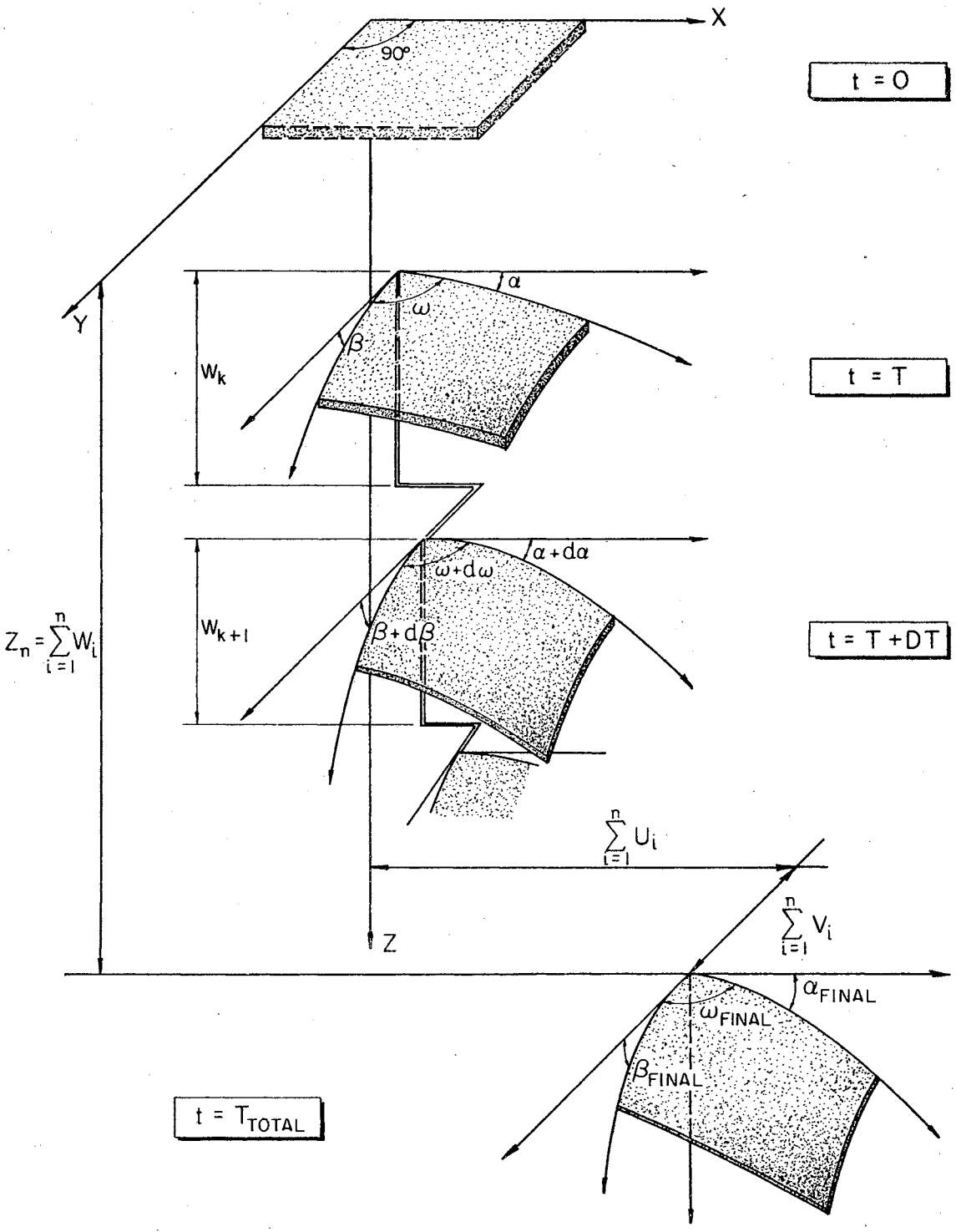

Figure 2. Progressive Incremental Deformation of Membrane Element

These comments indicate that each intermediate step in the deformation sequence is analogous to the total small deformation process of a translational shell of rectangular planform. In order to emphasize this connection in theory, the rectangular membrane is referred to as a "pseudo-shell" during intermediate states in the deformation procedure. In addition to the accumulation of the strains and displacements at the end of each step in the incremental process, the terminal conditions are reinstated as the initial conditions for the following deformation increment. Thus, established translational shell theory is an advantage of the incremental character of the problem and allows the nonlinearity of large deformation theory to be avoided.

2.3 Governing Equations

a) Equations of Motion - Using an orthogonal coordinate system exhibited in Figure 1, the deformed pseudo-shell surface is defined by function, Z, of the variables x and y. The intersection of this surface with planes perpendicular to the x and y axes defines a representative differential element. The dynamic equilibrium of this element is expressed using the appropriate skewed stress resultants and external and inertial forces shown in Figure 3. The resulting governing differential equations of motion are written using Pucher's Method (6). With this method, the equilibrium of the pseudo-shell element is stated in terms of the horizontal projections of skewed

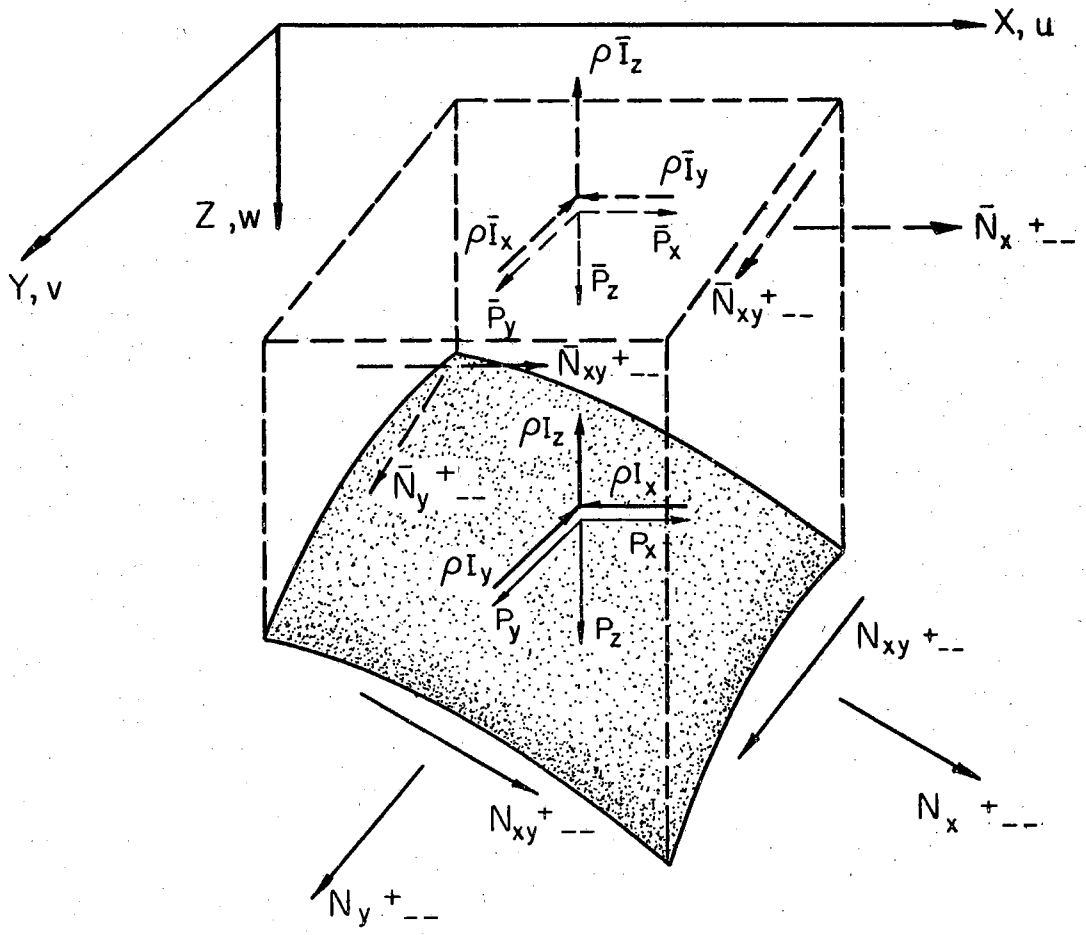

Figure 3. State of Dynamic Equilibrium

membrane forces, which are assumed to act on the horizontal line segments of the element's projection in the xy plane.

The derivation of the governing equation for static equilibrium using the Pucher Method is given in Appendix A for convenience. The equations are as follows:

$$\frac{\partial}{\partial x}\overline{N}_x + \frac{\partial}{\partial y}\overline{N}_{yx} + \overline{P}_x = 0 \tag{1a}$$

$$\frac{\partial}{\partial y}\overline{N}_y + \frac{\partial}{\partial x}\overline{N}_{xy} + \overline{P}_y = 0 \tag{1b}$$

$$\overline{N}_x\frac{\partial^2 Z}{\partial x^2} + 2\overline{N}_{xy}\frac{\partial^2 Z}{\partial x \partial y} + \overline{N}_y\frac{\partial^2 Z}{\partial y^2} = -\overline{P}_z + \overline{P}_x\frac{\partial Z}{\partial x} + \overline{P}_y\frac{\partial Z}{\partial y} \tag{1c}$$

where

$\overline{N}_{xy}$, $\overline{N}_x$, $\overline{N}_y$ = horizontal projections of skewed stress resultants N_{xy}, N_x and N_y respectively acting upon the sides of the projected element, dx and dy.

$\frac{\partial^2 Z}{\partial x^2}$, $\frac{\partial^2 Z}{\partial y^2}$, $\frac{\partial^2 Z}{\partial x \partial y}$ = the indicated derivatives of the function Z defining the reference undeformed configuration of the membrane shell.

$\overline{P}_x$, $\overline{P}_y$, $\overline{P}_z$ = equivalent external loads per unit area of the projected element.

These equations can easily be converted for use in this problem by accounting for the inertial forces shown in Figure 3 and certain changes in notation. In this manner, the equations of motion governing the state of

dynamic equilibrium become

$$\frac{\partial}{\partial x}\overline{N}_x + \frac{\partial}{\partial y}\overline{N}_{yx} + \overline{P}_x - \overline{I}_x = 0 \tag{2a}$$

$$\frac{\partial}{\partial y}\overline{N}_y + \frac{\partial}{\partial x}\overline{N}_{xy} + \overline{P}_y - \overline{I}_y = 0 \tag{2b}$$

and

$$\overline{N}_x \frac{\partial^2 R}{\partial x^2} + 2\overline{N}_{xy}\frac{\partial^2 R}{\partial x \partial y} + \overline{N}_y \frac{\partial^2 R}{\partial y^2} = -\overline{P}_z + \overline{I}_z + (\overline{P}_x - \overline{I}_x)\frac{\partial R}{\partial x} + (\overline{P}_y - \overline{I}_y)\frac{\partial R}{\partial y} \tag{2c}$$

where

$$\frac{\overline{P}_x}{P_x} = \frac{\overline{P}_y}{P_y} = \frac{\overline{P}_z}{P_z} = \frac{\overline{I}_x}{I_x} = \frac{\overline{I}_y}{I_y} = \frac{\overline{I}_z}{I_z} = \frac{dA}{dxdy} = \frac{(1 - \sin^2\alpha \sin^2\beta)^{\frac{1}{2}}}{\cos\alpha \cos\beta} \tag{3}$$

This relation is deduced from equation A10 in Appendix A.

Also, in the above equations,

R = replacement for notation Z used above to define reference "undeformed" configuration of pseudo-shell surface.

I_x, I_y, I_z = inertial forces per unit area acting on differential element in x, y and z directions respectively.

$I_x = \rho \frac{\partial^2 U}{\partial t^2}$

$I_y = \rho \frac{\partial^2 V}{\partial t^2}$

I_z $= \rho \frac{\partial^2 W}{\partial t^2} = \rho \frac{\partial^2 Z}{\partial t^2}$

$\bar{I}_x$, $\bar{I}_y$, $\bar{I}_z$ = inertial forces equivalents of I_x, I_y and I_z considered to be acting on the projected element.

dA = surface area of differential shell element.

In these equations, U, V, and W are the incremental deformations in the x, y, and z directions respectively. The function Z defines the configuration of the pseudo-shell in its deformed position.

Solutions to equations 2a, 2b, and 2c are now significantly simplified by neglecting the x and y components of inertia. As long as the slopes of the membrane surface are not so great that these terms approach that of the transverse inertial term in magnitude, this is a fair assumption. Previous investigators have applied this assumption successfully to cases of circular membranes (1) (7). On the basis of the same argument, the x and y components of the external loads are also omitted. The equations, in this manner, reduce to the forms

$$\frac{\partial}{\partial x} \bar{N}_x + \frac{\partial}{\partial y} \bar{N}_{yx} = 0 \qquad (4a)$$

$$\frac{\partial}{\partial y} \bar{N}_y + \frac{\partial}{\partial x} \bar{N}_{xy} = 0 \qquad (4b)$$

$$\bar{N}_x \frac{\partial^2 R}{\partial x^2} + 2\bar{N}_{xy} \frac{\partial^2 R}{\partial x \partial y} + \bar{N}_y \frac{\partial^2 R}{\partial y^2} = -\bar{P}_z + \bar{I}_z \qquad (4c)$$

b) Skewed Strain-Orthogonal Displacement Relations - Flügge and Geyling (5) used a skewed curvilinear coordinate system related to an orthogonal rectangular base system in developing a general deformation theory for membrane shells other than surfaces of revolution and cylinders. This development is included in Appendix B for reference.

In terms of the variables U, V, W, α, β, and ω, as indicated in Figure 4, the following expressions for skewed strain components were derived.

$$e_x = U_x \cos^2 \alpha + W_x \sin \alpha \cos \alpha \tag{5a}$$

$$e_y = V_y \cos^2 \beta + W_y \sin \beta \cos \beta \tag{5b}$$

$$\gamma_{xy} = \frac{1}{\sin \omega} [U_y \cos \alpha \cos \beta + V_x \cos \alpha \cos \beta + W_y \sin \alpha \cos^3 \beta + W_x \sin \beta \cos^3 \alpha - U_x \cos^2 \alpha \sin \beta \sin \alpha - V_y \cos^2 \beta \sin \beta \sin \alpha] \tag{5c}$$

where

e_x, e_y = total normal strains of the membrane in the x and y directions (considered to lie in tangent plane and, thus, are skewed)

U, V, W = displacements in the x, y, and z directions respectively.

α, β = angles between the horizontal and the curved line segments bounding the differential element.

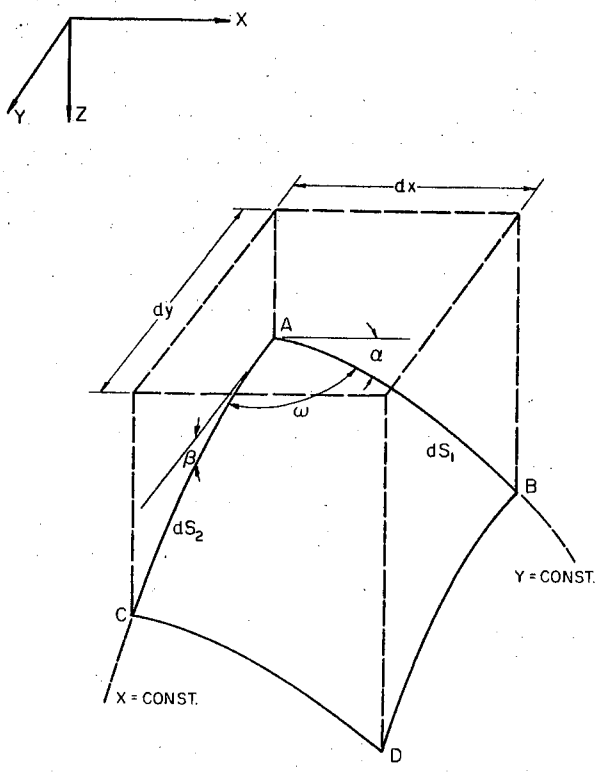

Figure 4. Geometry of Pseudo-Shell Element

ω = angle of skew between curved line segments in the plane tangent to the differential element.

Flügge and Geyling formulated these terms as the total deformation response of a membrane shell. In the present problem, however, they correspond only to an increment of deformation. Changing the notation in equation (5) to reflect this adjustment yields for the pseudo-shell membrane,

$$\delta e_x = U_x \cos^2 \alpha + W_x \sin \alpha \cos \alpha \tag{6a}$$

$$\delta e_y = V_y \cos^2 \alpha + W_y \sin \alpha \cos \alpha \tag{6b}$$

$$\delta\gamma_{xy} = \frac{1}{\sin\omega}\left[U_y \cos\alpha \cos\beta + V_x \cos\alpha \cos\beta + W_y \sin\alpha \cos^3\beta + W_x \sin\beta \cos^3\alpha - U_x \cos^2\alpha \sin\beta \sin\alpha - V_y \cos^2\beta \sin\alpha\right]$$

where

δe_x, δe_y = normal skewed strain increments associated with the current increment of deformations.

U, V, W = x, y, and z components, respectively, of the current increment of displacement.

c) Orthogonal Strain-Orthogonal Displacement Relations - In the preceding section, the kinematic relations in terms of skewed strains were developed. In order to use the constitutive equations, however, equivalent relations in terms of orthogonal strains must be formulated.

Flügge and Geyling, as shown in Appendix B, developed the following relations between the orthogonal and skewed strains

$$e_x = e_{\overline{x}}$$

$$\gamma_{xy}\frac{1}{\sin\omega} = \gamma_{\overline{xy}} \sin\omega + e_{\overline{x}} \cos\omega - e_{\overline{y}} \cos\omega$$

Converting to the notation of this thesis, these relations become

$$\delta e_x = \delta e_{\overline{x}} \qquad (7)$$

$$\delta\gamma_{xy} \frac{1}{\sin \omega} = \delta\gamma_{\bar{x}\bar{y}} \sin \omega + \delta e_{\bar{x}} \cos \omega - \delta e_{\bar{y}} \cos \omega \qquad (8)$$

The remaining required relation is derived using geometry from Figure 5 for the orthogonal strain increment, $\delta e_{\bar{y}}$.

From this figure,

$$\bar{AB} \sin \omega = \delta e_{\bar{y}} \frac{b}{\sin \omega}$$

$$\bar{AB} = \delta e_{\bar{y}} \frac{b}{\sin^2 \omega}$$

and

$$\tan \omega = \frac{\bar{EC}}{\bar{EB}}$$

$$\bar{EB} = \bar{EC} \cot \omega$$

$$\bar{EB} = \delta e_{\bar{x}} b \cot^2 \omega$$

Thus,

$$\delta e_y b = \bar{AB} - \bar{EB}$$

$$\delta e_y b = \delta e_{\bar{y}} \frac{b}{\sin^2 \omega} - \delta e_{\bar{x}} b \cot^2 \omega$$

or

$$\delta e_y = \delta e_{\bar{y}} \frac{1}{\sin^2 \omega} - \delta e_{\bar{x}} \cot^2 \omega \qquad (9)$$

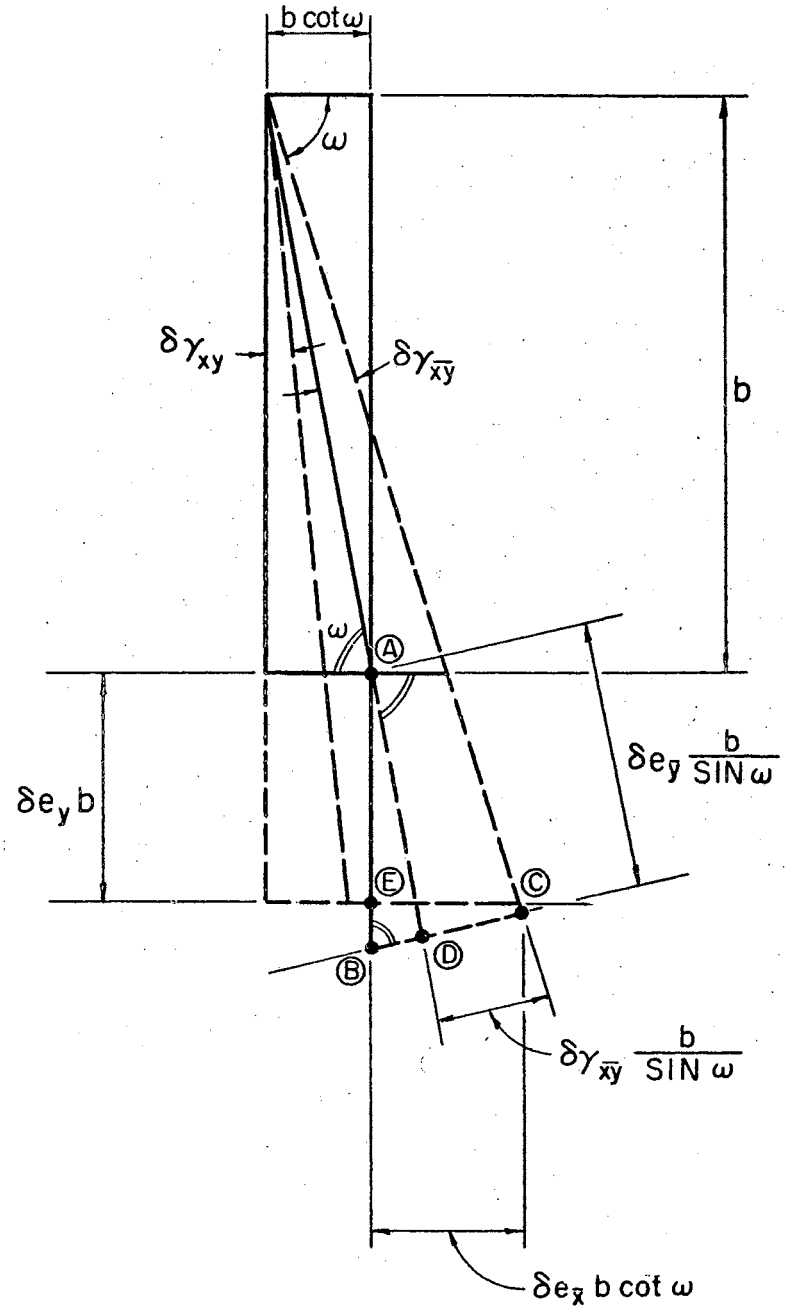

Figure 5. Skewed-Orthogonal Strain Relations

From equation (8),

$$\delta\gamma_{\bar{x}\bar{y}} = \frac{1}{\sin^2\omega}\left[\delta\gamma_{xy} - \delta e_{\bar{x}} \cot\omega + \delta e_{\bar{y}} \cot\omega\right] \tag{10}$$

Substituting equations (7) and (9) into (10) gives

$$\delta\gamma_{\bar{x}\bar{y}} = \frac{1}{\sin^2\omega}\left[\delta\gamma_{xy} - \delta e_{x} \cot\omega + \delta e_{y} \cot\omega\right] \tag{11}$$

Thus, the orthogonal strain increments in terms of the skewed strain increments are

$$\delta e_{\bar{x}} = \delta e_{x} \tag{12a}$$

$$\delta e_{\bar{y}} = \frac{1}{\sin^2\omega}\left[\delta e_{y} - \delta e_{x} \cos^2\omega\right] \tag{12b}$$

$$\delta\gamma_{\bar{x}\bar{y}} = \frac{1}{\sin^2\omega}\left[\delta\gamma_{xy} - \delta e_{x} \cot\omega + \delta e_{y} \cot\omega\right] \tag{12c}$$

With equations (12) and (6), the kinematic relations with orthogonal strains are written as follows:

$$\delta e_{\bar{x}} = U_x \cos^2\alpha + W_x \sin\alpha \cos\alpha \tag{13}$$

$$\delta e_{\bar{y}} = \frac{1}{\sin^2\omega}\left[V_y \cos^2\beta + W_y \sin\beta \cos\beta - (U_x \cos^2\alpha + W_x \sin\alpha \cos\alpha) \cos^2\omega\right] \tag{14}$$

$$\delta\gamma_{\bar{x}\bar{y}} = \frac{1}{\sin^3\omega}\left[V_y (\cos^2\beta \cos\omega - \cos^2\beta \sin\beta \sin\alpha) + U_y \cos\alpha \cos\beta + V_x \cos\alpha \cos\beta\right.$$

$$- U_x (\cos^2\alpha \sin\beta \sin\alpha + \cos^2\alpha \cos\omega)$$

$$+ W_y (\sin\alpha \cos^3\beta + \sin\beta \cos\beta \cos\omega)$$

$$+ W_x (\sin\beta \cos^3\alpha - \sin\alpha \cos\alpha \cos\omega)] \qquad (15)$$

d) Constitutive Equation - The constitutive equations for a rigid, work-hardening material involve consideration of the following: (a) an initial yield condition which the stresses must satisfy for initial yielding to begin; (b) a flow rule to associate the plastic strain increment with the current stress and (c) a hardening rule which serves to adjust the initial yield condition for continued plastic flow. The development in Appendix D of the constitutive equations combines the initial yield condition of von Mises-Henky and the Levy-Mises flow rule. These are

$$\begin{aligned} de_x &= \Delta\lambda(S_x - \tfrac{1}{2}N_y) \\ de_y &= \Delta\lambda(N_y - \tfrac{1}{2}S_x) \\ de_{xy} &= \tfrac{3}{2}\Delta\lambda\, T_1 \end{aligned} \qquad (16)$$

or in keeping with the finite incremental character of this problem, equations (16) are rewritten as

$$\begin{aligned} \delta e_x &= \Delta\lambda(S_x - \tfrac{1}{2}N_y) \\ \delta e_y &= \Delta\lambda(N_y - \tfrac{1}{2}S_x) \\ \delta e_{xy} &= \tfrac{3}{2}\Delta\lambda\, T_1 \end{aligned} \qquad (17)$$

where

S_x, $N_{\bar{y}}$ = normal stress resultants acting in the orthogonal x and y directions.

T_1 = shear stress associated with S_x and $N_{\bar{y}}$

$\Delta\lambda$ = plasticity parameter

$= \frac{\bar{\delta\epsilon}}{\bar{\sigma}\dot{t}}$

These equations are supplemented by the following work-hardening rule to describe the condition of continued yielding

$$\bar{\sigma} = H\ (\Sigma\overline{\delta\epsilon}) \tag{18}$$

where H is the universal stress-strain relationship usually taken to be the uniaxial stress-strain relationship for the material used. Such a hardening rule is an extension of the Mises-Henky initial yield criterion and was proposed by Ros and Eichinger (9). In this thesis, Ludwik's Power Law is chosen to represent the function and may be written

$$\bar{\sigma} = a + b\ (\Sigma\ \overline{\delta\epsilon})^c \tag{19}$$

where a, b, and c are material parameters.

Such a hardening rule describes the yield surface as uniformly increasing in size and retaining its form and center position. When unloading, the material is assumed to continue to act as a rigid-work-hardening solid. Thus, the constitutive equations given above are valid regardless of whether the material is loading, unloading or reloading.

From Appendix C, the following skew-to-orthogonal stress resultants are obtained

$$S_x = N_x \csc\omega + N_y \cot\omega \cos\omega + 2T_{xy} \cot\omega$$
$$N_y = N_y \sin\omega \qquad (20)$$
$$T_1 = N_{xy} + N_y \cos\omega$$

Substituting equations (20) into equations (17) the following constitutive equations in terms of skewed stress resultants are formed.

$$\delta e_x = \Delta\lambda[N_x \frac{1}{\sin\omega} + 2N_{xy} \cot\omega + N_y \sin\omega(\cot^2\omega - \tfrac{1}{2})]$$
$$\delta e_y = \Delta\lambda[-N_x \frac{1}{2\sin\omega} - N_{xy} \cot\omega + N_y \sin\omega(1 - \tfrac{1}{2}\cot^2\omega)]$$
$$\delta e_{xy} = \tfrac{3}{2}\Delta\lambda[N_{xy} + N_y \cos\omega] \qquad (21)$$

The existence of strain rate effects is still a controversial issue. The most common viewpoint is given by a quotation from a contribution by Henriksen et al (42); "Strain rate effects are a reality and are evidenced by variations in the mechanical properties". Among the methods for analytically accounting for such effects, the one that appears most tractable is that employed by Witmer et al (26). Basically, the yield stress of the material is assumed to increase with the strain rate while the strain hardening portion of the stress-strain curve retains the same shape of the static curve as indicated in Figure 6. An account, thereby, can be made by considering the material

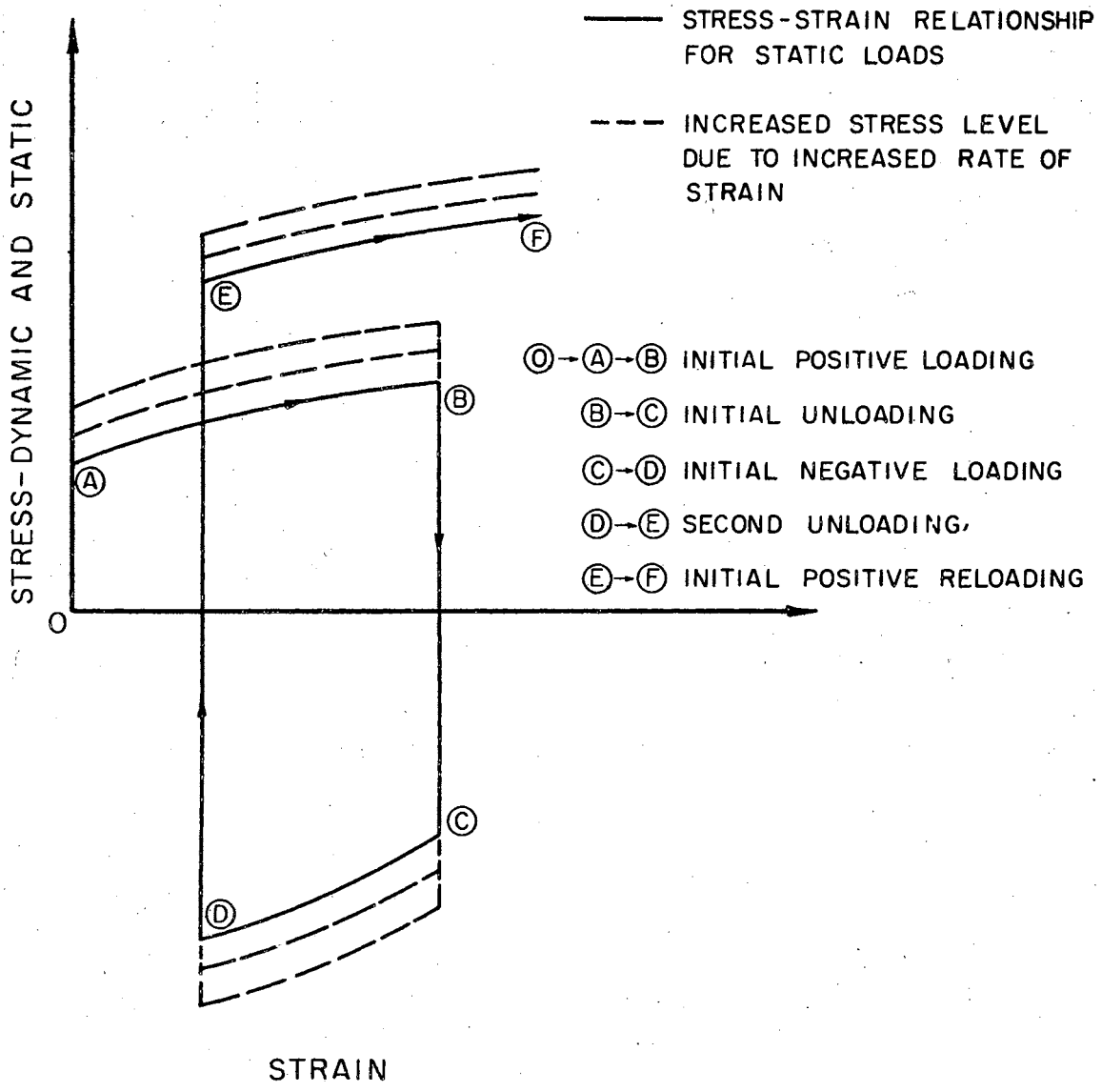

Figure 6. Typical Dynamic and Static Stress-Strain Relation

constants in equation (19) as functions of strain rate. The latter could be calculated at the end of each deformation increment using projected strain increment values. Other than this suggested procedure, no further consideration will be given to strain rate effects in the following formulation of the problem. The brevity of the formulation is considered more important than the benefit of illustrating the inclusion of strain rate effects.

e) Governing Differential Equations of Motion - In matrix form, equations (21) can be written as follows.

$$\begin{bmatrix} \frac{1}{\sin\omega} & \sin\omega(\cot^2\omega - \frac{1}{2}) & 2\cot\omega \\ -\frac{1}{2\sin\omega} & \sin\omega(1-\frac{1}{2}\cot^2\omega) & -\cot\omega \\ 0 & \cos\omega & 1 \end{bmatrix} \begin{bmatrix} N_x \\ N_y \\ N_{xy} \end{bmatrix} = \begin{bmatrix} \delta e_{\bar{x}}/\Delta\lambda \\ \delta e_{\bar{y}}/\Delta\lambda \\ \delta e_{\overline{xy}}/\beta\Delta\lambda \end{bmatrix}$$

By inversion, the following expressions of the skewed stress resultants as functions of orthogonal strain increments are obtained;

$$N_x = \frac{4\cos\omega}{3\Delta\lambda}[(\tan\omega + \tfrac{1}{2}\cot\omega)\delta e_{\bar{x}} + (\tfrac{1}{2}\tan\omega + \cot\omega)\delta e_{\bar{y}} - \delta e_{\overline{xy}}]$$

$$N_y = \frac{4}{3\Delta\lambda}\left[\frac{1}{2\sin\omega}\delta e_{\bar{x}} + \frac{1}{\sin\omega}\delta e_{\bar{y}}\right] \qquad (22)$$

$$N_{xy} = \frac{4}{3\Delta\lambda}[-\tfrac{1}{2}\cot\omega\,\delta e_{\bar{x}} - \cot\omega\,\delta e_{\bar{y}} + \tfrac{1}{2}\delta e_{\overline{xy}}]$$

From Appendix A, the horizontal projections of the skewed stress resultants in terms of the latter are

$$\bar{N}_x = N_x \frac{\cos\alpha}{\cos\beta}$$

$$\bar{N}_{xy} = \bar{N}_{yx} = N_{xy} = N_{yx} \tag{23}$$

$$\bar{N}_y = N_y \frac{\cos\beta}{\cos\alpha}$$

By substituting equations (22) in expressions (23) and substituting the results into the differential equation of motion, equations (4), the following governing differential equations of this problem are found;

$$\frac{\partial}{\partial x}\left\{\frac{4\cos\omega\cos\alpha}{3\Delta\lambda\cos\beta}\left[(\tan\omega + \tfrac{1}{2}\cot\omega)\delta e_{\bar{x}} + (\tfrac{1}{2}\tan\omega + \cot\omega)\delta e_{\bar{y}} - \delta e_{\overline{xy}}\right]\right\}$$
$$+ \frac{\partial}{\partial y}\left\{\frac{4}{3\Delta\lambda}\left[-\tfrac{1}{2}\cot\omega\,\delta e_{\bar{x}} - \cot\omega\,\delta e_{\bar{y}} + \tfrac{1}{2}\delta e_{\overline{xy}}\right]\right\} = 0$$

$$\frac{\partial}{\partial y}\left\{\frac{4}{3\Delta\lambda}\frac{\cos\beta}{\cos\alpha}\left(\frac{1}{2\sin\omega}\,\delta e_{\bar{x}} + \frac{1}{\sin\omega}\,\delta e_{\bar{y}}\right)\right\}$$
$$- \frac{\partial}{\partial x}\left\{\frac{4}{3\Delta\lambda}\left(\tfrac{1}{2}\cot\omega\,\delta e_{\bar{x}} + \cot\omega\,\delta e_{\bar{y}} - \tfrac{1}{2}\,\delta e_{\overline{xy}}\right)\right\} = 0, \tag{24}$$

and

$$\frac{\partial^2 R}{\partial x^2}\frac{\cos\alpha\cos\omega}{\cos\beta}\left[(\tan\omega + \tfrac{1}{2}\cot\omega)\delta e_{\bar{x}} + (\tfrac{1}{2}\tan\omega + \cot\omega)\delta e_{\bar{y}} - \delta e_{\overline{xy}}\right] - \frac{\partial^2 R}{\partial x\partial y}\left[\cot\omega\,\delta e_{\bar{x}} + 2\cot\omega\,\delta e_{\bar{y}} - \delta e_{\overline{xy}}\right] + \frac{\partial^2 R}{\partial y^2}\frac{\cos\beta}{\cos\alpha}\left[\frac{1}{\sin\omega}\left(\frac{\delta e_{\bar{x}}}{2} + \delta e_{\bar{y}}\right)\right] = \frac{3\Delta\lambda}{4}\left(\rho\frac{\partial^2 Z}{\partial t^2} - P_z\right)\left[\frac{(1 - \sin^2\alpha\sin^2\beta)^{\frac{1}{2}}}{\cos\alpha\cos\beta}\right].$$

As shown, equations (24) are in terms of orthogonal strain increments. This will permit the introduction of displacement boundary conditions through the intermediate kinematic relations, equations (13), (14), and (15).

CHAPTER III

NUMERICAL SOLUTION OF PROBLEM

3.1 Introduction

An analytical solution of the problem formulated in the preceding section appears to be highly improbable. This is due, of course, to the nonlinearity of the governing differential equations introduced through the equations relating stress to strain increment. Thus, a numerical approach to the solution is considered necessary. The selected method requires, first, the conversion of the governing differential equations to their finite difference equivalents and, second, the utilization of some numerical integration method, which is incremental in progression. The numerical procedure followed in this study is described in the following sections.

3.2 Finite Difference Formulation

The orthogonal strain-orthogonal displacement relations (13), (14), (15) can be written as follows:

$$\delta e_{\bar{x}} = tau_1 U_x + tau_2 W_x \tag{25}$$

$$\delta e_{\bar{y}} = tau_{22} (tau_4 V_y + tau_5 W_y - tau_6 U_x - tau_7 W_x)$$

$$\delta e_{\overline{xy}} = tau_{13}(tau_8\ V_y + tau_9\ U_x + tau_{10}\ U_y + tau_{10}\ V_x + tau_{11}\ W_y + tau_{12}\ W_x) \tag{25}$$

where the coefficients, tau_{ij}, are given in Appendix E.

Substituting equations (25) into the governing differential equations (24) and introducing, in addition, the D coefficient functions as defined in Appendix F, the former equations are converted to the following functions of displacements.

$$\frac{\partial}{\partial x}\left(D_1U_x + D_2W_x + D_3V_y + D_4W_y + D_5V_x\right) - \frac{\partial}{\partial y}\left(D_6U_x + D_7W_x + D_8V_y + D_9W_y + D_{10}U_y + D_{10}V_x\right) = 0 \tag{26}$$

$$\frac{\partial}{\partial y}\left(D_{11}U_x + D_{12}W_x + D_{13}V_y + D_{14}W_y\right) - \frac{\partial}{\partial x}\left(D_6U_x + D_7W_x + D_8V_y + D_9W_y + D_{10}U_y + D_{10}V_x\right) = 0 \tag{27}$$

and

$$D_{15}U_x + D_{16}W_x + D_{17}V_y + D_{18}W_y + D_{19}U_y + D_{20}V_x = D_{21}\left(\rho\frac{\partial^2 Z}{\partial t^2} - P_z\right) \tag{28}$$

In the above form, the governing differential equations are more compatible with both the use of displacement boundary conditions and the anticipated finite difference formulation procedure.

Figure 7 defines the notation used in this development.

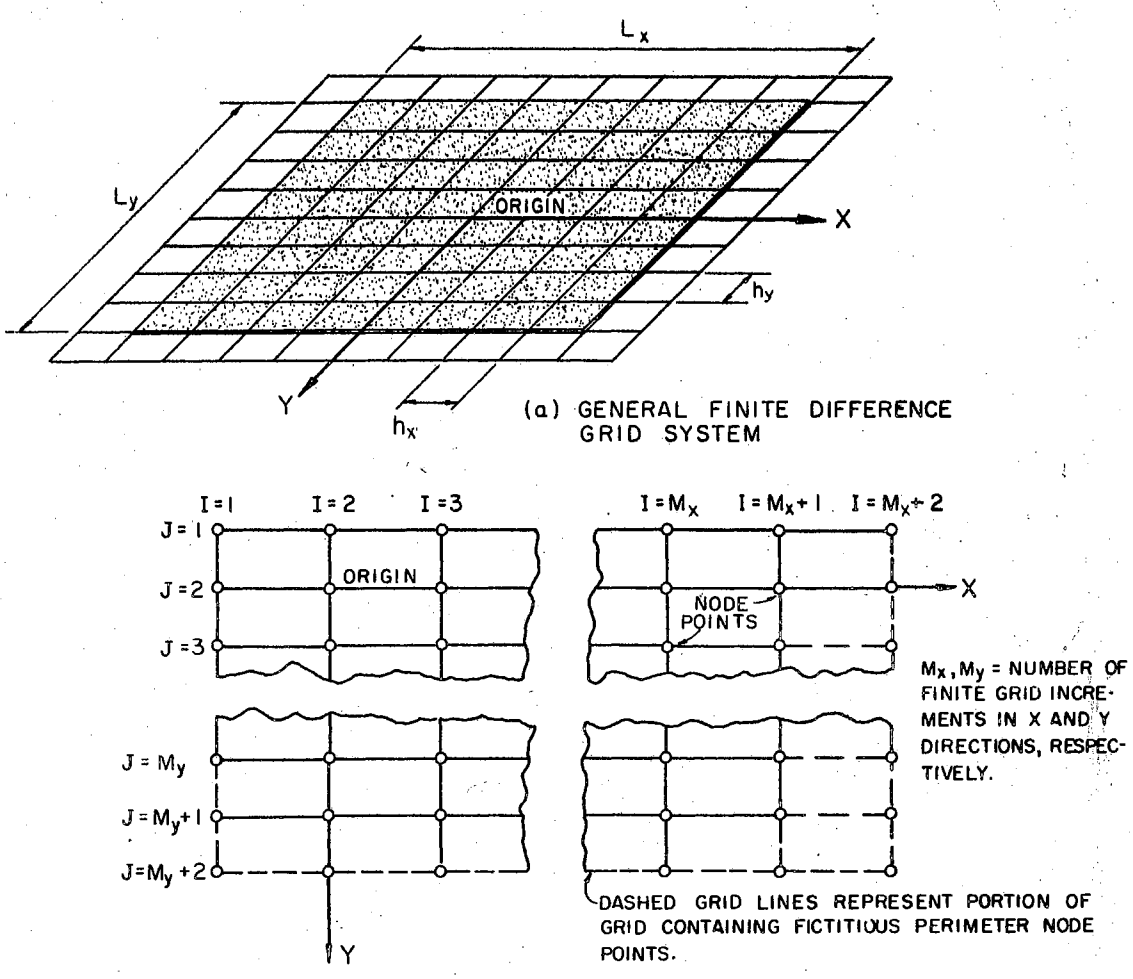

Figure 7. Finite Difference Representation

As shown the lines of the rectangular grid run parallel to the x and y axes. The intersection of these grid lines are known as node points. Their locations are specified using the indices i and j.

In order to transform equations (26) into finite differences, conventional use is made of general second degree parabolas or Taylor expansions. Choosing to use the central difference format as suggested by the reference system and position of the origin shown in Figure 7, the general finite difference equation becomes

$$
\begin{aligned}
&DU1_{i,j}U_{i-1,j-1} + DU2_{i,j}U_{i,j-1} + DU3_{i,j}U_{i+1,j-1} \\
&\quad + DU4_{i,j}U_{i-1,j} + DU5_{i,j}U_{i,j} + DU6_{i,j}U_{i+1,j} \\
&\quad + DU7_{i,j}U_{i-1,j+1} + DU8_{i,j}U_{i,j+1} + DU9_{i,j}U_{i+1,j+1} \\
&\quad + DV1_{i,j}V_{i-1,j-1} + DV2_{i,j}V_{i,j-1} + DV3_{i,j}V_{i+1,j-1} \\
&\quad + DV4_{i,j}V_{i-1,j} + DV5_{i,j}V_{i,j} + DV6_{i,j}V_{i+1,j} \\
&\quad + DV7_{i,j}V_{i-1,j+1} + DV8_{i,j}V_{i-1,j+1} + DV9_{i,j}V_{i+1,j+1} \\
&\quad + DW1_{i,j}W_{i-1,j-1} + DW2_{i,j}W_{i,j-1} + DW3_{i,j}W_{i+1,j-1} \\
&\quad + DW4_{i,j}W_{i-1,j} + DW5_{i,j}W_{i,j} + DW6_{i,j}W_{i+1,j} \\
&\quad + DW7_{i,j}W_{i-1,j+1} + DW8_{i,j}W_{i,j+1} + DW9_{i,j}W_{i+1,j+1} = 0
\end{aligned}
\tag{29}
$$

The variable coefficients introduced above are defined in Appendix G. This equation and others in its same general form will be referred to as pivotal equations.

In a similar manner, the desired finite difference form of equation (27) can be obtained. It can be shown to be identical to equations (29) except that the D coefficients are defined differently as indicated in Appendix G.

For the acceleration equation,

$$D15_{i,j}\left[\frac{U_{i+1,j} - U_{i-1,j}}{2h_x}\right] + D16_{i,j}\left[\frac{W_{i+1,j} - W_{i-1,j}}{2h_x}\right]$$

$$+ D17_{i,j}\left[\frac{V_{i,j+1} - V_{i,j-1}}{2h_y}\right] + D18_{i,j}\left[\frac{W_{i,j+1} - W_{i,j-1}}{2h_y}\right]$$

$$+ D19_{i,j}\left[\frac{U_{i,j+1} - U_{i,j-1}}{2h_y}\right] + D20_{i,j}\left[\frac{V_{i+1,j} - V_{i-1,j}}{2h_x}\right]$$

$$= D21_{i,j}\left[\rho\frac{\partial^2 Z}{\partial t^2} - Pz_{i,j}\right] \quad (30)$$

It should be noted in equation (30) that the acceleration term is not put into finite difference form in the time domain. The reason for this feature is explained in the next section. A side benefit, however, is that it facilitates the use of two general subscripts instead of the normal three.

3.3 Boundary Conditions

Because the governing differential equations are treated as first order linear partial differential equations in regards to spacial coordinates, the pertinent nodal points are those on the interior, on the boundary and those ficticious exterior points immediately adjacent to

the boundary. Along the boundary,

$$U(\pm \frac{L_x}{2},y) = U(x, \pm \frac{L_y}{2}) = 0$$

$$V(\pm \frac{L_x}{2},y) = V(x, \pm \frac{L_y}{2}) = 0 \qquad (31)$$

$$W(\pm \frac{L_x}{2},y) = W(x, \pm \frac{L_y}{2}) = 0$$

Also, boundary values must be prescribed for the function R which defines the intermediate reference configuration of the membrane. The Z function is defined as the sum of R and W expressions. These, however, are not required to be zero. The only restrictions, as previously mentioned, are that (1) the initial membrane configuration projects onto a rectangular planform in the xy plane, and (2) that there be a one-to-one functional correspondence between the membrane surface and its planform. In this work, however, the initial configuration is such that

$$R(\pm \frac{L_x}{2},y) = R(x, \pm \frac{L_y}{2}) = 0 \qquad (32)$$

Due to the symmetry of the problem with respect to each of its two axes, the first quadrant can be taken as representative of the deformation of the entire membrane. Thus, compensating for such symmetry, the following conditions are derived using a finite difference slope relation along the y axis.

$$U(2, J) = 0$$

$$U(1, J) = -U(3, J)$$

$$V(1, J) = V(3, J) \tag{33}$$

$$W(1, J) = W(3, j)$$

$$R(1, J) = R(3, J)$$

and along the x axis

$$V(I, 2) = 0$$

$$U(I, 1) = U(I, 3)$$

$$V(I, 1) = -V(I, 3) \tag{34}$$

$$W(I, 1) = W(I, 3)$$

$$R(I, 1) = R(I, 3)$$

For the ficticious nodal points located adjacent to the membrane perimeter, the lack of bending rigidity of a completely plastic membrane is considered by writing

$$U(M_x + 1, J) = U(M_x + 3, J)$$

$$V(M_x + 1, J) = -V(M_x + 3, J)$$

$$W(M_x + 1, J) = -W(M_x + 3, J)$$

$$R(M_x + 1, J) = -R(M_x + 3, J) \tag{35}$$

and

$$U(I, M_y + 1) = -U(I, M_y + 3)$$

$$V(I, M_y + 1) = V(I, M_y + 3)$$

$$W(I, M_y + 1) = -W(I, M_y + 3)$$

$$R(I, M_y + 1) = -R(I, M_y + 3) \qquad (36)$$

Using equations (35) and (36), the exterior fictitious displacement values at external nodal points are replaced by their equivalent expressions in terms of the desired interior values.

3.4 Initial Conditions

At the beginning of the membrane motion, either a velocity or pressure field is prescribed. If initial velocities are applied, no pressure is assumed to act on the membrane at any time. On the other hand, if a transient pressure distribution is prescribed, the initial velocity is taken as being zero. The determination of both of these sets of initial conditions is given in Appendix H. Thus, the implied initial conditions are

Case I

$$R(x, y, 0) = 0$$

Initial Impulse

$$\frac{\partial Z}{\partial t}(x, y, 0) = g(x, y)$$

Case II

$$R(x, y, 0) = 0$$

Applied Pressure

$$\frac{\partial Z}{\partial t}(x, y, 0) = 0$$

Upon the termination of each increment of deformation, the current velocities, accelerations and vertical displacements are calculated. These become the initial conditions for the following increment of deformation. These values will be referred to as the "subsequent initial" conditions.

3.5 Numerical Method of Solution

In essence, the solution of this problem is represented by the accumulated effects of many individual increments of deformations. For the purpose of clarity, the solution for each increment of deformation will be referred to as a "sub-solution". In the following discussion, a method will be developed, first, for obtaining a general sub-solution. This will be followed by the procedure with which each of these will be accumulated to adequately represent the total solution. A consideration of the definitions of the D coefficients, as given in Appendix F and introduced in the preceding section, reveals that they also serve to couple the three equations, the coefficients being functions of strains. Thus, in order to solve this system of simultaneous partial differential equations, complete U, V and W displacement fields must be assumed

initially. As will be shown later, the initial set of W displacements will be predicted using an established structural dynamic procedure. The initial U and V displacement fields will be approximated using Mostow's derivations contained in reference (13). Assuming the numerical procedure to be convergent, the solution of the equations will provide better approximations of these dependent variables. Using the improved approximations, a repeat of the solution procedure would yield an even better set of approximations to the displacement fields. Such an iterative process would continue until the error induced by neglecting the differences in the present and the previously calculated displacement fields would be of a tolerable magnitude. Here and in the following discussion, a "tolerable magnitude" of error is defined as an induced error which is of the same relative magnitude as the errors caused by the general assumptions of Chapters I and II. Such a convergence marks the end of the particular increment of deformation. At this point, the determined strain and displacement values are accumulated and a new increment commenced.

The question now encountered is that of which numerical method or combination of methods to use in constructing such an iterative procedure. As shown, equation (30) is a direct function of time. The other two are only indirectly related to the time variable; this dependency being due to the coupling effect of the dependent variable,

W. Noting this distinction, equation (29) and the similar expression formed from equation (27) are to be approached as boundary value problems whereas the solutions of equation (30) is identified as a propagation problem of a continuous system.

With this acknowledgement, an iterative procedure suggested by Boyd (1) is selected. The general procedure is to use the U and V displacement fields calculated in a particular increment as first estimates in the following stage of deformation. The new displacement field is obtained using a suitable predictor formula. Substituting these values in a finite difference form of equation (26), new values for the U displacements are calculated. Using this calculated set and carrying over the same V and W terms, equation (27) is used to calculate an improved set of V displacements. These calculated values are then used in equation (28) to calculate the acceleration field acting at the end of the present cycle. Next the newly calculated acceleration values are used in a corrector formula to derive an improved W displacement field. This entire sequence is repeated until the calculated differences between the new and old displacement field converge to an acceptable minimum and then a new increment of deformation is started. Thus, one sub-solution is completed and another is started. The intermediate step of revising initial conditions and accumulating strains and displacements is also necessary.

The preceding description of the sub-solution procedure is general. The necessary additional details are provided through the following discussion of the solution of each individual equation. The entire solution procedure is implied by the flow diagram given in Appendix I. In this development, equation (26) will be referred to as the "U displacement equation" implying the variable for which it is used to solve. Likewise, equations (27) and (28) are designated the "V displacement" and the "acceleration equations", respectively.

a) Solution of the U and V Displacement Equation - These equations are of the boundary value type. Applying the pivotal equation for the U displacement (equation (29)) to each of the n interior nodal points contained in the first quadrant and utilizing the boundary conditions given in Section 3.3, a set of n homogeneous, linear algebraic equation is derived in terms of the 3n unknown displacements U, V, and W. In symbolic matrix form, this operation yields

$$[C]\{U\} + [D]\{V\} + [E]\{W\} = 0 \qquad (39)$$

where

$[C]$, $[D]$, $[E]$	= first order finite difference matrices (square)
$\{U\}$	= U displacement matrix (vector)
$\{V\}$	= V displacement matrix (vector)
$\{W\}$	= W displacement matrix (vector)

The general format of the matrices products $[C]\{U\}$, $[D]\{V\}$, and $[E]\{W\}$ is identical.

Assuming known V and W displacement fields

$$[C]\{U\} = -([D]\{V\} + [E]\{W\}) \tag{40}$$

$$[C]\{U\} = \{UDISP\} \tag{41}$$

$$\{U\} = [C]^{-1}\{UDISP\} \tag{42}$$

The operation implied by equation (42) results in an improved set of values for the U displacements.

The finite difference equation established for the V displacements is used in the same manner to obtain

$$[F]\{U\} + [G]\{V\} + [H]\{W\} = 0$$

$$[G]\{V\} = -[H]\{W\} - [F]\{U\}$$

$$[G]\{V\} = \{VDISP\}$$

and

$$\{V\} = [G]^{-1}\{VDISP\}$$

Equation (43) gives the V displacement field in terms of the U and W displacements. It is apparent that if the correct value of the W displacement is assumed, if the procedure is convergent, and if the most recently corrected values of the U and V displacement values are used, the continued cyclic use of equations (42) and (43) would result in progressively improving U and V displacement values.

b) Solution of the Acceleration Equation - Pertinent methods of dynamic analysis can be divided into three major categories; open method, closed method, or a combination of the preceding two methods. An open method is one with which the displacements for the projected time increment are functions only of the displacement, velocity, and acceleration calculated for the past time increment. As such, it is sometimes referred to as a forward method. The closed method formulates the projected displacement as functions of the velocities and accelerations of the projected time increment. Thus, a varying number of iterations are required to converge within a reasonable tolerance to the true values. The closed method is the more accurate of these two methods.

The joint use of open and closed methods in solving problems of dynamic propagation is conventional. Boyd applied such a combination in his analysis of the circular membrane problem. Basically, an open method serves to predict a displacement field and then a closed method is used to correct such a prediction. Unless the formulation is numerically unstable, repetition results in convergence.

A simple Euler finite difference approximation to the acceleration term,

$$\frac{\partial^2 Z_{i,j}}{\partial t^2} = [(Z_{i,j})_{t-\Delta t} - (Z_{i,j})_t + (Z_{i,j})_{t+\Delta t}]\frac{1}{\Delta t^2} \qquad (44)$$

yields the following predictor equation for the accumulated membrane configuration in the projected time period.

$$(Z_{i,j})_{t+\Delta t} = (Z_{i,j})_t - (Z_{i,j})_{t-\Delta t} + \Delta t^2(\ddot{Z}_{i,j})_t \tag{45}$$

where $\ddot{Z}_{i,j}$ denotes $\frac{\partial^2 Z_{i,j}}{\partial t^2}$. The desired predicted W displacement values are obtained as follows

$$(W_{i,j})_{t+\Delta t} = (Z_{i,j})_{t+\Delta t} - (Z_{i,j})_t \tag{46}$$

Therefore, by using equations (45) and (46), the W displacement field for a new increment of deformation can be predicted entirely on the basis of known past values of displacement, velocity and acceleration.

Consider now the acceleration equation written in an abbreviated form as

$$\begin{aligned}\ddot{Z}_{i,j} = f(&U_{i-1,j};\ U_{i+1,j};\ U_{i,j-1};\ U_{i,j+1};\\ &V_{i-1,j};\ V_{i+1,j};\ V_{i,j-1};\ V_{i,j+1};\\ &W_{i-1,j};\ W_{i+1,j};\ W_{i,j-1};\ W_{i,j+1})\end{aligned} \tag{47}$$

Assuming that the U and V displacement fields are either known or have been predicted, equation (47) can be treated as a function of displacements only. Thus,

$$\ddot{Z}_{i,j} = f(W_{i-1,j};\ W_{i+1,j};\ W_{i,j-1};\ W_{i,j+1}) \tag{48}$$

By using predicted values of $(W_{i,j})_{t+\Delta t}$ in equation (48), a set of values can be calculated for $(\ddot{Z}_{i,j})_{t+\Delta t}$. At this

point, a closed method sometimes designated as Stormer's Method, is introduced to obtain "corrected" values of the displacement field. This corrector formula is given by Crandall (29) as

$$(Z_{i,j})_{t+\Delta t} = 2(Z_{i,j})_t - (Z_{i,j})_{t-\Delta t} + \frac{\Delta t^2}{12}[(\ddot{Z}_{i,j})_{t+\Delta t} + 10(\ddot{Z}_{i,j})_t + (\ddot{Z}_{i,j})_{t-\Delta t}] \quad (49)$$

from which the improved values are derived using the following equation

$$(W_{i,j})_{t+\Delta t} = (Z_{i,j})_{t+\Delta t} - (Z_{i,j})_t \quad (50)$$

As implied in the beginning of this section, these values and the calculated $(V_{i,j})_{t+\Delta t}$ displacement field are then substituted into the U displacement equation and a more improved set of $(U_{i,j})_{t+\Delta t}$ displacements calculated. Then, of course, this revised set of U displacements and the same W displacements are used in the V displacements equation to obtain corrected values of $(V_{i,j})_{t+\Delta t}$ displacements. At this point, equation (48) can be used to calculate a better value for the acceleration $(\ddot{Z}_{i,j})_{t+\Delta t}$. Following this, from equations (49) and (50) are obtained still better approximations to the $(W_{i,j})_{t+\Delta t}$ displacement field. This procedure is repeated until the corrected acceleration yields an insignificant change in the $(W_{i,j})_{t+\Delta t}$ displacement field. The computer program block

diagram in Appendix I illustrates more clearly this general iterative procedure.

3.6 Selection of Space and Time Intervals

The accuracy and execution time of the preceding solution procedure will be affected to a great extent by the selection of the space and time intervals. In the interest of computer programming efficiency, the selection of the largest intervals possible is desirable. The analytical determination of such optimum values for this problem appears to be highly improbable if not impossible. A numerical determination by trial is suggested in Figure 8.

As indicated in Figure 8a the optimum time interval was found by repeating the solution process with a steadily decreasing time interval until the resulting deformation field varied to within a reasonable tolerance of the field corresponding to the preceding time interval. Figure 8b indicates what variation could be expected with changes in the space intervals. For the two trials plotted, no sensitivity to moderate change in the latter is evident. Of course, no optimum space interval is concluded. In this case, however, the suggested insensitivity made further space interval investigation impracticable. The space and time intervals established by trial in this manner vary with the loading conditions and, of course, the physical properties of the membrane. A change in the initial velocity field would result in different stability data.

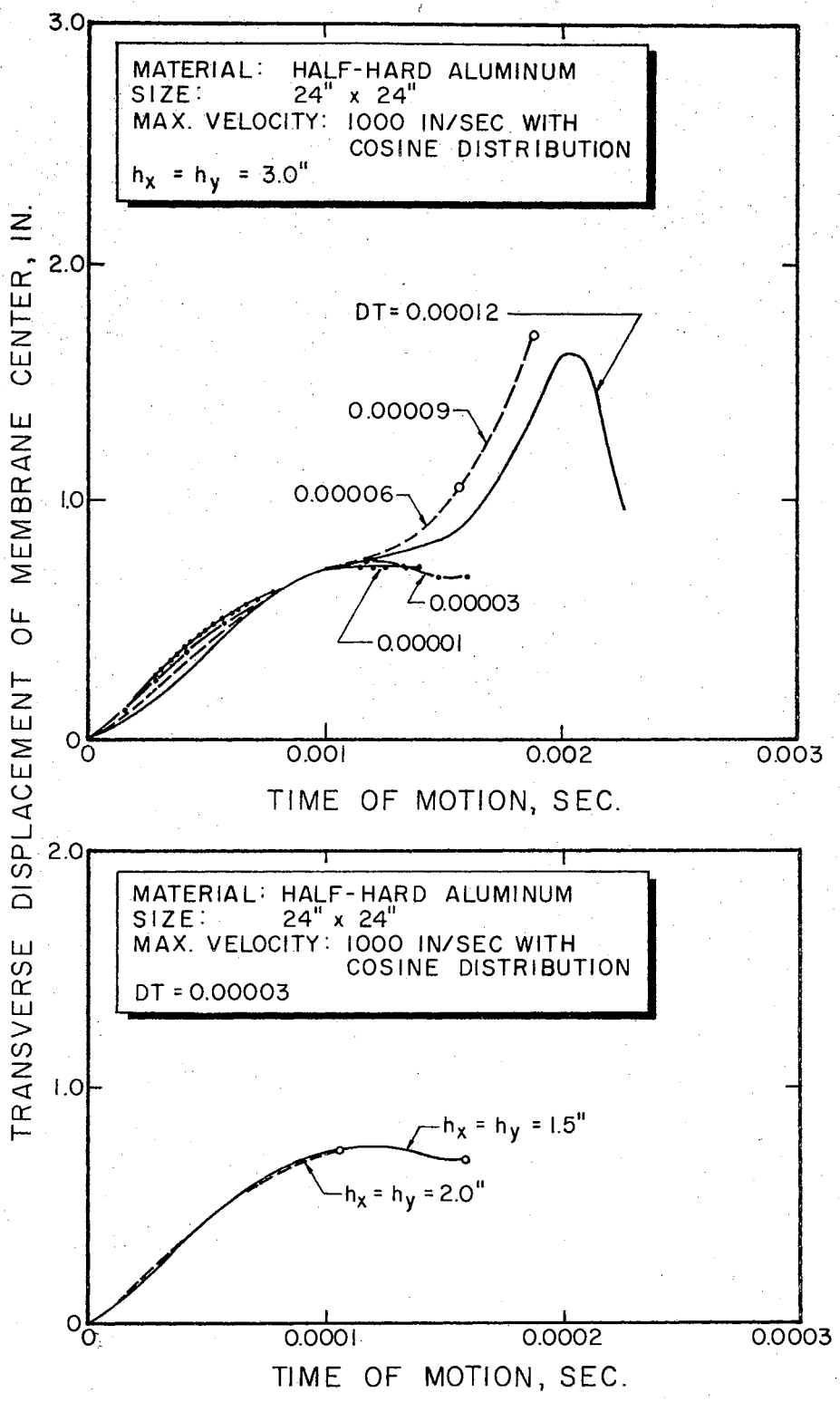

Figure 8. Dependency of Numerical Stability upon Time and Spacial Internal Magnitudes

The results in Figure 8 are still useful, however, as they often indicate possible corrective measures in other cases.

The instability which occurred during this investigation occurred primarily at the center nodal point. The other points appeared to converge in a relatively stable manner. Such behavior is indicated in Figure 9a. A comparison of this data with that given in Figure 8a indicates that a reduction in the size of the time interval might stabilize the response of the center point A. Another indication of instability is given by the results illustrated in Figure 9b. A reduction in the size of the time interval would probably also correct this response. If the reduction was made, a steadily reducing oscillatory motion about the final equilibrium position would probably result.

While desirable, such a refinement in stability cannot justify the additional computer time for most problems of application. The results without the improvement are normally very satisfactory. By interpolating using the relatively well behaved neighboring points, the final displacement of the fluctuating center point can be defined very well. In the cases of cosine distribution of initial velocity, no significant numerical instability was experienced.

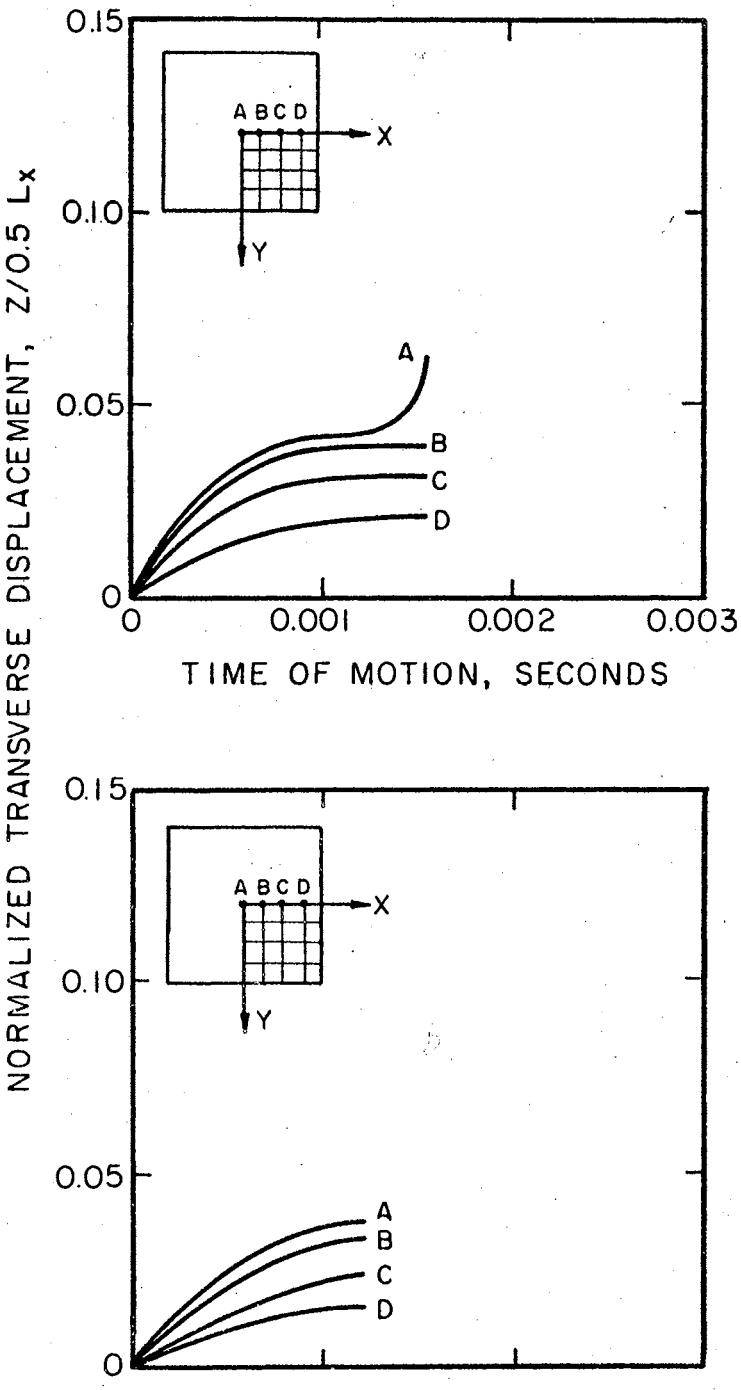

Figure 9. Evidence of Numerical Instability

3.7 Displacement Function Approximation

At the end of an increment of deformation, the points on the membrane surface for which the displacement values have been calculated are no longer beneath their initial nodal point. The continued use of the initial rectangular finite difference grid, then, requires some adjustment if the continuity of deformation is to be preserved exactly. An elaborate interpolation scheme to re-establish the values at the grid intersections could be employed. However, this degree of accuracy is inconsistent with other assumptions of this development. Certainly, the increased computing time would be undesirable. Instead, the increments will be accumulated at each intersection assuming that the displacement values at the beginning of an increment of deformation are equal to those located at the same nodal point at the end of the previous deformation increment.

CHAPTER IV

NUMERICAL RESULTS

4.1 General

The computer program block diagram is shown in Appendix I. The associated general computer program uses data cards to introduce the particular membrane's physical properties, the initial velocity field, the initial membrane configuration, and the transient pressures. The output gives the accumulated strains and displacements.

A brief parametric investigation is used in the chapter to illustrate the preceding theoretical developments. The major areas include (a) the variation of the initial velocity configuration, (b) the variation of the transient pressure profile, (c) the variation of the aspect ratio and (d) the variation of initial impulses and stress-strain relationships. In all cases, a rectangular, initially plane membrane with fixed edges is used with the general finite difference grid system shown in Figure 10.

4.2 Variation of Initial Velocity Configuration

The exact initial velocity distribution in most practical cases would be difficult if not impossible to

describe mathematically. Useful approximations, however, are the cosine and uniform configurations. These are discussed in Appendix H. Also included is the least practical but interesting pyramid shape. To determine the effects of varying the initial velocity fields, these three configurations are used to deliver an impulse of 25.92 lb-inches to a 24" square membrane. This equivalence of the velocity fields is described in Appendix H. The velocity value V_o shown in Figure 11 is 2,000 inches/second.

Figure 11 illustrates the effects of varying the velocity configurations on the terminal transverse displacement field. The displacement of the membrane surface

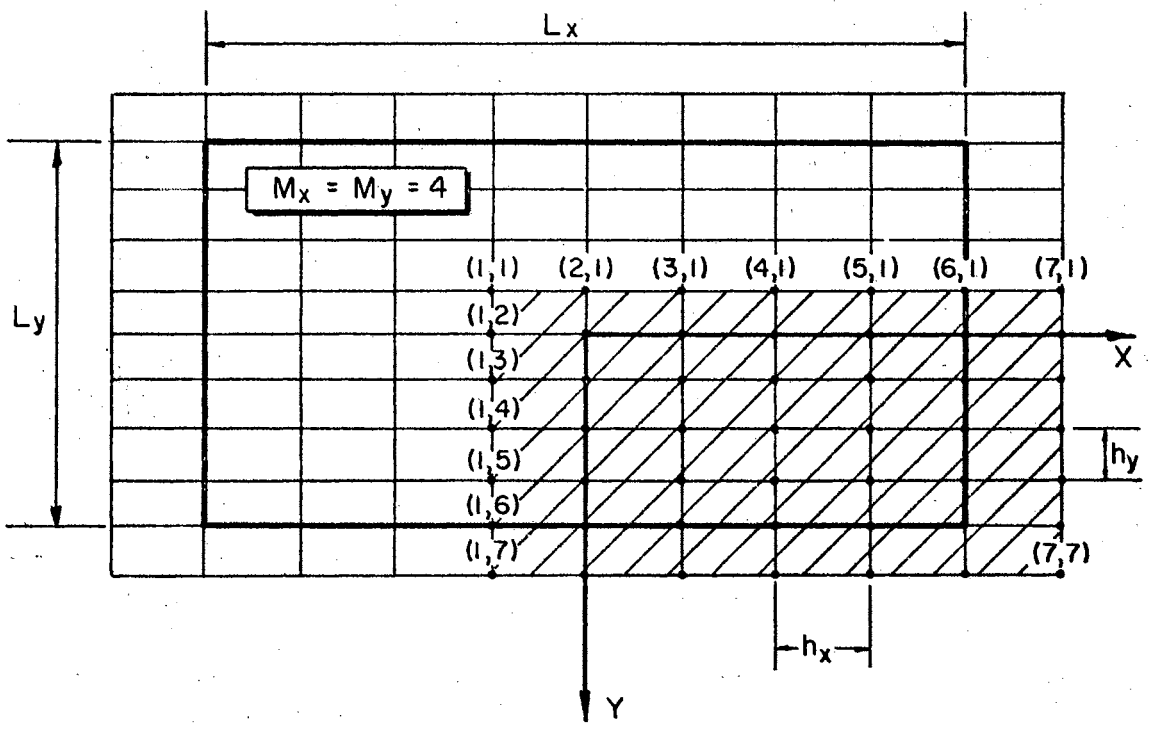

Figure 10. Representative Finite Difference Grid System

along the x-axis is also shown. The physical properties and membrane dimensions are given in the same figure.

Figure 12 shows the variation in the horizontal "U" displacement field due to the change in initial velocity fields. These values are given in the form of contour plots for the same square membrane used in Figure 11.

The effects of the same velocity variations on the transient transverse displacements are indicated in Figure 13. The displacement progress in each case is plotted at 1/10 millisecond intervals for the duration of the motion. The final configuration is also given. The data was taken from the same solutions reported in Figure 10.

A typical displacement response of a square membrane to a larger impulse is given in Figure 14. A contour plot of the transverse displacements with a profile along the x-axis is shown.

4.3 Variation of Transient Pressure

As explained in Appendix H, the initial velocity field is taken as zero if a transient pressure is applied. The distribution of such pressure is governed by equation H19 which is given below.

$$P(x,y) = P_M e^{-t/\Theta} \cos^p \left(\frac{\pi x}{L_x}\right) \cos^q \left(\frac{\pi y}{L_y}\right)$$

where

$$P_M = k\left(\frac{W^{1/3}}{R}\right)^{\emptyset}$$

$k, \emptyset$ = explosive material constants. Table H-1 gives some typical values.

W = weight in pounds of explosive material.

R_o = vertical distance of explosive material above membrane surface.

p, q = spatial shape parameters.

The distribution of the pressure at any time, t, can be varied using the spacial shape parameters p and q. Figure 15 illustrates the cases $p = q = 1$ and $p = q = 3$.

The investigation of the response to pressure variations uses a membrane with the following material properties and dimensions.

$L_x = L_y = 24$ inches

$t = 0.075$ inches

$W = 0.0214$ lbs.

$k = 2.16\ 10^4$

$\emptyset = 1.13$

For TNT from Table H-1

$a = 0.222$

$b = 0.25$

$c = 22{,}200$

For half-hard aluminum from Table D-1

The impulse is generated by an explosive charge suspended in water at a height of 168 inches above the clamped membrane.

The influence of pressure distribution on the transient transverse displacements is indicated in Figure 16. The transient displacements were plotted for the two cases given in Figure 15; p = q = 1 and p = q = 3. The delivered pressures are

$$P_z(x,y,t) = e^{-4.87x10^{-5}t} \cos\left(\frac{\pi x}{L_x}\right) \cos\left(\frac{\pi y}{L_y}\right)$$

and

$$P_z(x,y,t) = e^{-4.87x10^{-5}t} \cos^3\left(\frac{\pi x}{L_x}\right) \cos^3\left(\frac{\pi y}{L_y}\right)$$

Contour plots of the final horizontal U-displacement field for each of the pressure loading cases are given in Figure 17.

The transient transverse displacement response of a square membrane to a typical pressure loading is illustrated in Figure 18. The displacement profile along the x-axis is used. The shaded curve represents the final configuration.

4.4 Variation of the Aspect Ratio

The effects of changing from a square to a rectangular membrane configuration are indicated in Figure 19, 20, and 21. These give, respectively, the effects on the transverse Z, the horizontal U, and the horizontal V displacement fields. An initial velocity field of a cosine

TABLE 4-1

ASPECT RATIO DATA

Case	L_x(in.)	L_y(in.)	Aspect Ratio
1	24.00	24.00	1
2	16.98	33.96	1/2
3	19.60	29.40	2/3

distribution is prescribed in each case with the maximum velocity ordinate chosen so that the total delivered impulse is constant. The specific side lengths and aspect ratios are given in Table 4-1. The use of half-hard aluminum is continued.

4.5 Variation of Initial Impulse and Stress-Strain Relationships

The permanent transverse displacement response of the center node of a square membrane is plotted for several values of total impulse in Figure 22. The membrane is of half-hard aluminum and has the physical properties given in the figure.

In Figure 23 the effects of varying the stress-strain relationships are illustrated using three different materials. The latter include a 1020 hot rolled steel, a 70-30 annealed brass, and an 1100 annealed aluminum. All materials have been given a 10% initial coldworking. A 24 inch square membrane is used. As in all of the

investigations, the edges are fixed.

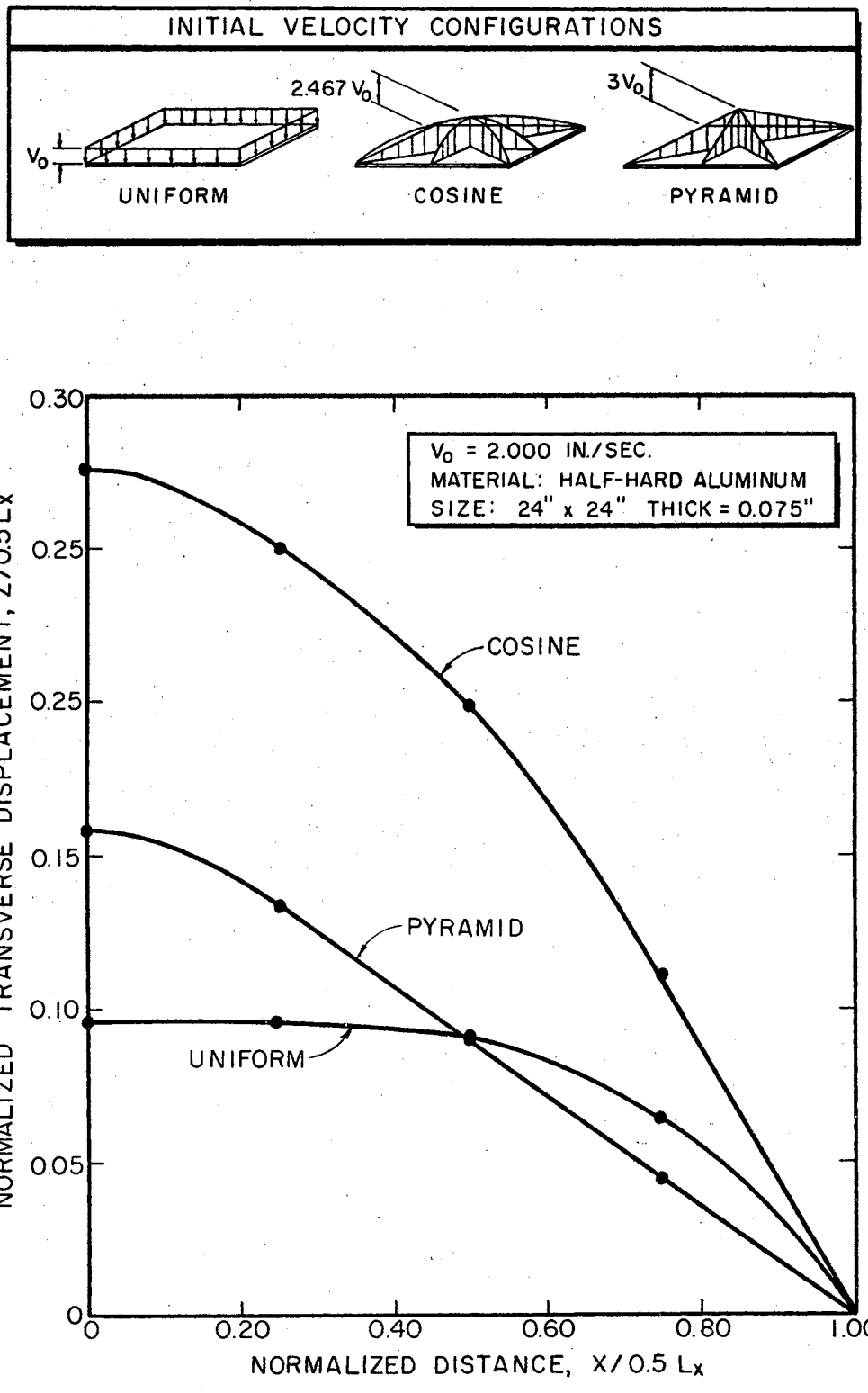

Figure 11. Variation of Terminal Transverse Displacements with Initial Velocity Configuration

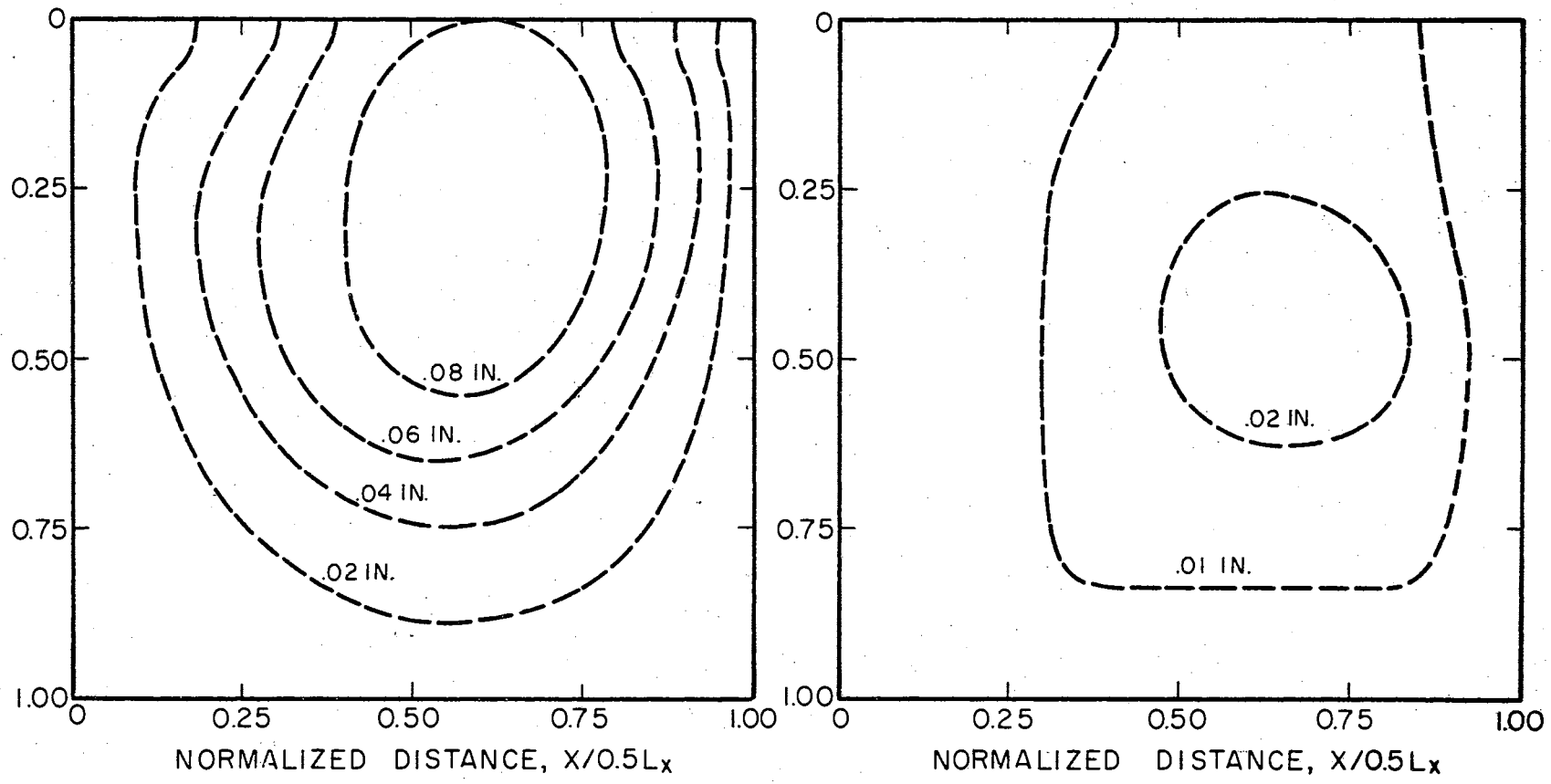

(a) COSINE DISTRIBUTION OF INITIAL VELOCITY (b) UNIFORM DISTRIBUTION OF INITIAL VELOCITY

Note: First Quadrant Only Is Shown.

Figure 12. Effect of Initial Velocity Distribution on "U" Displacement Field

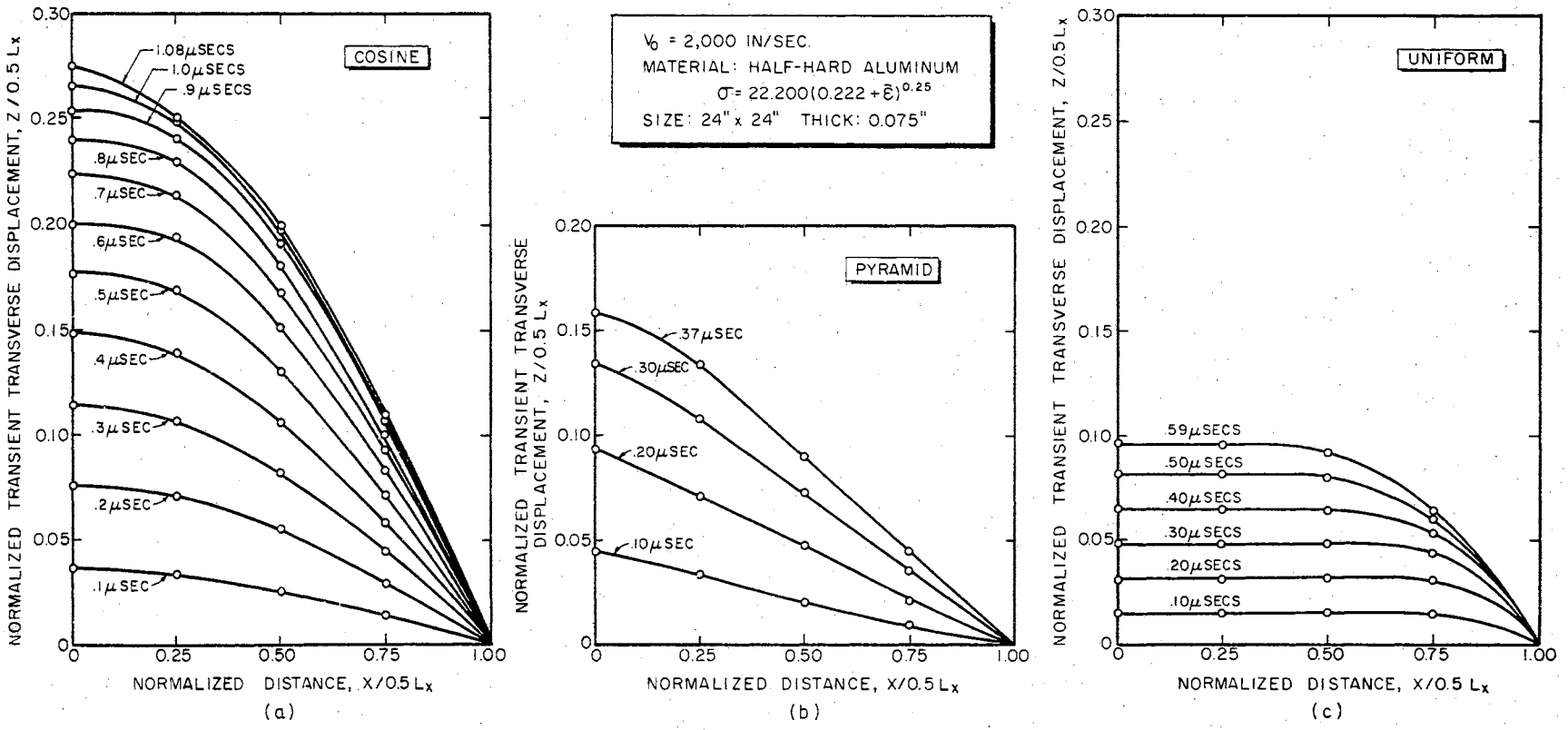

Figure 13. Variation of Transient Transverse Displacements with Initial Velocity Configuration

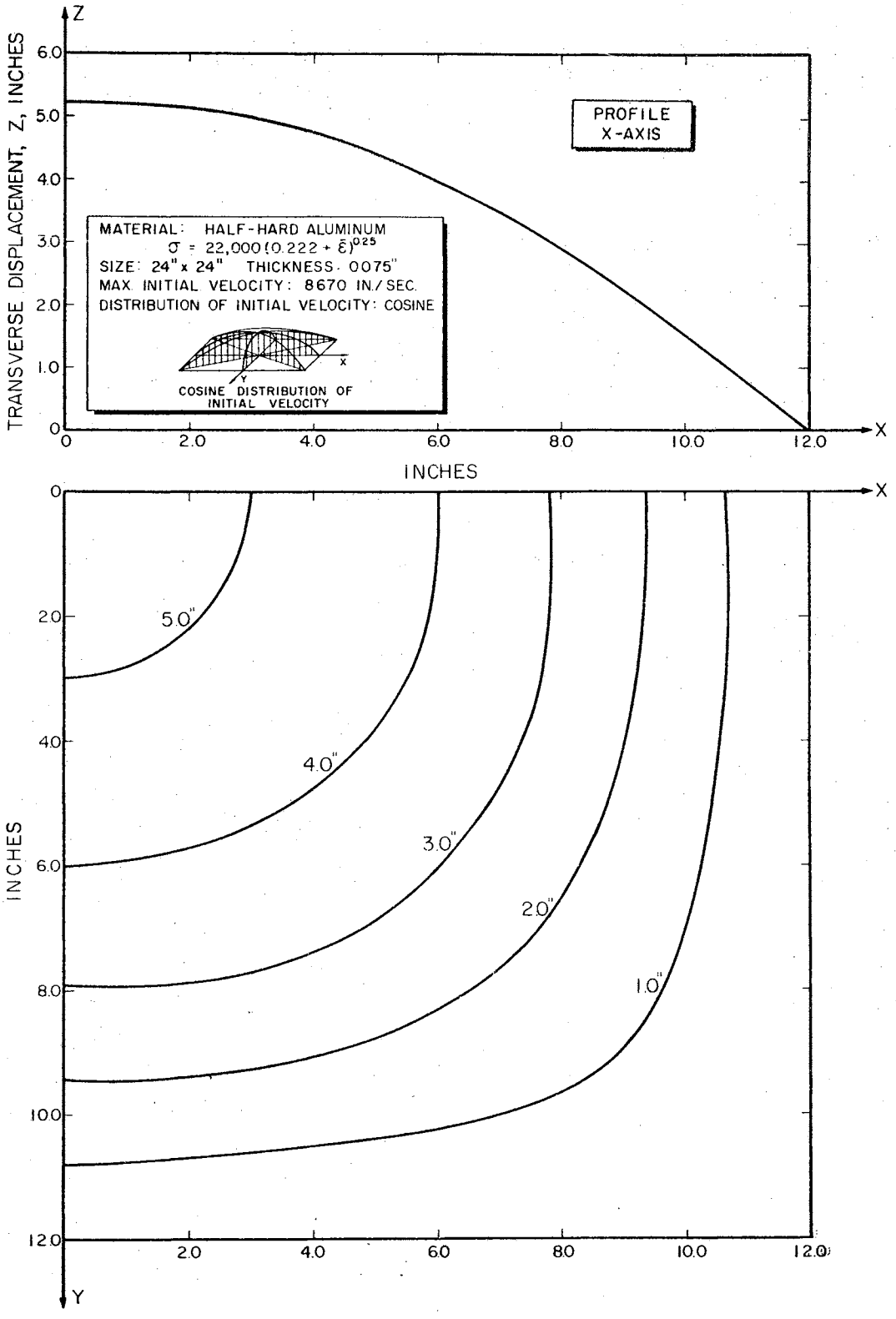

Figure 14. Terminal Transverse Displacements for Square Membrane

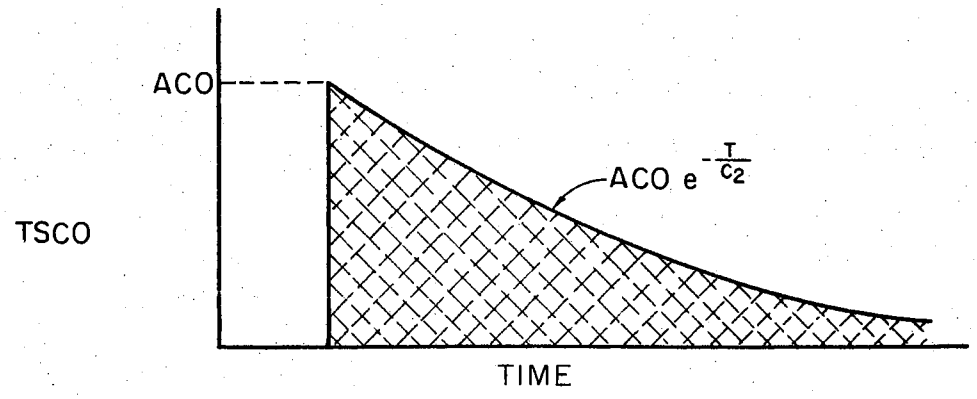

(a)

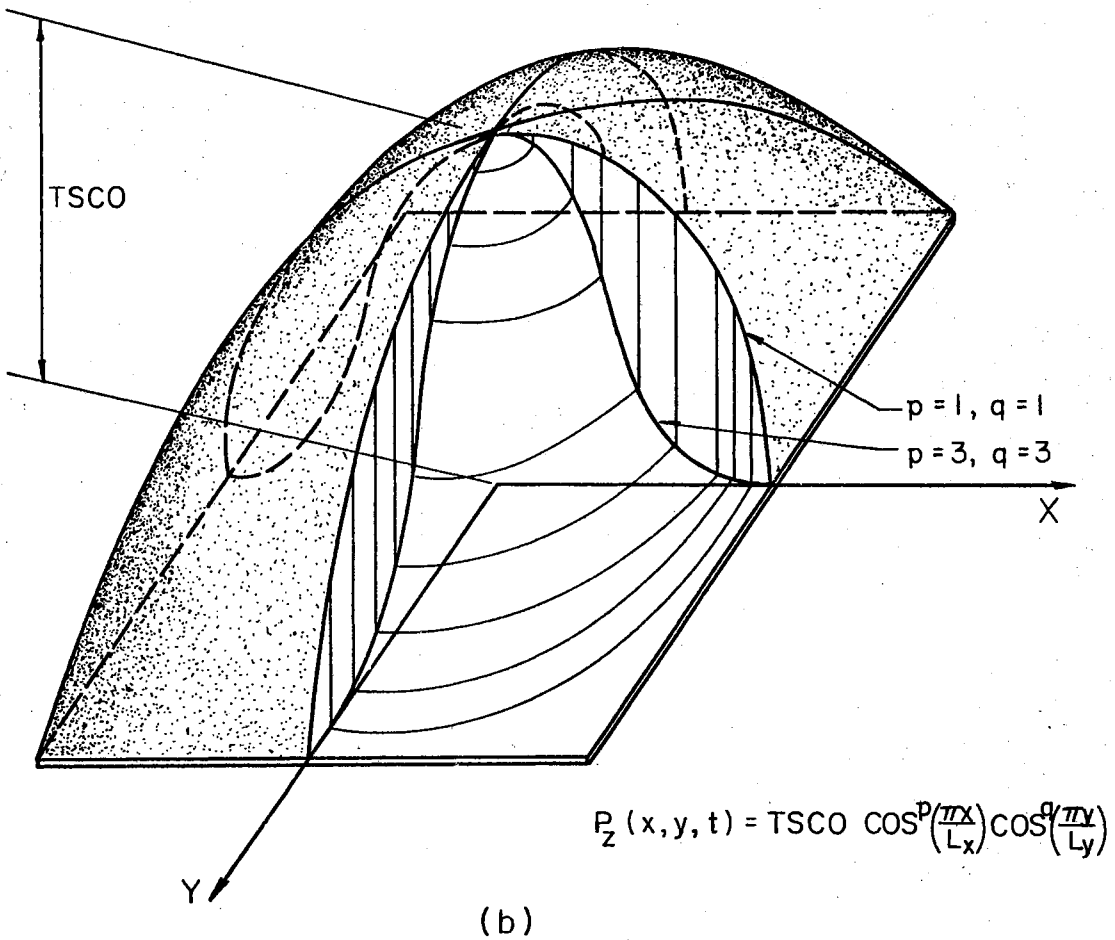

(b)

Figure 15. Transient Pressure Profile

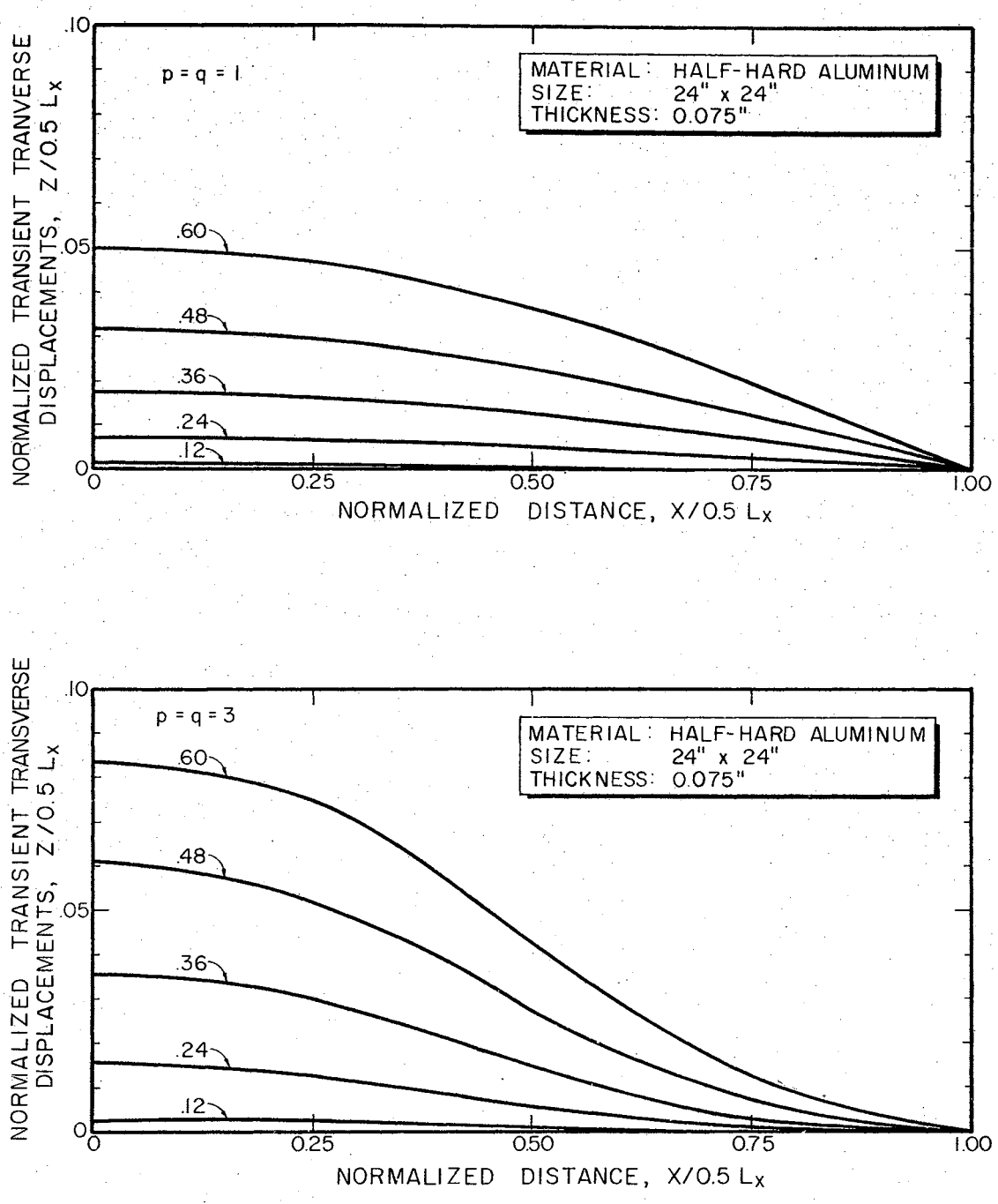

Figure 16. Effect of Pressure Distribution on Transient Transverse Displacements

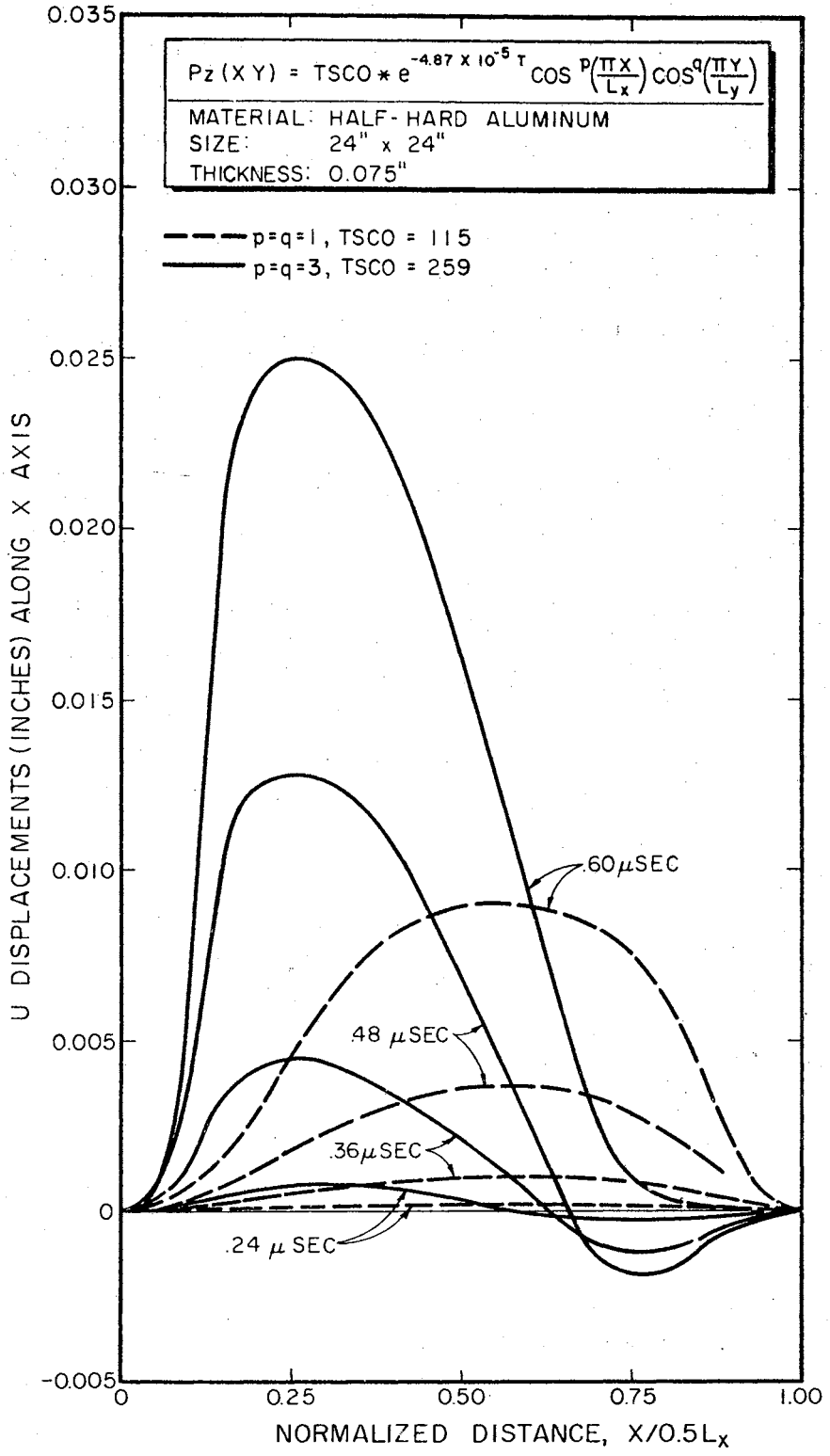

Figure 17. Effect on Pressure Distribution on U Displacement Response

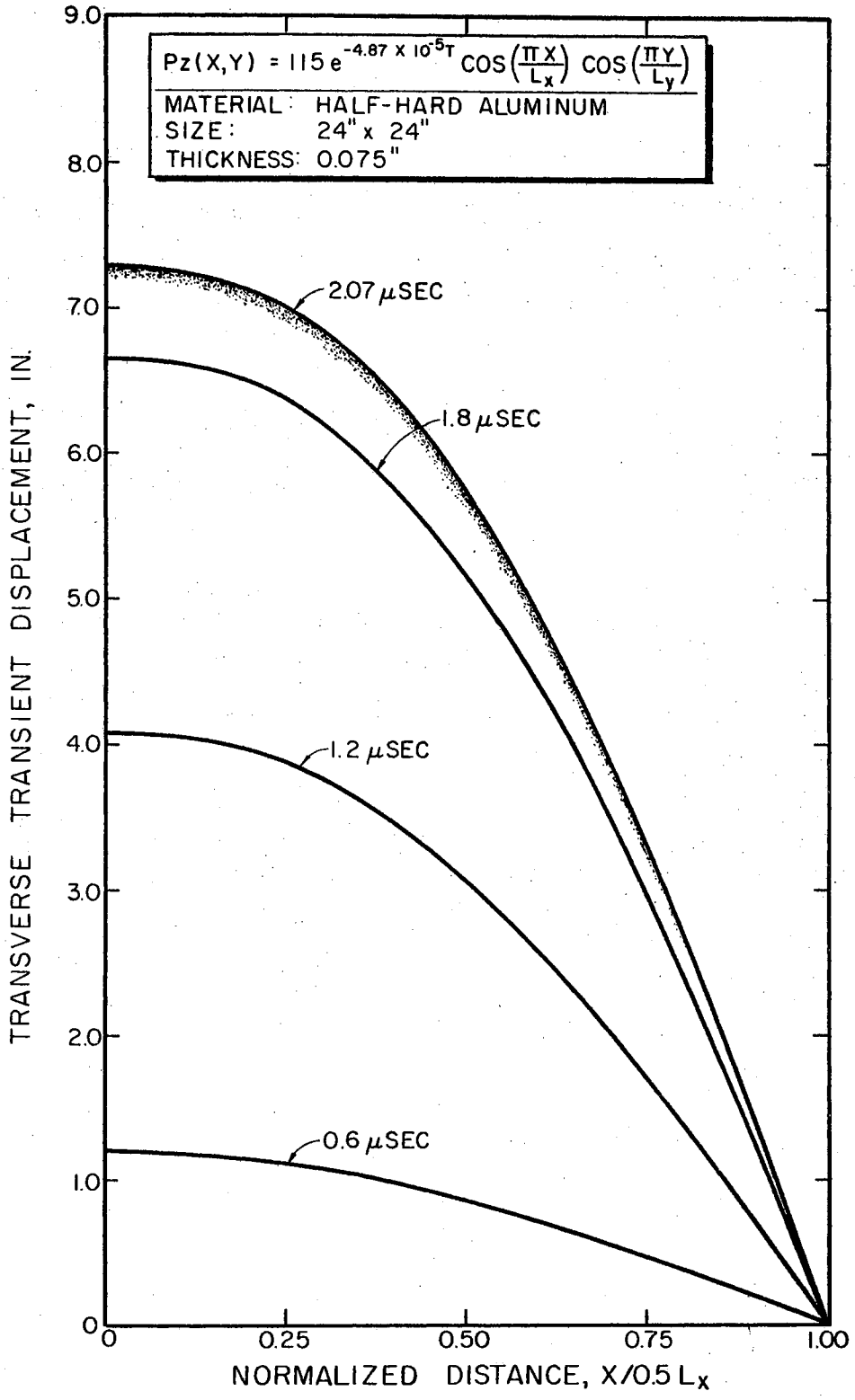

Figure 18. Typical Deformation Response of Square Membrane to Impulsive Pressure

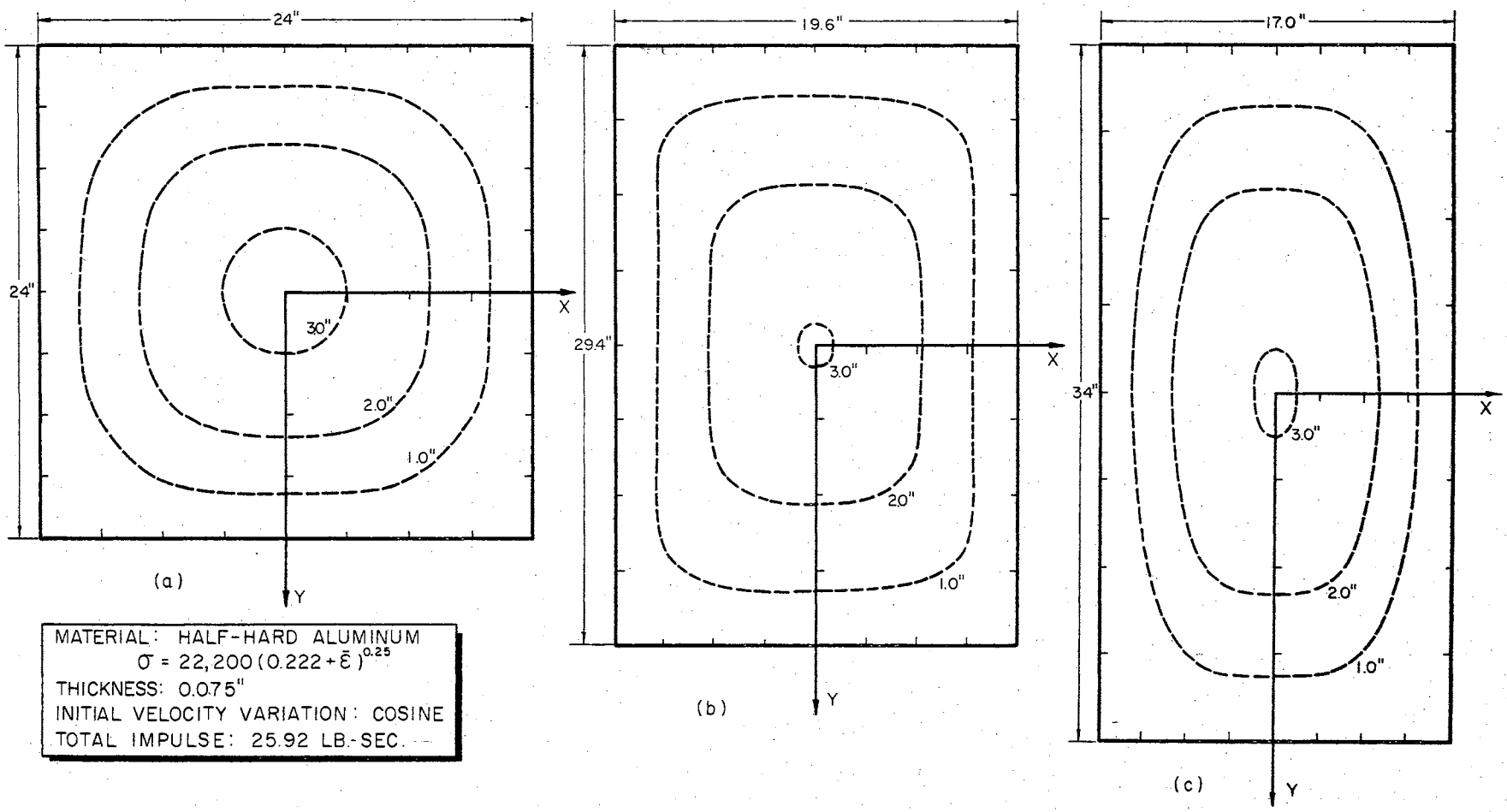

Figure 19. Effect of Aspect Ratio on the Transverse Displacement Field

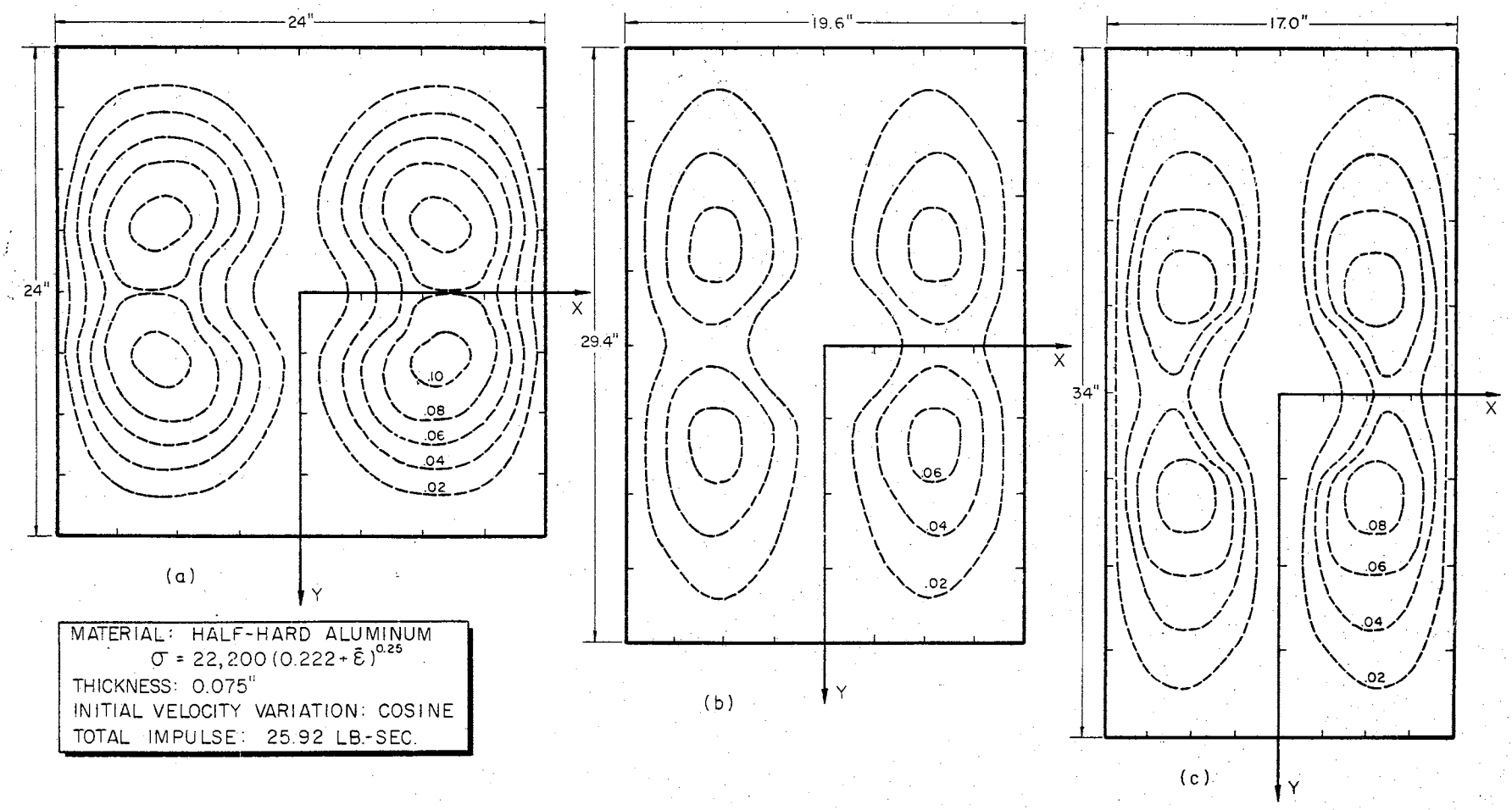

Figure 20. Effect of Aspect Ratio on the Horizontal U Displacement Field

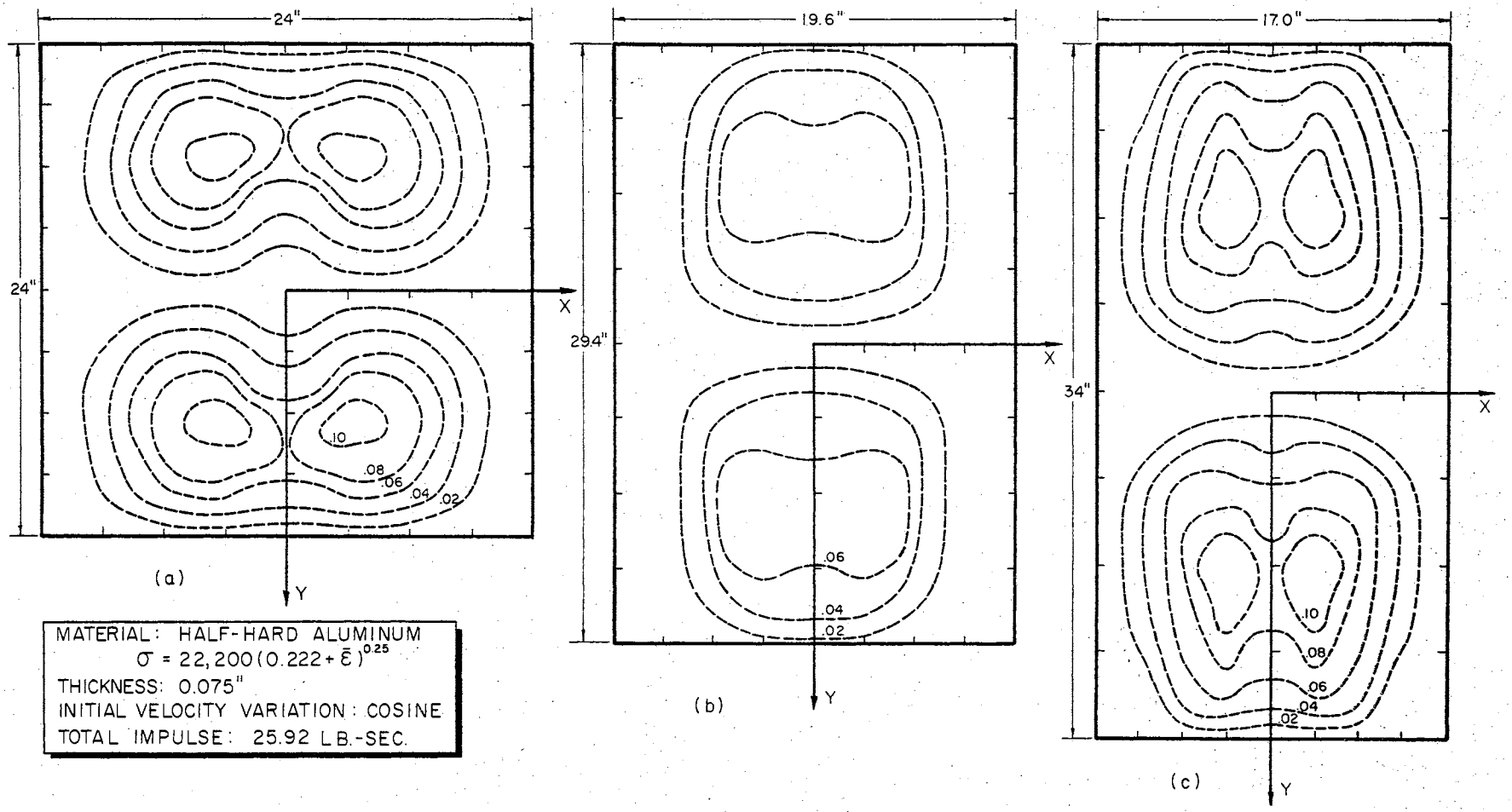

Field 21. Effect of Aspect Ratio on the Horizontal V Displacement Field

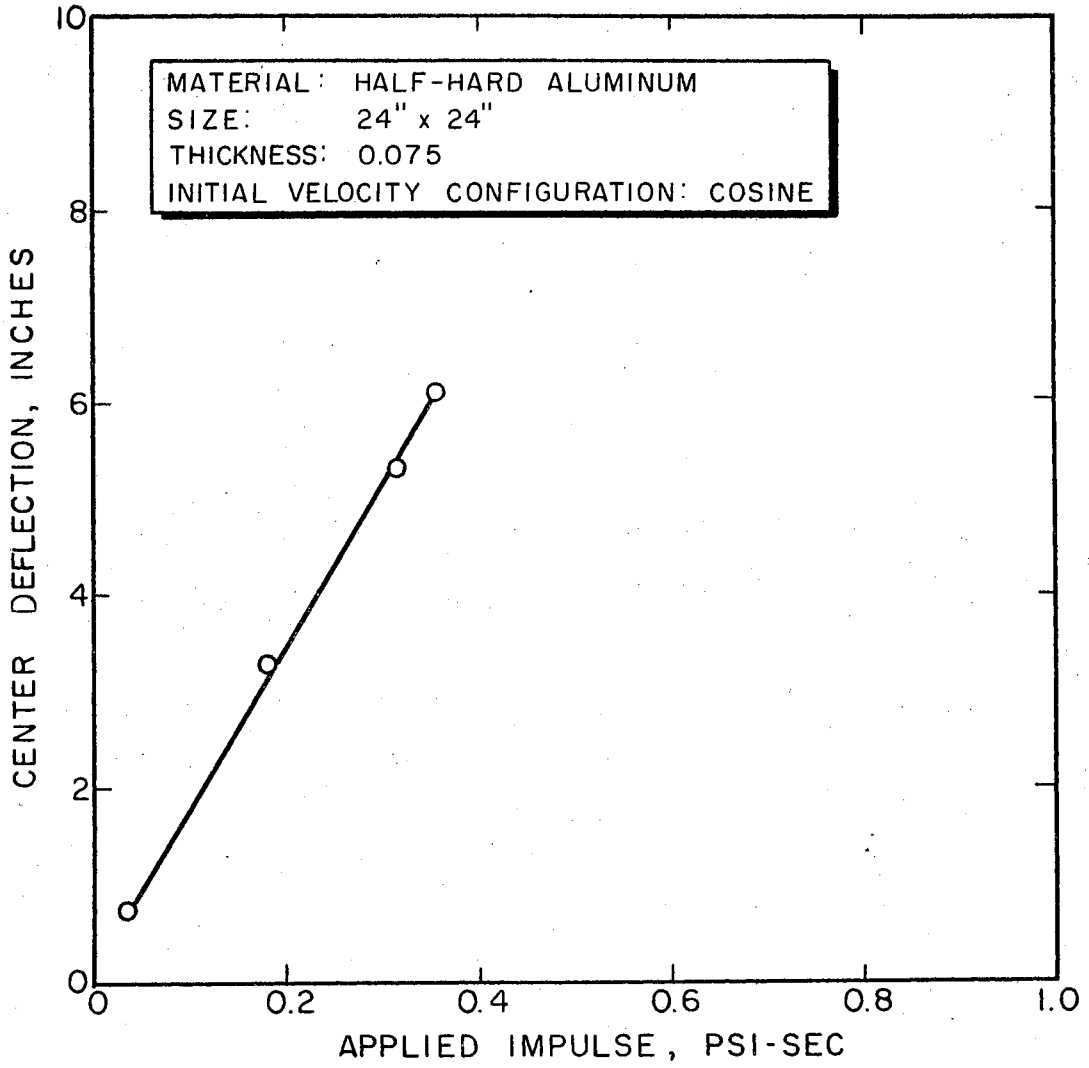

Figure 22. Variation of Permanent Center Displacement with Applied Impulse

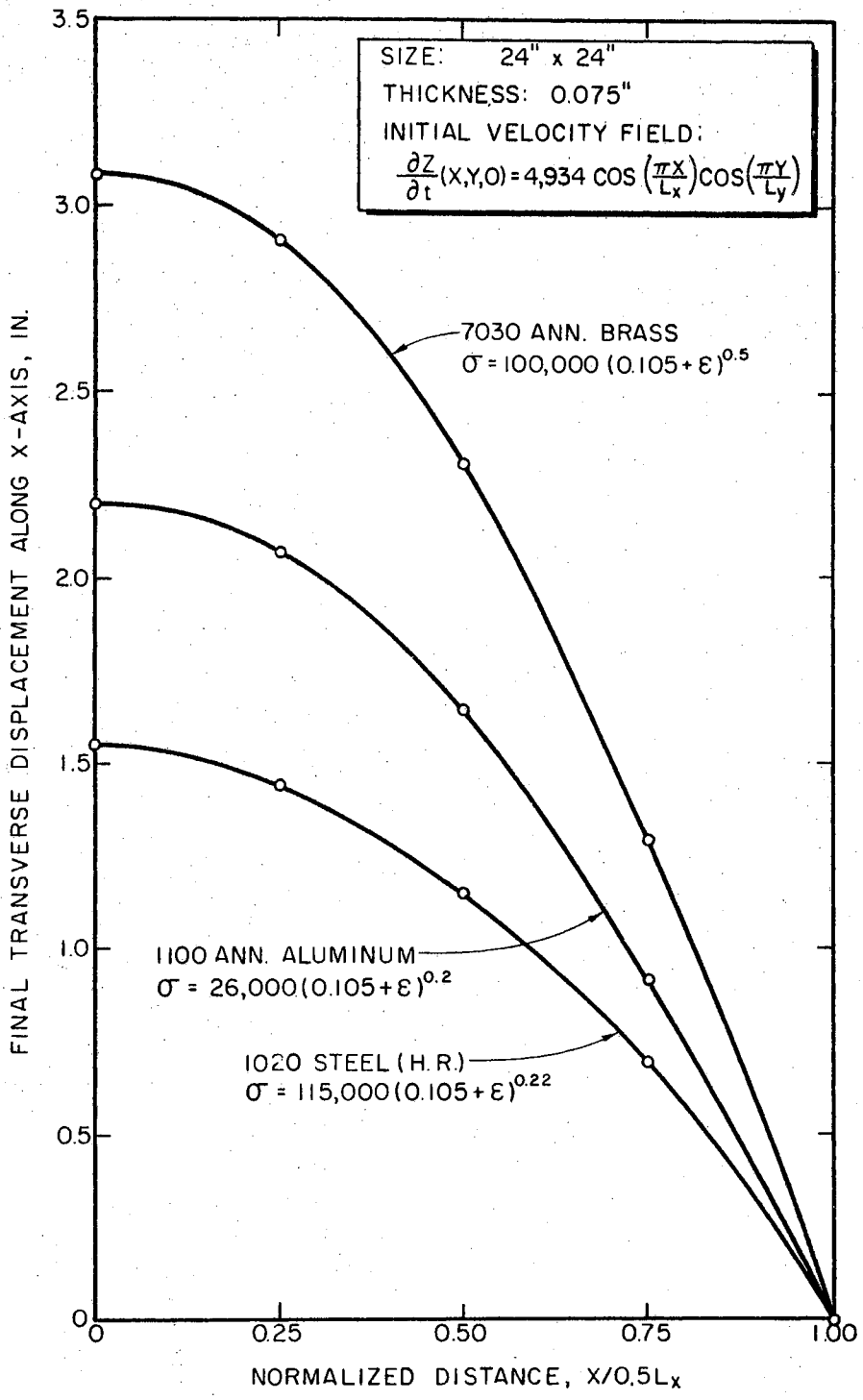

Figure 23. Influence of the Effective Stress-Strain Relationship on the Total Transverse Displacements

CHAPTER V

SUMMARY AND CONCLUSIONS

5.1 Summary

A method is developed for determining the finite, inelastic deformation of a clamped, rectangular membrane subjected to impulsive loading. An accumulation of numerous increments of deformation is assumed to represent the total deformation process. In this manner, the nonlinearity of the formulation is minimized through the use of kinematic relations for small displacement shell theory. The dynamic equilibrium of a representative differential element is mathematically formulated. The resulting three nonlinear, coupled, partial differential equations, converted to functions of displacements, form the governing differential equations of motion. The numerical solution of this set of equations is obtained using a digital computer.

The derivation is much more general than implied by the thesis title. The membrane can have initial curvature and be prestrained. The incremental formulation also permits the recording of the total deformation response to repeated blast loadings. Also, the membrane, the pressure loadings, and/or the initial velocity field do not have to

be symmetrical with respect to the horizontal axes. If such is the case, a finite difference grid system for the entire membrane surface must be used.

A limited parametric investigation is performed to illustrate the development.

5.2 Discussion of Results

An evaluation of the results is limited by the non-availability of experimental data and other numerical investigations. An objective discussion is still possible, however, through the use of comparable circular membrane studies and experimental reports on the static loading of rectangular membranes.

Figures 11 through 14 indicate the effects of varying the configuration of the initial velocity field. The terminal displacements in Figure 11 appear to be reasonable. The cosine distribution accounts for a larger quantity of initial kinetic energy within the center quarter section of the membrane. The uniform distribution places the smallest amount of kinetic energy in this center section. This comparison supports the order of displacement magnitude illustrated; i.e. cosine, pyramid and finally the uniform velocity configuration. The pyramid configuration also accounts for less transverse displacement around the perimeter of the membrane. This also is to be expected. Figure 12 shows the change in the U displacement field accompanying a revised velocity configuration. The values

and contours are reasonable. The U displacements as well as the transverse displacements are expected to be less for the uniform case because the associated initial kinetic energy, both for the center section and the membrane as a whole is the smallest. The greater rate of change in the U displacement field being along the boundary parallel to the y-axis (rather than the x-axis) is consistent with statically loaded membrane results. The transient transverse displacement responses are depicted in Figure 13. Those shown for the cosine and pyramid cases approach their final values in a smooth manner. The response to the uniform configuration, however, takes the form of a perimeter wave moving inward. The extent of its travel evidently varies directly with the magnitude of the transverse displacements. If the deformation sequence is continued, a travel distance would be encountered at which unloading would commence to follow the wave. Boyd reported a similar circumferential wave for circular membranes.

The transverse displacements shown in Figure 14 for a typical case of specified initial velocities are reasonable. The exhibited symmetry with respect to a diagonal through the origin is encouraging. The transition from circular contours at the center to those approaching a rectangular shape at the boundary is also the expected behavior.

The results of the pressure variation study are

reasonable; Figures 15, 16, 17, and 18 illustrate. The transverse displacements given in Figure 16 for the two cases, $p = q = 1$ and $p = q = 3$, show the effects of favoring the center section with delivered pressure. Greater center displacements for $p = q = 3$ case are accompanied by a loss in uniformity as displayed in the other case. Such a transition in loading patterns could be affected by varying the height above the membrane of a pressure producing device. Figure 17 describes the related effect on the U displacement field. For the $p = q = 1$ case, the U displacements uniformly increase with the greater magnitudes being at the midpoint between the origin and the boundary. In the other case, a negative displacement region exists beyond the midpoint for practically the entire first millisecond of motion. These results are very similar to Boyd's data for the circular membrane. As the latter indicated, this unusual activity is caused by the magnitude of the initial transverse displacements being much greater in the center portion of the membrane. The horizontal pull-in of the membrane's perimeter region continues until the transverse displacements start to displace uniformly.

The aspect ratio study also supports the general validity of the results. The contours plotted in Figure 19 for transverse displacements are as suggested by known rectangular plate responses (57). For a square membrane the transition of the form from the center circle to a

boundary rectangle is entirely reasonable. The increasing dominance of the rectangular over the circular form as the aspect ratio increases is acceptable. As shown, the oval contour configuration appears for $\frac{L_x}{L_y} = {}^2/_3$. The U and V displacement contours in Figures 20 and 21 are also acceptable. The equivalence of the U and V displacement fields for square membranes is clearly reflected. The steeper gradient of that portion of U displacement field located along the perimeter and parallel to the y axis is consistent with experimental results give given by Mostow (13). The magnitudes of the horizontal displacements seem to be reasonably consistent with the related transverse displacement field.

Finally, a linear relationship between the center transverse displacement of a square membrane and the total applied impulse is depicted in Figure 22. It appears to be consistent with comparable circular membrane data by Boyd.

5.3 General Conclusion and Possible Extensions

The numerical results support the general validity of the method as a means of analytically investigating the response of clamped rectangular membranes to impulsive loads. A detailed evaluation and confirmation of the method's accuracy is not presently possible. Other analytical or some experimental results are needed. At the present, however, it is believed that this is the first

and only general solution of the subject dynamic membrane problem.

The only significant deficiency of the method appears to be scattered instances of numerical instability. These principally occurred when discontinuous functions were used to represent initial velocity fields.

Any extension of this work should first include a numerical stability investigation. The stability investigation on an individual problem basis is recommended only as an interim measure. A satisfactory general method of prescribing the optimum space and time intervals would not only reduce the amount of required computer time but would also allow the use of a greater variation in velocity field configurations.

An adjustment to the present development to accomodate membrane surfaces of other planforms is also possible. The Flügge and Geyling small deformation theory has already been applied to translational shell surfaces with other planform configurations such as those triangular and trapezoidal in shape (29), (37). These works could be extended to the dynamic problems as indicated in this dissertation.

In the design of many armaments, mass is used to dissipate high quantities of kinetic energy. In other cases, thick plates of high tensile strength metals are used with strain energy accounting for the change in kinetic energy. The results of this dissertation suggest the possible

advantage of using a baffle arrangement of thin membranes in preference to the thick plates or objects of great mass. The idea is based upon more efficiently producing strain energy to dissipate the kinetic energy.

Also, the degeneration of the governing differential equations to those for the general case of static loadings is recommended. A satisfactory solution for the static finite deformation of membranes of rigidly plastic-strain hardening or elastic-plastic materials is not known to exist. Such a conversion would involve solving all three equations using the matrix iteration scheme presently used for the U and V displacement equations.

Finally, an experimental investigation is needed to complete the evaluation of this development.

BIBLIOGRAPHY

SELECTED BIBLIOGRAPHY

(1) Boyd, D. E., "Dynamic Deformations of Circular Membranes," ASCE, EMD, Vol. 92, June 1966.

(2) Cole, R. H., Underwater Explosions, Princeton University Press, Princeton, New Jersey, 1958.

(3) Chubbuck, E. R., "Large Deformations of Thin Shells of Revolution by Internal-Pressure Loading," Proc. of 1st Southwestern Conf. on Theoretical & Applied Mech., Vol. 1, 1962.

(4) Day, J. W., "Hydrostatic Pressure Tests on Thin Rectangular Diaphragms 21" x 13½", David Taylor Model Basin Report 635, March 1951.

(5) Flügge and Geyling, "A General Theory of Deformations of Membrane Shells," Int. Cong. of Appl. Mech., 1956, Proc., Vol. 6, p. 250.

(6) Flügge, W. and F. T. Geyling, "A General Theory of Deformations of Membrane Shells," Vol. 17, 1957, pp. 23-46, Memoiries, Int. Assoc. for Bridge and Structural Engr.

(7) Frederick, D., "A Simplified Analysis of Circular Membranes Subjected to an Impulsive Loading Producing Large Plastic Deformation," Proc. of 4th Midwestern Cong. on Solid Mech., p. 18, Austin, Texas, 1959.

(8) Gleyzal, A., "Plastic Deformation of a Circular Diaphragm under Pressure," ASME Vol. 70, pp. 288-296, 1948.

(9) Hill, R., The Mathematical Theory of Plasticity, Oxford University Press, London, 1964.

(10) Hill, R., "A Theory of the Plastic Bulging of a Metal Diaphragm by Lateral Pressure," Phil. Mag. Vol. 41, 7th Series, pp. 1137-1142, November 1950.

(11) Hudson, G. E., "Theory of the Dynamic Plastic Deformation of a Thin Diaphragm," Journal of Applied Physics, Vol. 22, No. 1, p. 1, 1955.

(12) Hwang, Chintsuh, "Incremental Stress-Strain Law Applied to Work Hardening Plastic Materials," Trans. ASME, 81, 594, 1959.

(13) Kachanow, Beliaev, Ilyushin, Mostow, and Gleyzal, Plastic Deformation Principles and Theories, Mapleton House Publishers, New York, 1948.

(14) Levy, S., "Square Plate with Clamped Edges Under Normal Pressure Producing Large Deformations," NASA Report #740, 1942.

(15) Levy, S., "Bending of Rectangular Plates with Large Deformations," NASA Report #737, 1942.

(16) Oden, J. T. and T. Sato, "Finite Strains and Displacements of Elastic Membranes by the Finite Element Method," (to be published).

(17) Pope, G. G., "A Discrete Element Method for the Analysis of Plane Elasto-Plastic Stress Problems," The Aeron. Quart., February 1966.

(18) Perrone and Hodge, Jr., "Strain-Hardening Solutions to Plate Problems," Trans. ASME 81, p. 276, 1959.

(19) Prager, W., "On the Use of Singular Yield Conditions and Associated Flow Rules," J. of Appl. Mech., Trans. ASME, Vol. 75, 1953, pp. 317-320.

(20) Reissner, Eric, "On Some Aspects of the Theory of Thin Elastic Shells," Jour. of Boston Society of C.E., Vol. 42, April 1955, pp. 100-133.

(21) Salmon, M. A., "Large Plastic Deformation of Pressurized Cylinders," ASCE, EMD, Vol. 92, June 1966.

(22) Salvadori and Baron, Numerical Methods in Engineering, Prentice-Hall, Inc., Englewood Cliffs, N.J., 1961.

(23) Timoshenko, S., Vibration Problems in Engineering, D. Van Nostran Co., Inc., New York, 1955.

(24) Wang, A. J., "Permanent Deflection of a Plastic Plate Under Blast Loading," J. Appl. Mech. 22, pp. 375-376, 1955.

(25) Way, S., "Uniformly Loaded, Clamped Rectangular Plates with Large Deflections," Proc. 5th Int. Cong. Appl. Mech., 1938, pp. 123-128.

(26) Witmer, Herrmann, Lerch, and Pian, "Responses of Plates and Shells to Intense External Load of Short Duration," W.P. Air Devel. Div. TR 60.433 Ap 1960.

(27) Witmer, Balmer, Leech, and Pian, "Large Dynamic Deformations of Beams, Rings, Plates, and Shells," AIAA Journal, Vol. 1, No. 8, p. 1848, 1963.

GENERAL BIBLIOGRAPHY

(28) Boyce, W. E. and W. Prager, "On Rigid Work-Hardening Solids with Singular Yield Conditions," J. Mech. Phys. Solids, Vol. 6, 1957, No. 1, pp. 9-12.

(29) Crandall, S. H., Engineering Analysis, McGraw-Hill Book Company, 1956.

(30) Csonka, P., "Specially Shaped Membrane Shells on a Base Comprising an Equilateral Triangle," Acta. Tech. Acad. Sci. Hungaricae, Budapest 39, 1/2, p. 187, 1962.

(31) Davis, H. E. and E. R. Parker, "Behavior of Steel Under Biaxial Stress as Determined by Tests in Tubes," J. Appl. Mech., 15, 201 (1948).

(32) Drucker, D. C., "On the Coincidence of Plasticity Solutions Obtained with Incremental and Deformation Theories," Proc., 1st U. S. Natl. Cong. for Appl. Mech., 1951.

(33) Drucker, D. C., "Some Implication of Work Hardening and Ideal Plasticity," Q. Appl. Math. 7, pp. 411-418, 1949.

(34) Drucker, D. C., "Variational Principles in the Mathematical Theory of Plasticity," Proc., Symp. Appl. Math., Vol. 8, Calculus of Variations and Its Applications, 1958, pp. 7-22.

(35) Flügge, W., Stresses in Shells, Springer-Verlag, Berlin, 1962.

(36) Föppl, A. L., Drang und Zwang, p. 226, R. Oldenbourg, Munich, Germany, 1924.

(37) Foti, C., "The Static State and Deformations of an Elliptic Paraboloid over a Trapezoidal Base," G. Genio Civile 103,3, p. 95, March 1965.

(38) Handelman, Lin, and Prager, "On the Mechanical Behavior of Metals in the Strain Hardening Range," Q. Appl. Math., Vol. 4, pp. 397-407, 1947.

(39) Handelman, G. H. and W. M. Warner, "Loading Paths and the Incremental Strain Law," J. Math. Phys., Vol. 33, 1954, No. 2.

(40) Head, R. M. and E. E. Sechler, Normal Pressure Tests on Unstiffened Flat Plates, N.A.C.A. T.N. No. 943, September 1944.

(41) Hencky, H., "Die Berechnung Dunner Rechteckiger Platten Mit Verschwindender Biegungsteifigkeit," ZAMM, p. 8, April 1921.

(42) Henriksen, E. K., I. Lieberman, J. F. Wilkin, and W. B. McPherson, "Metallurgical Effects of Explosive Straining," ASTM Special Technical Publication No. 336, 1962.

(43) Hodge, P. G., Jr., "Piecewise Linear Plasticity," IX Congress International de Mecanique Appliquee, 1957, pp. 65-72.

(44) Lubalin and Felgar, Plasticity and Creep of Materials, John Wiley & Sons, Inc., New York, 1962.

(45) Morley, L. S. D., Skew Plates and Structures, Int. Series of Monographs in Aeronautics and Astronautics, MacMillian Co., New York, 1963.

(46) Neubert, M. and A. Sommer, "Rectangular Shell Plating Under Uniformly Distributed Hydrostatic Pressure," N.A.C.A. T.M. No. 965, December 1940.

(47) Nowinski, J., "Note on an Analysis of Large Deflections of Rectangular Plates," Appl. Sci. Res., Sec. A, The Hague 11, 1962, 85-96, AMR 16, 1409.

(48) Olszak, W., Z. Mroz, and P. Perzyna, Recent Trends in the Development of the Theory of Plasticity, MacMillan Co., New York, 1963.

(49) Phillips, A., Plasticity, Ronald Press Company, New York, 1956.

(50) Prager, W., "A New Method of Analyzing Stresses and Strains in Work-Hardening Plastic Solids," Jour. of Appl. Mech., Vol. 23, Trans. ASME, Vol. 78, 1956, pp. 413-96.

(51) Prager, W., "Theory of Plastic Flow Versus Theory of Plastic Deformation," J. of Appl. Phy., Vol. 19,

1948, pp. 540-543.

(52) Prager, W. and P. G. Hodge, Theory of Perfectly Plastic Solids, John Wiley & Sons, Inc., New York, 1963.

(53) Prager, W., "Recent Developments in the Mathematical Theory of Plasticity," J. Appl. Physics, 20, pp. 235-241, 1949.

(54) Rinehart, Behavior of Metals Under Impulsive Loads, Dover Publications, Inc., New York, 1965.

(55) Shizud, Ban, "Formandernng Der Differential Gleichung Der Formanderung," Vol. 13, 1953, pp. 1-16, Memoiries, Int. Assoc. for Bridge and Structural Engineers.

(56) Sokolvsky, W. W., "The Theory of Plasticity - An Outline of the Work in Russia," J. Appl. Mech., Vol. 13, No. 1, pp. A1-A10, 1946.

(57) Timoshenko, S., Theory of Plates and Shells, McGraw-Hill Book Co., Inc., New York and London, 1940.

(58) Wah, T., "Large Deflection Theory of Elasto-Plastic Plates," ASCE, Proc., Vol. 84, EM4, October 1958.

(59) Weil, N. A. and N. M. Newmark, "Large Plastic Deformations of Circular Membranes," ASME, December 1965, Jour. of Appl. Mech.

(60) White, G. N. and D. C. Drucker, "Effective Stress and Effective Strain in Relation to Stress Theories of Plasticity," J. Appl. Phys., Vol. 21, Oct. 1950, pp. 1013-1021.

(61) Young, K. C. and R. C. Binker, "Response of Models to Water-Shock Loading," ASCE Mech. Div., Vol. 91, December, 1965, pp. 67-89.

APPENDIX A

PUCHER STRESS THEORY

The Pucher solution of the shell membrane stress problem greatly simplifies the general equilibrium equations of the membrane theory by stating them in terms of equivalent projected stress resultants acting on a hypothetical projected element in the horizontal plane. Such a projection of the differential element is illustrated in Figure A-1. The curved line segments are related to the projected horizontal sides by

$$ds_1 = \frac{dx}{\cos \alpha}$$

$$ds_2 = \frac{dy}{\cos \beta} \qquad \text{A1}$$

The total forces on the sides of the curved element are found by multiplying the pertinent skew stress resultants, shown in Figure A-2, by the length of the related curved line segment. These forces are inclined at an angle of either α or β with the horizontal plane. The components in the horizontal plane in the x direction form the equivalence

$$N_x \frac{dy}{\cos \beta} \cos \alpha = \bar{N}_x dy \qquad \text{A2}$$

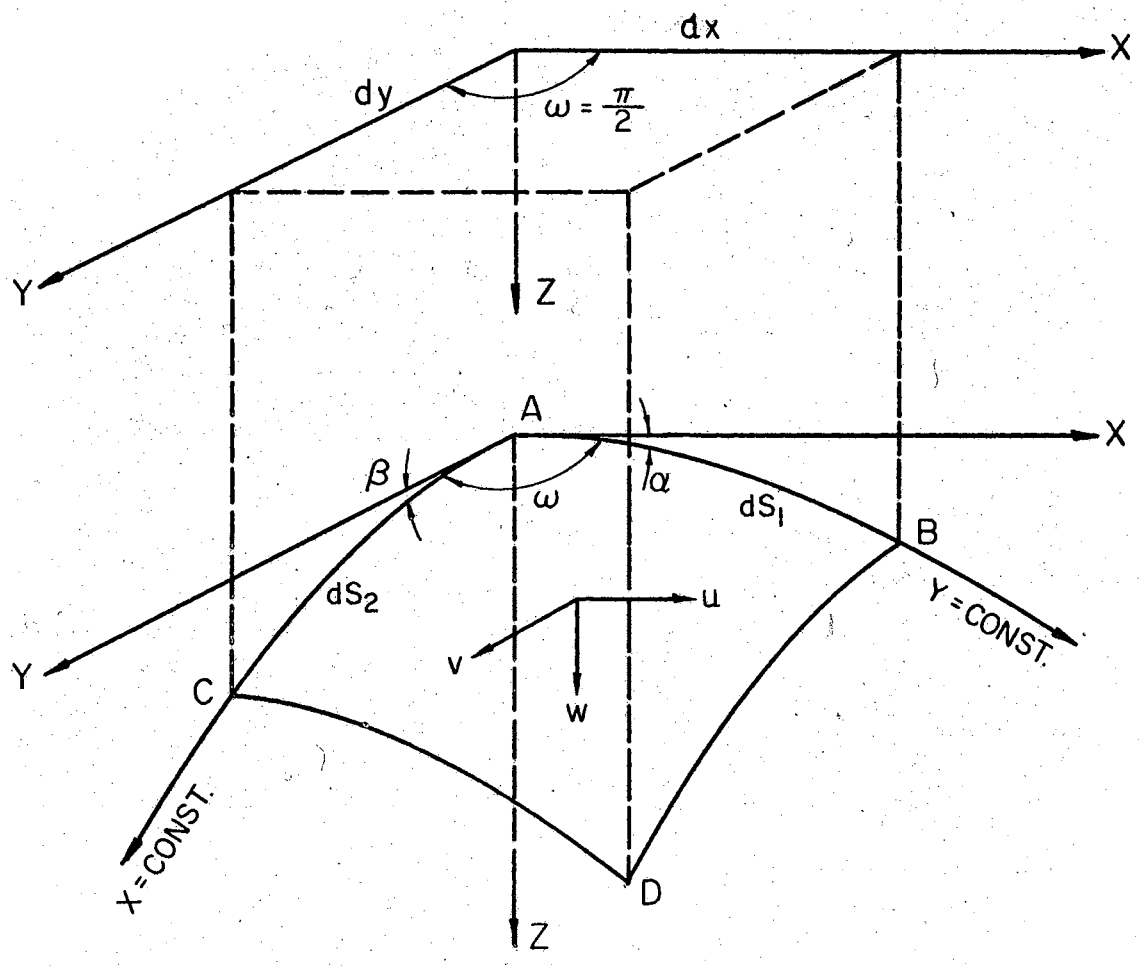

Figure A-1. Projection of Element of Double Curvature

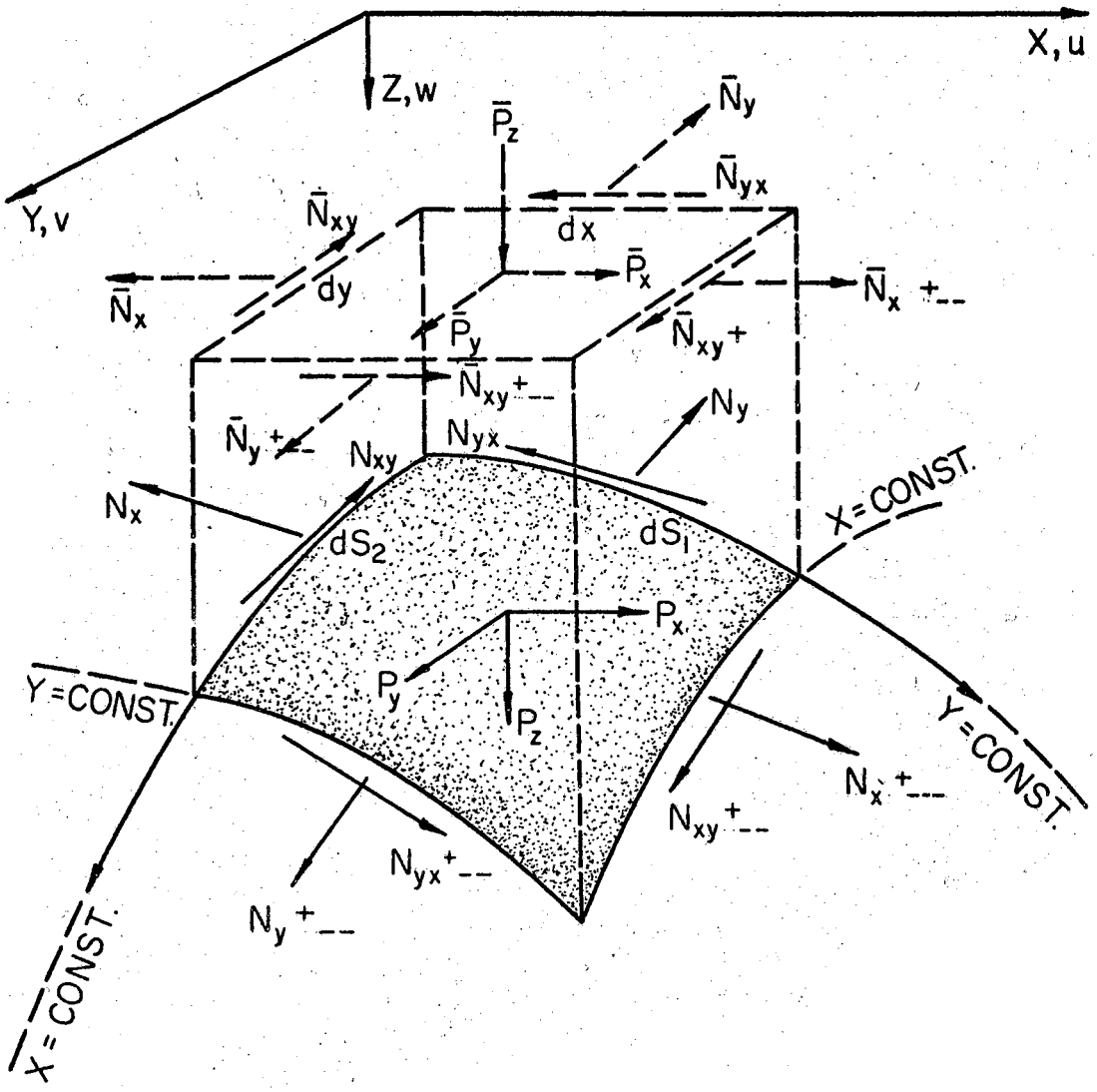

Figure A-2. State of Static Equilibrium

$$N_{yx} \frac{dx}{\cos \alpha} \cos \alpha = \overline{N}_{yx} dx \qquad A3$$

while those in the y direction

$$N_y \frac{dx}{\cos \alpha} \cos \beta = \overline{N}_y dx \qquad A4$$

$$N_{xy} \frac{dy}{\cos \beta} \cos \beta = \overline{N}_{xy} dy \qquad A5$$

Thus, the following equalities are obtained

$$\overline{N}_x = N_x \frac{\cos \alpha}{\cos \beta} \qquad A6a$$

$$\overline{N}_{xy} = \overline{N}_{yx} = N_{xy} = N_{yx} \qquad A6b$$

$$\overline{N}_y = N_y \frac{\cos \beta}{\cos \alpha} \qquad A6c$$

P_x, P_y, P_z are the x, y, and z components, respectively of the exterior load per unit shell area. These distributed external loads are now replaced by their equivalents acting over the horizontal projected area, dxdy. Considering P_x,

$$P_x dA = \overline{P}_x dxdy = \overline{P}_x dA_z \qquad A7$$

Where

dA_z = horizontal projection of shell differential element

dA = area of shell element

$\overline{P}_x$ = component of P_x which acts on the projected area dA_z,

and

$$\frac{\overline{P}_x}{P_x} = \frac{dA}{dA_z} \tag{A8}$$

it can be shown that

$$\frac{\overline{P}_x}{P_x} = \frac{(1 - \sin^2 \alpha \sin^2 \beta)^{\frac{1}{2}}}{\cos \alpha \cos \beta} \tag{A9}$$

In general, then, the following relation exists between $\overline{P}_x$, $\overline{P}_y$, $\overline{P}_z$ and the forces P_x, P_y, P_z, per unit area of the differential shell element.

$$\frac{\overline{P}_x}{P_x} = \frac{\overline{P}_y}{P_y} = \frac{\overline{P}_z}{P_z} \frac{(1 - \sin^2 \alpha \sin^2 \beta)^{\frac{1}{2}}}{\cos \alpha \cos \beta} \tag{A10}$$

Two of the equilibrium equations are formed by directly considering the summation of forces acting on the projected element and in the x and y directions.

Considering the x direction, the following is derived.

$$-\overline{N}_x dy + (\overline{N}_x + \frac{\partial \overline{N}_x}{\partial x} dx)dy - \overline{N}_{yx} dx + (\overline{N}_{yx} + \frac{\partial \overline{N}_{yx}}{\partial y} dy)dx + \overline{P}_x dxdy = 0$$

$$\frac{\partial \overline{N}_x}{\partial x} + \frac{\partial \overline{N}_{yx}}{\partial y} + \overline{P}_x = 0 \tag{A11}$$

Similarly, using the y direction

$$-\bar{N}_y dx + (\bar{N}_y + \frac{\partial}{\partial y}\bar{N}_y dy)dx - \bar{N}_{xy}dy +$$

$$+ (\bar{N}_{xy} + \frac{\partial}{\partial x}\bar{N}_{xy}dx)dy + \bar{P}_y dxdy = 0$$

$$\frac{\partial}{\partial y}\bar{N}_y + \frac{\partial}{\partial x}\bar{N}_{xy} + \bar{P}_y = 0 \qquad \text{A12}$$

For the third equation, equilibrium in the z direction is considered. Noting that,

$$N_x \sin\alpha\, dq = \bar{N}_x \frac{\cos\beta}{\cos\alpha} \sin\alpha\, dq$$

$$= \bar{N}_x \tan\alpha \cos\beta\, dq$$

$$= \bar{N}_x \frac{\partial z}{\partial x} dy \qquad \text{A13a}$$

$$N_y \sin\beta\, dp = \bar{N}_y \frac{\partial z}{\partial y} dx \qquad \text{A13b}$$

$$N_{xy} \sin\beta\, dq = \bar{N}_{xy} \sin\beta \frac{dy}{\cos\beta}$$

$$= \bar{N}_{xy} \tan\beta\, dy$$

$$= \bar{N}_{xy} \frac{\partial z}{\partial y} dy \qquad \text{A13c}$$

$$N_{yx} \sin\phi\, dp = \bar{N}_{yx} \sin\phi \frac{dx}{\cos\phi}$$

$$= \bar{N}_{yx} \tan\phi\, dx$$

$$= \bar{N}_{yx} \frac{\partial z}{\partial x} dx \qquad \text{A13d}$$

Thus for equilibrium in the z direction.

$$-\bar{N}_x \frac{\partial z}{\partial x} dy + \bar{N}_x \frac{\partial z}{\partial x} dy + \frac{\partial}{\partial x} (\bar{N}_x \frac{\partial z}{\partial x} dy) dx$$

$$-\bar{N}_y \frac{\partial z}{\partial y} dx + \bar{N}_y \frac{\partial z}{\partial y} dx + \frac{\partial}{\partial y} (\bar{N}_y \frac{\partial z}{\partial y} dx) dy$$

$$-\bar{N}_{xy} \frac{\partial z}{\partial y} dy + \bar{N}_{xy} \frac{\partial z}{\partial y} dy + \frac{\partial}{\partial x} (\bar{N}_{xy} \frac{\partial z}{\partial y} dy) dx$$

$$-\bar{N}_{yx} \frac{\partial z}{\partial x} dx + \bar{N}_{yx} \frac{\partial z}{\partial x} dx + \frac{\partial}{\partial y} (\bar{N}_{yx} \frac{\partial z}{\partial x} dx) dy$$

$$+\bar{P}_z - \bar{P}_x \frac{z}{x} - \bar{P}_y \frac{\partial z}{\partial y} = 0$$

or

$$\frac{\partial}{\partial x} (\bar{N}_x \frac{\partial z}{\partial x}) + \frac{\partial}{\partial y} (\bar{N}_{yx} \frac{\partial z}{\partial x}) + \frac{\partial}{\partial x} (\bar{N}_{xy} \frac{\partial z}{\partial y}) + \frac{\partial}{\partial y} (\bar{N}_y \frac{\partial z}{\partial y})$$

$$+ \bar{P}_z - \bar{P}_x \frac{z}{x} - \bar{P}_y \frac{\partial z}{\partial y} = 0 \qquad \text{A14}$$

the moment equilibrium equation can be used to prove

$$\bar{N}_{xy} = \bar{N}_{yx} \qquad \text{A15}$$

differentiating the products in equation (A14) gives

$$\bar{N}_x \frac{\partial^2 z}{\partial x^2} + 2\bar{N}_{xy} \frac{\partial^2 z}{\partial x \partial y} + \bar{N}_y \frac{\partial^2 z}{\partial y^2}$$

$$= -\bar{P}_z - (\frac{\partial \bar{N}_x}{\partial x} + \frac{\partial \bar{N}_{xy}}{\partial y}) \frac{\partial z}{\partial x} - (\frac{\partial}{\partial x} \bar{N}_{xy} + \frac{\partial}{\partial y} \bar{N}_y) \frac{\partial z}{\partial y} \qquad \text{A16}$$

incorporating the other two equilibrium equations (A11) and (A12) results in

$$\bar{N}_x \frac{\partial^2 z}{\partial x^2} + 2\bar{N}_{xy} \frac{\partial^2 z}{\partial x \partial y} + \bar{N}_y \frac{\partial^2 z}{\partial y^2} = -\bar{P}_z + \bar{P}_x \frac{\partial z}{\partial x} + \bar{P}_y \frac{\partial z}{\partial y} \qquad \text{A17}$$

Equations (A11), (A12), and (A17) are known as Pucher's equations of equilibrium for general translational shells. In summary, they are

$$\frac{\partial}{\partial x} \bar{N}_x + \frac{\partial}{\partial y} \bar{N}_{yx} + \bar{P}_x = 0$$

$$\frac{\partial}{\partial y} \bar{N}_y + \frac{\partial}{\partial x} \bar{N}_{xy} + \bar{P}_y = 0$$

$$\bar{N}_x \frac{\partial^2 z}{\partial x^2} + 2\bar{N}_{xy} \frac{\partial^2 z}{\partial x \partial y} + \bar{N}_y \frac{\partial^2 z}{\partial y^2} = -\bar{P}_z + \bar{P}_x \frac{\partial z}{\partial x} + \bar{P}_y \frac{\partial z}{\partial y} \qquad \text{A18}$$

APPENDIX B

FLÜGGE AND GEYLING KINEMATIC RELATIONS

Flügge and Geyling (6) extended Pucher's method of stress analysis given in Appendix A by developing a general deformation theory for membrane shells. The purpose of this appendix is to summarize the development of the kinematic relations as initially given in the preceding work.

The differential shell element shown in Figure 4 shows the three applicable displacement components; U, V, and W; as well as the parameters which are necessary to describe the reference geometry of the shell surface; α, β, and ω. The displacements U, V, and W are the displacement components acting in the $\dot{x}$, $\dot{y}$, and z directions respectively. α and β are the angles between the horizontal and the curved line segments bounding the differential element. The lines AC and BC are in the $\dot{x}z$ and $\dot{y}z$ planes respectively. The angle ω is the angle at which the curved lines segments are skewed in the plane tangent to the differential element. Considering the angles α and β to be nonzero, the angle, ω, which is formed by the intersection of the line segments must be other than 90 degrees in magnitude. With such geometric parameters, the need for the joint use of a skewed

curvilinear coordinate system and an orthogonal rectangular base system becomes clear. The skewed strains will be related to the orthogonal displacements first. Then, by using geometric relations, the orthogonal strain-orthogonal displacement relationships will be derived.

Considering Figure B-1(b), the following relation is derived for skewed strain increment in the x direction, e_x.

$$(1 + e_x)ds_1 = ds_1 + U_x dx \cos \alpha + W_x dx \sin \alpha$$

$$e_x = U_x \cos^2 \alpha + W_x \sin \alpha \cos \alpha \qquad B1$$

Similarily,

$$e_y = V_y \cos^2 \beta + W_y \sin \beta \cos \beta$$

For γ_{xy}, consider Figure B-1(a). The shearing action has caused line segments AC and AB to relocate to AC^1 and AB^1 respectfully. Assuming the latter to be straight, the following condition can be used as written in vector notation.

$$\overline{AC}^1 \cdot \overline{AB}^1 = |AC^1| \, |AB^1| \cos \gamma_{xy} \qquad B2$$

Substituting the equivalents

$$\overline{AC}^1 = (U_y dy)\hat{i} + (1 + V_y)dy \, \hat{j} + (\tan \beta + W_y)dy \, \hat{k}$$

$$\overline{AB}^1 = (1 + U_x)dx \, \hat{i} + V_x dx \, \hat{j} + (\tan \alpha + W_x)dx \, \hat{k} \qquad B4$$

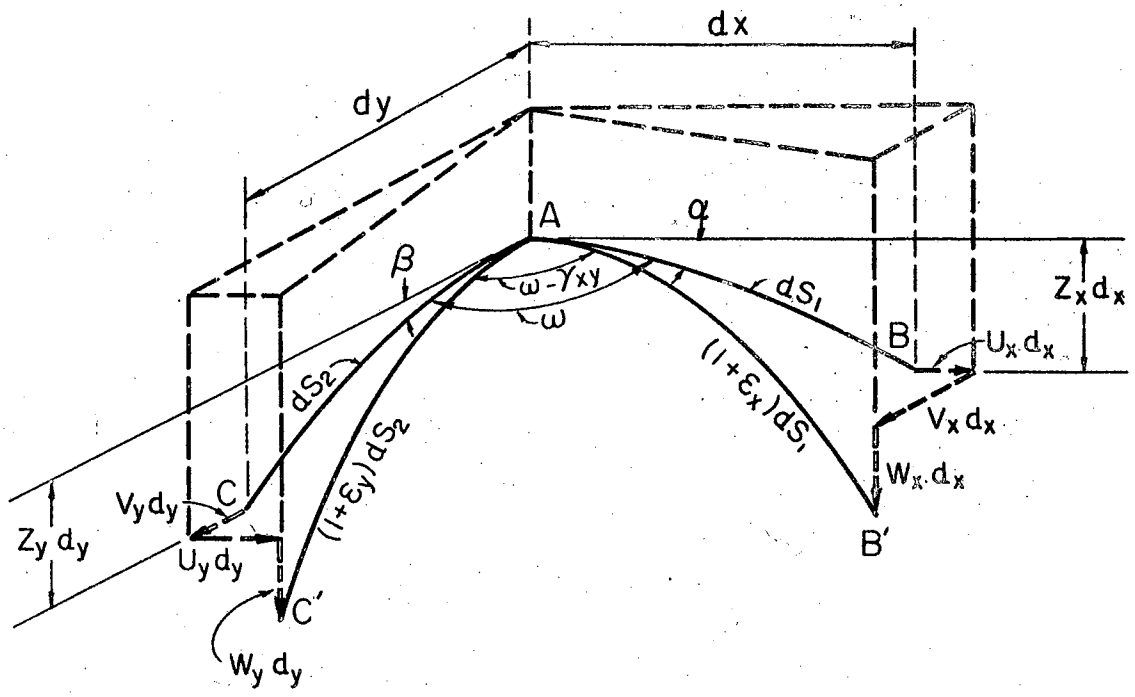

(a)

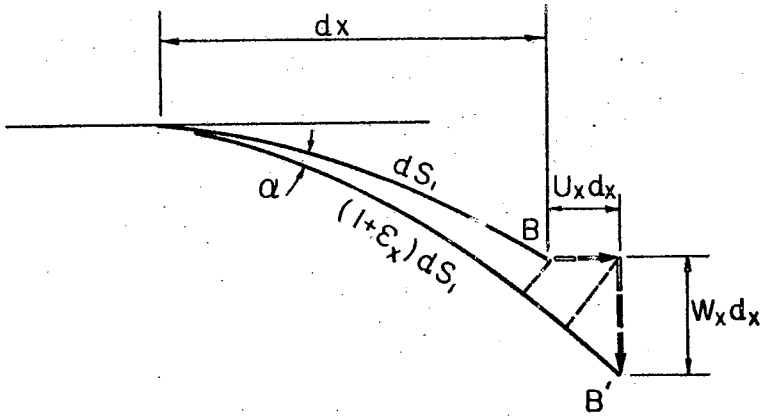

(b)

Figure B-1. Deformation of Curvilinear Element

leads to

$$(U_y dy)(1 + U_x)dx + (1 + V_y)dyV_x dx + (\tan \beta + W_y)dy_x \qquad B5$$

$$(\tan \alpha + W_x)dx = (1 + \epsilon_x)ds_1(1 + \epsilon_y)ds_2 \cos (W - \gamma_{xy})$$

Substituting equations B1 and B2 into equation B5 and neglecting higher order terms gives

$$[U_y + V_x + \tan \beta \tan \alpha + W_y \tan \alpha + W_x \tan \beta]\cos \alpha \cos \beta$$

$$= [1 + U_x \cos^2 \alpha + W_x \sin \alpha \cos \alpha + W_y \sin \beta \cos \beta +$$

$$+ V_y \cos^2 \alpha][\cos \omega + \sin \omega \gamma_{xy}] \qquad B6$$

Again using the definition of a dot product as given in vector algebra, the following relation between ω, α, and β is derived.

$$[dx\ \hat{i} + dx \tan \alpha\ \hat{k}][dy\ \hat{j} + dy \tan \beta\ \hat{k}] = \frac{dy}{\cos \beta} \frac{dx}{\cos \alpha} \cos \omega \qquad B7$$

or

$$\tan \beta \tan \alpha = \frac{1}{\cos \beta \cos \alpha} \cos \omega$$

Thus,

$$\cos \omega = \sin \beta \cos \alpha \qquad B8$$

and considering

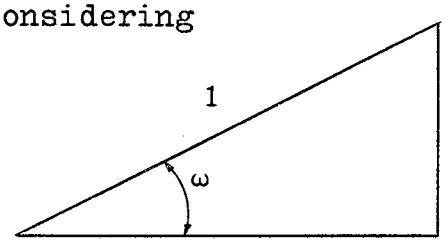

$(1 - \sin^2 \alpha \sin^2 \beta)^{1/2}$

the following is formed

$$\sin \omega = (1 - \sin^2 \alpha \sin^2 \beta)^{\frac{1}{2}} \qquad \text{B9}$$

After substituting with equations B8 and B9 and neglecting higher order terms, equation B6 is developed into

$$\gamma_{xy} = \frac{1}{\sin \alpha} [U_y \cos \alpha \cos \beta + V_x \cos \alpha \cos \beta \qquad \text{B10}$$

$$+ W_y \sin \alpha \cos^3 \beta + W_x \sin \beta \cos^3 \alpha$$

$$- U_x \cos^2 \alpha \sin \beta \sin \alpha - V_y \cos^2 \beta \sin \beta \sin \alpha]$$

Thus, in summary, the kinematic relations for the skewed strain components are

$$e_x = U_x \cos^2 \alpha + W_x \sin \alpha \cos \alpha \qquad \text{B11a}$$

$$e_y = V_y \cos^2 \beta + W_y \sin \beta \cos \beta$$

$$\gamma_{xy} = \frac{1}{\sin \omega} [U_y \cos \alpha \cos \beta + V_x \cos \alpha \cos \beta \qquad \text{B11c}$$

$$+ W_y \sin \alpha \cos^3 \beta + W_x \sin \beta \cos^3 \alpha$$

$$- U_x \cos^2 \alpha \sin \alpha \sin \beta - V_y \cos^2 \beta \sin \theta \sin \alpha] \quad \text{B11c}$$

Flügge and Geyling also use Figure B-2 to deduce the following relations between the orthogonal and the skewed strain components.

$$e_x = e_{\bar{x}} \quad \text{B12}$$

$$\gamma_{xy} \frac{1}{\sin} = \bar{\gamma}_{xy} \sin \omega + e_{\bar{x}} \cos \omega - e_{\bar{y}} \cos \omega \quad \text{B13}$$

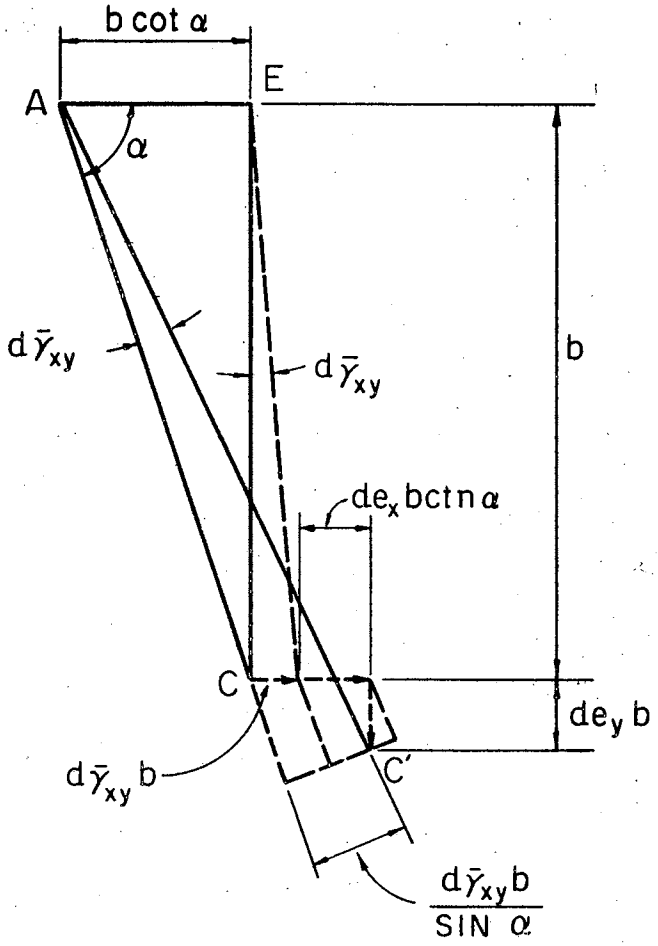

Figure B-2. Orthogonal-Skewed Strain Relations

APPENDIX C

STRESS RESULTANT TRANSFORMATION

The following development of equations governing the transformation to orthogonal stress resultants from those in an oblique or skewed coordinate system is by Morley (45). The notation has been changed to be consistent with Flügge and Geyling (6). Consider the orthogonal and skewed coordinate force systems represented in Figure C-1.

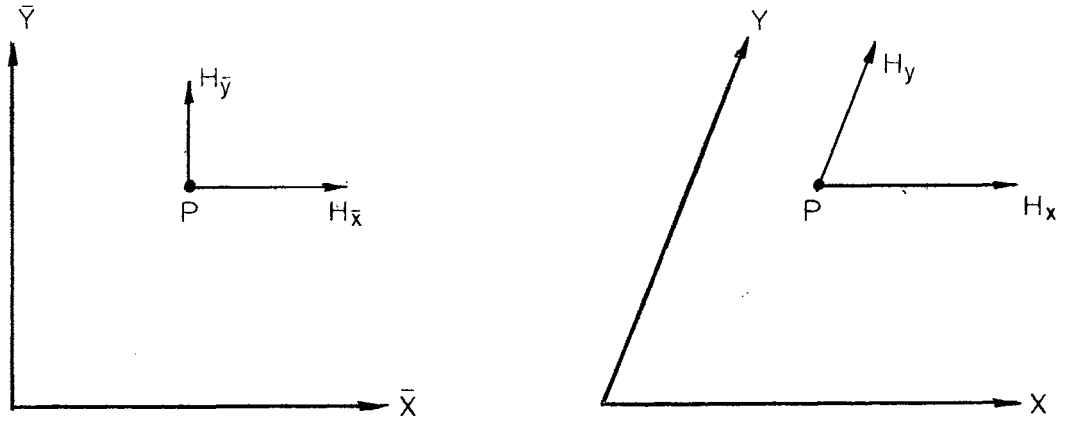

Figure C-1. Orthogonal-Skewed Force System

From geometry,

$$N_{\bar{x}} = N_x + N_y \cos \alpha \qquad C1$$

$$N_{\bar{y}} = N_y \sin \alpha \qquad C2$$

or

$$N_x = N_{\bar{x}} - N_{\bar{y}} \cot \alpha \qquad C3$$

$$N_y = N_{\bar{y}} \csc \alpha \qquad C4$$

where

N_x, N_y = components of force in the skewed system

$N_{\bar{x}}$, $N_{\bar{y}}$ = components of force in the orthogonal system

Considering equilibrium in the orthogonal system,

$$\Sigma M @ 0 = 0 = x H_{\bar{y}} - y H_{\bar{x}}$$

thus,

$$\Sigma F_{\bar{x}} = F_{\bar{y}} = x H_{\bar{y}} - y H_{\bar{x}} = 0 \qquad C5$$

and for the skewed system,

$$\Sigma M @ 0 = 0 = x H_y - y H_x$$

thus,

$$\Sigma F_x = F_y = x H_y - y H_x = 0 \qquad C6$$

Now consider Figure C-2.

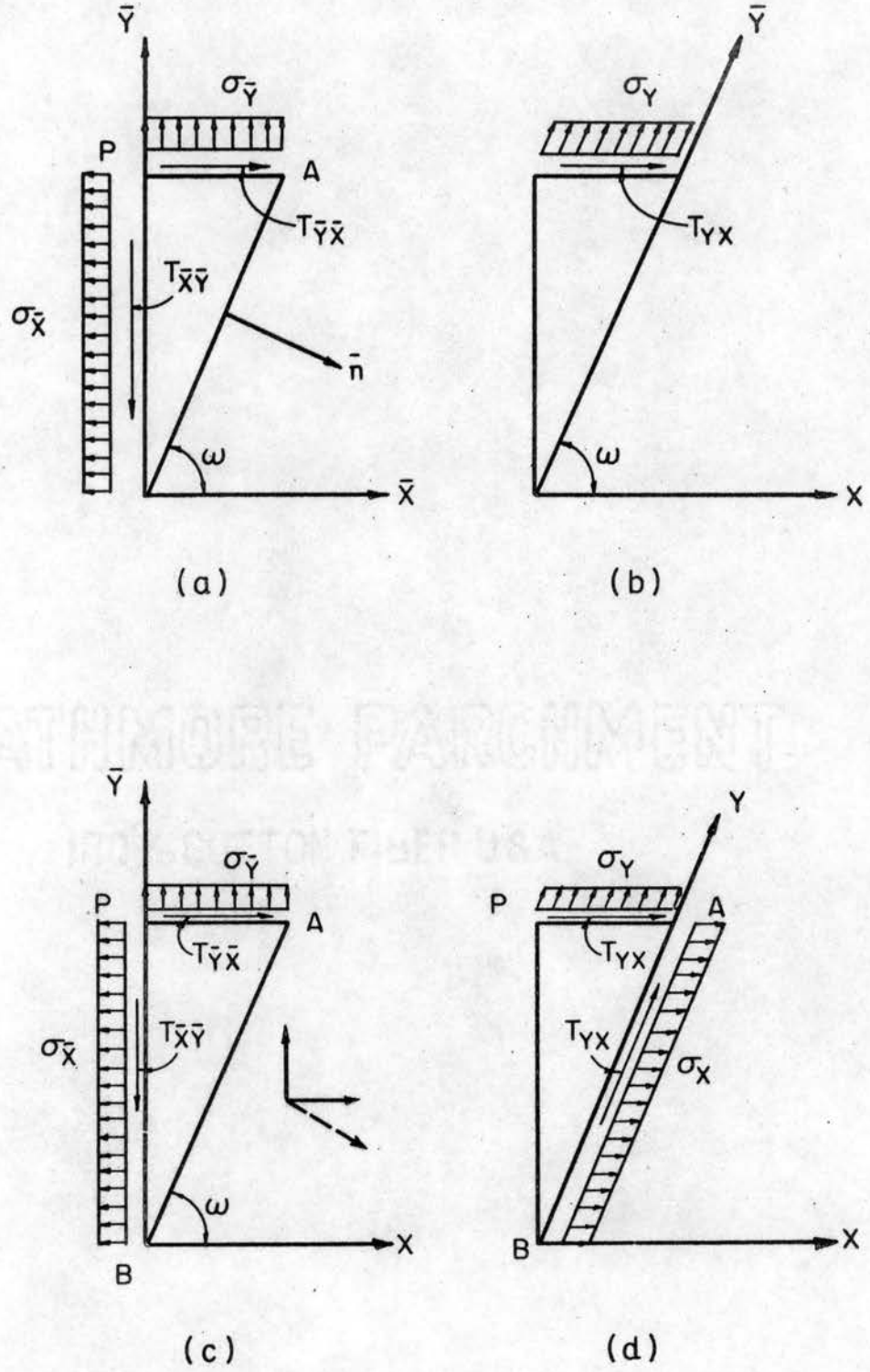

Figure C-2. Orthogonal-Skewed Stress System

Let stresses $\sigma_{\overline{x}}$, $\sigma_{\overline{y}}$, and $\gamma_{\overline{xy}}$ at point P in a plate be assumed to act on the sides of triangular element APB as shown in Figure C-2(a). Using equations C1 through C4 the stresses on side PA are resolved into stresses σ_y and σ_{xy} as shown in Figure C-2(b) and derived below

$$\sigma_{\overline{y}} = \sigma_y \sin \omega \qquad C7$$

$$T_{\overline{xy}} = T_{xy} \cos \omega \qquad C8$$

or

$$T_{xy} = T_{\overline{xy}} - \sigma_{\overline{y}} \cot \omega \qquad C9$$

$$\sigma_y = \sigma_{\overline{y}} \operatorname{cosec} \omega \qquad C10$$

In Figure C-2(a), the directional cosines of the inclined normal are

$$l = \cos (90 - \omega) = \sin \omega \qquad C11$$

$$m = \cos (180 + \omega) = -\cos \omega \qquad C12$$

Let $N_{\overline{x}}$ and $N_{\overline{y}}$ be the components of stress parallel to the axes of the rectangular coordinates and acting on side AB.

$$N_{\overline{x}} = \sigma_x l + T_{\overline{xy}} m = \sigma_x \sin \omega - T_{\overline{xy}} \cos \omega \qquad C13$$

$$N_{\overline{y}} = T_{\overline{xy}} l + \sigma_{\overline{y}} m = T_{\overline{xy}} \sin \omega - \sigma_{\overline{y}} \cos \omega \qquad C14$$

as shown in Figure C-1 and stated in equations C3 and C4.

$N_{\bar{x}}$ and $N_{\bar{y}}$ can be put in terms of σ_y and T_{yx}. In this manner,

$$\sigma_x = N_{\bar{x}} - N_{\bar{y}} \cot \omega \qquad C15$$

$$T_{yx} = N_{\bar{y}} \operatorname{cosec} \omega \qquad C16$$

Substituting equations C13 and C14 into C15 and C16 gives

$$\sigma_x = \sigma_{\bar{x}} \sin \omega + \sigma_{\bar{y}} \cos \omega \cot \omega - 2T_{\overline{xy}} \cos \omega \qquad C17$$

$$T_{yx} = T_{\overline{xy}} - \sigma_{\bar{y}} \cot \omega \qquad C18$$

The quantities σ_x, σ_y, and $T_{xy} = T_{yx}$ are the components of stress for the skewed coordinate system for they completely define the state of stress at point P provided $\omega \neq 0, \pi$. Collectively, they are

$$\sigma_x = \sigma_{\bar{x}} \sin \omega + \sigma_{\bar{y}} \cos \omega \cot \omega - 2T_{\overline{xy}} \cos \omega \qquad C19$$

$$\sigma_y = \sigma_{\bar{y}} \operatorname{cosec} \omega \qquad C20$$

$$T_{xy} = T_{\overline{xy}} - \sigma_{\bar{y}} \cot \omega \qquad C21$$

The rectangular components in terms of the skewed stresses are

$$\sigma_{\bar{x}} = \sigma_x \operatorname{cosec} \omega + \sigma_y \cos \omega \cot \omega + 2T_{xy} \cot \omega$$

$$\sigma_{\bar{y}} = \sigma_y \sin \omega$$

$$T_{\overline{xy}} = T_{\overline{yx}} = T_{xy} + \sigma_y \cos\omega \qquad C22$$

In terms of stress resultants, the preceding equations are

$$S_x = N_x \operatorname{cosec}\omega + N_y \cos\omega \cot\omega + 2T_{xy} \cot\omega$$

$$N_{\overline{y}} = N_y \sin\omega$$

$$T_1 = N_{xy} + N_y \cos \qquad C23$$

APPENDIX D

PLASTIC CONSTITUTIVE EQUATIONS

There are two current theories of deformation from which the constitutive equations may be chosen; the incremental theory and the deformation theory. The incremental theory requires that the current stress and strain increment be used to solve for the current strain increment whereas only the current stress state is necessary to find the current strain in the total deformation theory. The latter is the least complex to apply in a mathematical sense. This simplicity, however, is over ruled by its relative inaccuracy. As Hill (9) points out, the only case when the deformation theory satisfactorily describes the plastic behavior of a metal is when two conditions exist; (1) the principal axes of successive strain increments do not rotate relative to the element and (2) the components of any strain-increment bear constant ratios to one another. Such cases are not the most common and certainly do not pertain to this problem. Thus, the incremental theory of plasticity is selected for use.

Considering the membrane material to be an elastic-perfectly plastic solid, the Reuss-Prandtl equation is applicable.

$$d\varepsilon_{ij} = d\varepsilon^{P}_{ij} + d\varepsilon^{e}_{ij} \qquad D1$$

$$d\varepsilon_{ij} = \sigma'_{ij} d\lambda + \frac{d\sigma'_{ij}}{2G} + \frac{(1 - 2\nu)}{E} \delta_{ij} d\sigma_{M} \qquad D2$$

where:

σ'_{ij} = deviatoric stress tensor

$d\lambda$ = non-negative constant of proportionality

δ_{ij} = kronecker delta

$d\sigma_{M}$ = hydrostatic stress increment

E = modulus of elasticity

G = mosulus of rigidity

The equation, as given above, states that the plastic strain increment is at any instant proportional to the instantaneous stress deviation and the shear stresses.

In problems of large deformations, the elastic strains are only evident during the first few increments of deformation and then become part of the plastic response. The latter strains account for practically the entire distortion. On this basis, the elastic component of the strain is neglected and the less complex Levy-Mises equations replace equations D2. These assume only plastic strains are present and are written as follows

$$d\varepsilon_{ij} = d\lambda \sigma'_{ij} \qquad D3$$

where $d\lambda$ is a scalar factor of proportionality.

In defining the state of stress causing initial yield, the condition based upon the energy of distortion and known as Von Mises' yield criterion is used. This statement is written as follows for the case of plane stress.

$$\sigma_o = (\sigma_x^2 - \sigma_x\sigma_y + \sigma_y^2 + 3T_{xy}^2)^{\frac{1}{2}} \qquad \text{D4}$$

where

σ_o = yield stress in simple tension

σ_x, σ_y = normal stresses in the X and Y directions respectfully

T_{xy} = shearing stress in XY plane

Equation D4 implies that whenever the indicated function of stresses equal σ_o then initial yielding occurs. If the material was rigid perfectly plastic, such a condition would also govern any additional yielding.

For subsequent yielding of a work hardening material, the constant σ_o is replaced by the parameter $\bar{\sigma}$ defined as the effection stress. Thus, the yield condition becomes

$$\bar{\sigma} = (\sigma_x^2 - \sigma_x\sigma_y + \sigma_y^2 + 3T_{xy}^2)^{\frac{1}{2}} \qquad \text{D5}$$

this condition can be rewritten as

$$f(\sigma_x, \sigma_y, T_{xy}) = \sigma_x^2 - \sigma_x\sigma_y + \sigma_y^2 + 3T_{xy}^2 = \bar{\sigma}^2 \qquad \text{D6}$$

or, if stated in terms of tensor notation,

$$f(\sigma_{ij}) = \bar{\sigma} \qquad \text{D7}$$

The function $f(\sigma_{ij})$ mathematically describes the expansion of the yield surface which occurs during work-hardening. Such a function depends both upon stresses and plastic strains. In addition, its argument should be expressed in terms of scalar quantities. Most authors acknowledge the existence of two hypotheses. The first is that the amount of strain hardening is a function only of the total plastic work done. This is expressed mathematically as

$$f(\sigma_{ij}) = F(\xi) \qquad \text{D8}$$

where

$$\xi = \sigma_{ij} d\epsilon^{P}_{ij} \qquad \text{D9}$$

The second hypothesis is that the same function, $f(\sigma_{ij})$, is a measure of the total plastic deformation. This is written

$$f(\sigma_{ij}) = H(\bar{\epsilon}^{P}) \qquad \text{D10}$$

where

$$\bar{\epsilon}^{P} = \text{effective strain} = \sqrt{\tfrac{2}{3}} \int \sqrt{d\epsilon_{ij}\, d\epsilon_{ij}} \qquad \text{D11}$$

The equation D3 is a statement that the principal axes of stress and the plastic strain increment are coincident. Under the terms of this assumption, the two working-hardening hypotheses D8 and D10 are equivalent. That is, they reduce to $\sigma = H(\int d\varepsilon^P)$. Hill shows that the equations D3 can then be written in terms of the following two statements.

$$d\varepsilon_{ij}^P = \frac{3d\varepsilon^P}{2\bar{\sigma}} \sigma'_{ij} , \quad \sigma = H(\int d\varepsilon^P) \qquad \text{D12}$$

where

$d\varepsilon^P$ = effective strain increment

$$= \frac{2}{3} (de_x^2 + de_x de_y + de_y^2 = \frac{1}{4} d\gamma_{xy}^2)^{\frac{1}{2}}$$

H = function relating effective stress to effective strain and referred to as the "universal" stress-strain relationship.

Instead of using the effective stress and effective strain in the universal stress-strain relationship, at least three other sets of quantities could have been used; the maximum shear stress vs. the maximum shear strain, the maximum shear vs. the numerically largest strain, or the octahedral shear stress vs. the octahedral shear strain. The effective stress-effective strain relationship was chosen as its possible reduction to that of the uniaxial stress and strain makes it more convenient.

The universal stress-strain relationship is taken as the uniaxial stress-strain curve for the applicable

material. It is recognized that such a representation is not most accurate but current developments allow no recourse. Biaxial tests which have been made (29), (9), (44) are limited in number and deficient in agreement with predicted results. Also, the constant stress ratios used in most of these tests are not a true reflection of the variable stress conditions of this problem.

The constitutive equations D12 are expanded to give the following desired expressions.

$$de_x = \frac{\overline{d\epsilon}}{\bar{\sigma}} (\sigma_x - \frac{1}{2}\sigma_y)$$

$$de_y = \frac{\overline{d\epsilon}}{\bar{\sigma}} (\sigma_y - \frac{1}{2}\sigma_x)$$

$$de_{xy} = \frac{3}{2} (\frac{\overline{d\epsilon}}{\bar{\sigma}})\sigma_{xy}$$

or in terms of the orthogonal stress resultants, the constitutive equations become

$$de_x = \Delta\lambda(S_x - \frac{1}{2} N_{\bar{y}})$$

$$de_y = \Delta\lambda(N_{\bar{y}} - \frac{1}{2} S_x)$$

$$de_{xy} = \frac{3}{2}\Delta\lambda T_1 \qquad \text{D14}$$

where

$$\bar{\sigma} = H(\Sigma \overline{d\epsilon}^P) \qquad \text{D15}$$

and

$$\Delta\lambda = \text{plasticity parameter}$$

$$= \frac{\overline{d\epsilon}}{\bar{\sigma}_t}$$

TABLE D-1

UNIVERSAL STRESS-STRAIN RELATIONSHIP PARAMETERS

Material	a	b	c
70-30 Annealed Brass (10% prior coldwork)	100,000	0.105	0.5
1100 Annealed Aluminum (10% prior coldwork)	26,000	0.105	0.20
1020 Hot Rolled Steel (10% prior coldwork)	115,000	0.105	0.22
Half-Hard Aluminum	22,200	0.222	0.25

APPENDIX E

TAU VALUES

$$tau_1 = \cos^2 \alpha$$

$$tau_2 = \sin \alpha \cos \alpha$$

$$tau_3 = \frac{\cos^2 \beta}{\sin^2 \omega}$$

$$tau_4 = \cos^2 \beta$$

$$tau_5 = \sin \beta \cos \beta$$

$$tau_6 = \cos^2 \alpha \cos^2 \omega$$

$$tau_7 = \sin \alpha \cos \alpha \cos^2 \omega$$

$$tau_8 = \cos^2 \beta \cos \omega - \cos^2 \beta \sin \beta \sin \alpha$$

$$tau_9 = \cos^2 \alpha \sin \beta \sin \alpha + \cos^2 \alpha \cos \omega$$

$$tau_{10} = \cos \alpha \cos \beta$$

$$tau_{11} = \sin \alpha \cos^3 \beta + \sin \beta \cos \beta \cos \omega$$

$$tau_{12} = \sin \beta \cos^3 \alpha - \sin \alpha \cos \alpha \cos \omega$$

$$tau_{13} = \frac{0.5}{\sin^3 \omega}$$

$$tau_{14} = \cos \omega \cos \alpha$$

$$tau_{15} = \sin \omega + 0.5 \frac{\cos^2 \omega}{\sin \omega}$$

$$tau_{16} = 0.5 \sin \omega + \frac{\cos^2 \omega}{\sin \omega}$$

$$tau_{17} = \frac{\cos \omega}{\sin \omega}$$

$$tau_{18} = \frac{\cos^2 \omega}{\sin^2 \omega}$$

$$tau_{19} = \frac{\cos \beta}{\cos \alpha \sin \omega}$$

$$tau_{20} = \frac{1}{\sin \omega}$$

$$tau_{21} = \frac{(1.0 - \sin^2 \alpha \sin^2 \beta)^{\frac{1}{2}}}{\cos \alpha \cos \beta}$$

$$tau_{22} = \frac{1}{\sin^2 \omega}$$

where

$$\sin \alpha = \frac{Z_x}{(1 + Z_x^2)^{\frac{1}{2}}} \quad , \quad \cos \alpha = \frac{1}{(1 + Z_x^2)^{\frac{1}{2}}}$$

$$\sin \beta = \frac{Z_y}{(1 + Z_y^2)^{\frac{1}{2}}} \quad , \quad \cos \beta = \frac{}{(1 + Z_y^2)^{\frac{1}{2}}}$$

$$\sin \omega = \frac{(1 + \tan^2 \alpha + \tan^2 \beta)^{\frac{1}{2}}}{(1 + \tan^2 \alpha + \tan^2 \beta + \tan^2 \alpha \tan^2 \beta)^{\frac{1}{2}}}$$

$$\cos \omega = \frac{\tan \alpha \tan \beta}{(1 + \tan^2 \alpha + \tan^2 \beta + \tan^2 \alpha \tan^2 \beta)^{\frac{1}{2}}}$$

APPENDIX F

D COEFFICIENTS

$$D_1 = [\tau_{15}\,\tau_1 - \tau_{16}\,\tau_{22}\,\tau_6 + \cos\,\tau_{13}\,\tau_9]\,[(plas1)\,\tau_{14}]$$

$$D_2 = [\tau_{15}\,\tau_2 - \tau_{16}\,\tau_{22}\,\tau_7 - \cos\,\tau_{13}\,\tau_{12}]\,[(plas1)\,\tau_{14}]$$

$$D3 = [\tau_{16}\,\tau_{22}\,\tau_4 - \cos\,\tau_{13}\,\tau_8][(plas1)\,\tau_{14}]$$

$$D4 = [\tau_{16}\,\tau_{22}\,\tau_5 - \cos\,\tau_{13}\,\tau_{11}][(plas1)\,\tau_{14}]$$

$$D5 = [-\cos\,\tau_{13}\,\tau_{10}]\,\tau_{14}\,plas1$$

$$D6 = [0.5\,\tau_1\,\tau_{17} - \tau_{17}\,\tau_{22}\,\tau_6 + 0.5\,\tau_{13}\,\tau_9]plas1$$

$$D7 = [0.5\,\tau_2\,\tau_{17} - \tau_{17}\,\tau_{18}\,\tau_2 - 0.5\,\tau_{13}\,\tau_{12}]plas1$$

$$D8 = [\tau_{17}\,\tau_4\,\tau_{22} - 0.5\,\tau_{13}\,\tau_8]plas1$$

$$D9 = [\tau_{17}\,\tau_{22}\,\tau_5 - 0.5\,\tau_{13}\,\tau_{11}]plas1$$

$$D10 = -0.5\ tau_{13}\ tau_{10}\ plas1$$

$$D11 = [0.5\ tau_{1} - tau_{22}\ tau_{6}]tau_{19}\ plas1$$

$$D12 = [0.5\ tau_{2} - tau_{22}\ tau_{7}]tau_{19}\ plas1$$

$$D13 = tau_{22}\ tau_{4}\ tau_{19}\ plas1$$

$$D14 = tau_{22}\ tau_{5}\ tau_{19}\ plas1$$

$$D15 = tau_{23}\ tau_{1} - tau_{24}\ tau_{22}\ tau_{6} - tau_{25}\ tau_{13}\ tau_{9}$$

$$D16 = tau_{23}\ tau_{2} - tau_{24}\ tau_{22}\ tau_{7} + tau_{25}\ tau_{13}\ tau_{12}$$

$$D17 = tau_{24}\ tau_{22}\ tau_{4} + tau_{25}\ tau_{13}\ tau_{3}$$

$$D18 = tau_{24}\ tau_{22}\ tau_{5} + tau_{25}\ tau_{13}\ tau_{11}$$

$$D19 = tau_{25}\ tau_{13}\ tau_{10}$$

$$D20 = D19$$

$$D21 = 0.75\ tau_{21}\ plas$$

where

$$plas = \frac{\overline{\delta\varepsilon}}{\bar{\sigma}^{t}}$$

$$plas1 = \frac{4.0}{3.0\ plas}$$

APPENDIX G

DU_i, DV_i, AND DW_i COEFFICIENTS FOR THE DISPLACEMENT EQUATIONS

The coefficients used in the U displacement equation are defined as

$$DU1 = (D5_{i-1,j} + D5_{i,j} - D6_{i,j-1} - D6_{i,j}) \frac{1}{8h_x h_y}$$

$$DU2 = (D5_{i-1,j} - D5_{i+1,j}) \frac{1}{8h_x h_y} - (D10_{i,j} + D10_{i,j-1}) \frac{1}{2h_y^2}$$

$$DU3 = (-D5_{i+1,j} - D5_{i,j} + D6_{i,j-1} + D6_{i,j}) \frac{1}{8h_x h_y}$$

$$DU4 = (D6_{i,j+1} - D6_{i,j-1}) \frac{1}{8h_x h_y} + (D1_{i-1,j} + D1_{i,j}) \frac{1}{2h_x^2}$$

$$DU5 = (D10_{i,j+1} + 2D10_{i,j} + D10_{i,j-1}) \frac{1}{2h_y^2} - (D1_{i+1,j} + 2D1_{i,j} + D1_{i-1,j}) \frac{1}{2h_x^2}$$

$$DU6 = (D6_{i,j-1} - D6_{i,j+1}) \frac{1}{8h_x h_y} + (D1_{i+1,j} + D1_{i,j}) \frac{1}{2h_x^2}$$

$$DU7 = -(D5_{i-1,j} + D5_{i,j}) \frac{1}{8h_x h_y} + (D6_{i,j+1} + D6_{i,j}) \frac{1}{8h_x h_y}$$

$$DU8 = (D5_{i+1,j} - D5_{i-1,j}) \frac{1}{8h_x h_y} - (D10_{i,j+1} + D10_{i,j}) \frac{1}{2h_y^2}$$

$$DU9 = (D5_{i+1,j} + D5_{i,j} - D6_{i,j+1} - D6_{i,j}) \frac{1}{8h_x h_y}$$

$$DV1 = (D3_{i-1,j} + D3_{i,j}) \frac{1}{8h_x h_y} - (D10_{i,j-1} + D10_{i,j}) \frac{1}{8h_x h_y}$$

$$DV2 = (D3_{i-1,j} - D3_{i+1,j}) \frac{1}{8h_x h_y} - (D8_{i,j-1} + D8_{i,j}) \frac{1}{2h_y^2}$$

$$DV3 = (-D3_{i+1,j} - D3_{i,j} + D10_{i,j-1} + D10_{i,j}) \frac{1}{8h_x h_y}$$

$$DV4 = (D5_{i,j} + D5_{i-1,j}) \frac{1}{2h_x^2} + (D10_{i,j+1} - D10_{i,j-1}) \frac{1}{8h_x h_y}$$

$$DV5 = (D8_{i,j+1} + 2D8_{i,j} + D8_{i,j-1}) \frac{1}{2h_y^2} - (D5_{i+1,j} + 2D5_{i,j} + D5_{i-1,j}) \frac{1}{2h_x^2}$$

$$DV6 = (D5_{i+1,j} + D5_{i,j}) \frac{1}{2h_x^2} - (D10_{i,j+1} - D10_{i,j-1}) \frac{1}{8h_x h_y}$$

$$DV7 = (D10_{i,j+1} + D10_{i,j}) \frac{1}{8h_x h_y} - (D3_{i-1,j} + D3_{i,j}) \frac{1}{8h_x h_y}$$

$$DV8 = (D3_{i+1,j} - D3_{i-1,j}) \frac{1}{8h_x h_y} - (D8_{i,j+1} + D8_{i,j}) \frac{1}{2h_x^2}$$

$$DV9 = (D3_{i+1,j} + D3_{i,j}) \frac{1}{8h_x h_y} - (D10_{i,j+1} + D10_{i,j}) \frac{1}{8h_x h_y}$$

$$DW1 = (D4_{i-1,j} + D4_{i,j}) \frac{1}{8h_x h_y} - (D7_{i,j-1} + D7_{i,j}) \frac{1}{8h_x h_y}$$

$$DW2 = (D4_{i-1,j} - D4_{i+1,j}) \frac{1}{8h_x h_y} - (D9_{i,j-1} + D9_{i,j}) \frac{1}{2h_y^2}$$

$$DW3 = (D7_{i,j-1} + D7_{i,j}) \frac{1}{8h_x h_y} - (D4_{i+1,j} + D4_{i,j}) \frac{1}{8h_x h_y}$$

$$DW4 = (D2_{i,j} + D2_{i-1,j}) \frac{1}{2h_x^2} + (D7_{i,j+1} - D7_{i,j-1}) \frac{1}{8h_x h_y}$$

$$DW5 = (D9_{i,j+1} + 2D9_{i,j} + D9_{i,j-1}) \frac{1}{2h_y^2}$$

$$- (D2_{i+1,j} + 2D2_{i,j} + D2_{i-1,j}) \frac{1}{2h_x^2}$$

$$DW6 = (D2_{i+1,j} + D2_{i,j}) \frac{1}{2h_x^2} - (D7_{i,j+1} - D7_{i,j-1}) \frac{1}{8h_x h_y}$$

$$DW7 = (D7_{i,j+1} + D7_{i,j}) \frac{1}{8h_x h_y} - (D4_{i-1,j} + D4_{i,j}) \frac{1}{8h_x h_y}$$

$$DW8 = (D4_{i+1,j} - D4_{i-1,j}) - (D9_{i,j+1} + D9_{i,j}) \frac{1}{2h_y^2}$$

$$DW9 = (D4_{i+1,j} + D4_{i,j}) \frac{1}{8h_x h_y} - (D7_{i,j+1} + D7_{i,j}) \frac{1}{8h_x h_y}$$

The coefficients used in the V displacement equation are defined as

$$DV1 = -(D8_{i-1,j} + D8_{i,j}) \frac{1}{8h_x h_y}$$

$$DV2 = (D13_{i,j-1} + D13_{i,j}) \frac{1}{2h_y^2} + (D8_{i+1,j} - D8_{i-1,j}) \frac{1}{8h_x h_y}$$

$$DV3 = (D8_{i+1,j} + D8_{i,j}) \frac{1}{8h_x h_y}$$

$$DV4 = -(D10_{i-1,j} + D10_{i,j}) \frac{1}{2h_x^2}$$

$$DV5 = -(D13_{i,j+1} + 2D13_{i,j} + D13_{i,j-1}) \frac{1}{2h_y^2}$$

$$+ (D10_{i+1,j} + 2D10_{i,j} + D10_{i-1,j}) \frac{1}{2h_x^2}$$

$$DV6 = -(D10_{i+1,j} + D10_{i,j}) \frac{1}{2h_x^2}$$

$$DV7 = (D8_{i-1,j} + D8_{i,j}) \frac{1}{8h_x h_y}$$

$$DV8 = (D13_{i,j+1} + D13_{i,j}) \frac{1}{2h_y^2} - (D8_{i+1,j} - D8_{i-1,j}) \frac{1}{8h_x h_y}$$

$$DV9 = -(D8_{i+1,j} + D8_{i,j}) \frac{1}{8h_x h_y}$$

$$DU1 = (D11_{i,j-1} + D11_{i,j}) \frac{1}{8h_x h_y} - (D10_{i-1,j} + D10_{i,j}) \frac{1}{8h_x h_y}$$

$$DU2 = (D10_{i+1,j} - D10_{i-1,j}) \frac{1}{8h_x h_y}$$

$$DU3 = -(D11_{i,j-1} + D11_{i,j}) \frac{1}{8h_x h_y} + (D10_{i+1,j} + D10_{i,j}) \frac{1}{8h_x h_y}$$

$$DU4 = (D11_{i,j-1} - D11_{i,j+1}) \frac{1}{8h_x h_y} - (D6_{i,j} + D6_{i-1,j}) \frac{1}{2h_x^2}$$

$$DU5 = (D6_{i+1,j} + 2D6_{i,j} + D6_{i-1,j}) \frac{1}{2h_x^2}$$

$$DU6 = (D11_{i,j+1} - D11_{i,j-1}) \frac{1}{8h_x h_y} - (D6_{i+1,j} + D6_{i,j}) \frac{1}{2h_x^2}$$

$$DU7 = -(D11_{i,j+1} + D11_{i,j}) \frac{1}{8h_x h_y} + (D10_{i-1,j} + D10_{i,j}) \frac{1}{8h_x h_y}$$

$$DU8 = (D10_{i-1,j} - D10_{i+1,j}) \frac{1}{8h_x h_y}$$

$$DU9 = (D11_{i,j+1} + D11_{i,j}) \frac{1}{8h_x h_y} - (D10_{i+1,j} + D10_{i,j}) \frac{1}{8h_x h_y}$$

$$DW1 = (D12_{i,j-1} + D12_{i,j}) \frac{1}{8h_x h_y} - (D9_{i-1,j} + D9_{i,j}) \frac{1}{8h_x h_y}$$

$$DW2 = (D14_{i,j-1} + D14_{i,j}) \frac{1}{2h_y^2} + (D9_{i+1,j} - D9_{i-1,j}) \frac{1}{8h_x h_y}$$

$$DW3 = (D9_{i+1,j} + D9_{i,j}) \frac{1}{8h_x h_y} - (D12_{i,j-1} + D12_{i,j}) \frac{1}{8h_x h_y}$$

$$DW4 = (D12_{i,j-1} - D12_{i,j+1}) \frac{1}{8h_x h_y} - (D7_{i,j} + D7_{i-1,j}) \frac{1}{2h_x^2}$$

$$DW5 = (D7_{i+1,j} + 2D7_{i,j} + D7_{i-1,j}) \frac{1}{2h_x^2} - (D14_{i,j+1} + 2D14_{i,j} + D14_{i,j-1}) \frac{1}{2h_y^2}$$

$$DW6 = (D12_{i,j+1} - D12_{i,j-1}) \frac{1}{8h_x h_y} - (D7_{i+1,j} + D7_{i,j}) \frac{1}{2h_x h_y}$$

$$DW7 = (D9_{i-1,j} + D9_{i,j}) \frac{1}{8h_x h_y} - (D12_{i,j+1} + D12_{i,j}) \frac{1}{8h_x h_y}$$

$$DW8 = (D14_{i,j+1} + D14_{i,j}) \frac{1}{2h_y^2} - (D9_{i+1,j} - D9_{i-1,j}) \frac{1}{8h_x h_y}$$

$$DW9 = (D12_{i,j+1} + D12_{i,j}) \frac{1}{8h_x h_y} - (D9_{i+1,j} + D9_{i,j}) \frac{1}{8h_x h_y}$$

APPENDIX H

INITIAL CONDITIONS

H-1. Initial Velocity - No Transient Pressure

Much experimental data (2) regarding peak impulse intensities delivered to normal surface areas has been obtained. For small charges, the best analytical fit to this data is given by the following.

$$I = BW^{1/3}\left(\frac{W^{1/3}}{R_o}\right)^F \qquad \text{H1}$$

where

I = peak impulse intensity (lb-sec./in^2.)

F,B = material constants, given for typical materials in TABLE H-1.

R_o = normal distance to charge

W = weight of explosive in pounds

TABLE H-1

EXPLOSIVE MATERIAL PROPERTIES

Explosive Type	B	F	Ø	$10^{-4}k$
Pentolite	2.18	1.05	1.13	2.25
Tetryl	1.73	0.98	1.15	2.14
TNT	1.46	0.89	1.13	2.16

Equation H1 written with units of lb-sec/ft^2, is

$$I = 144 \frac{BW^{\frac{F+1}{3}}}{R^F} \qquad \text{H2}$$

Consider Figure H-1.

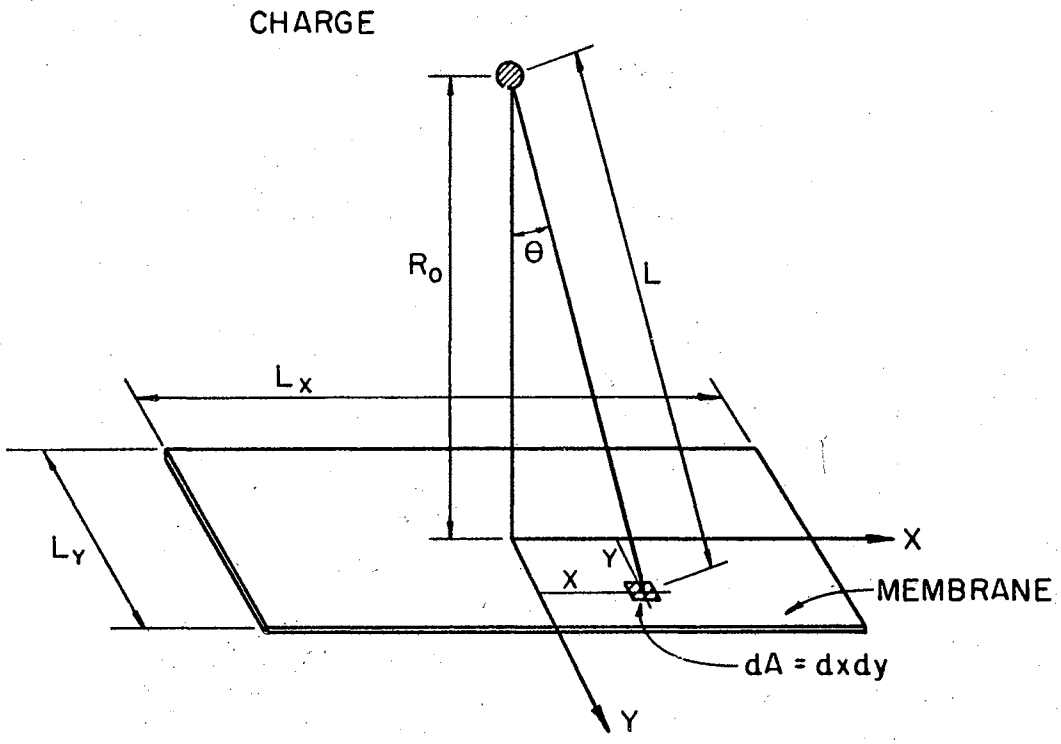

Figure H-1. Development of Impulse for Deformation Process

In this schematic, a rectangular membrane is shown positioned below an explosive charge. Assuming that no membrane motion occurs until the spherical blast wave front has contacted each point on the membrane surface, the total impulse can be considered as having been applied in one instant of time. The initial velocities can thereby be computed as given in the remaining part of this section.

The distance from the charge to a typical element of the surface is

$$L = (R_o^2 + x^2 + y_2)^{\frac{1}{2}} \qquad H3$$

substituting equation H3 into equation H2 gives

$$dI_R = 144\ BW^{\frac{F+1}{3}} \left[\frac{1}{(R_o^2 + x^2 + y^2)^{\frac{1}{2}}}\right]^F dA_R \qquad H4$$

the projected area of the surface normal to the radius, R_o.

$$dA_R = \frac{1}{\cos\ \theta}\ dxdy \qquad H5$$

The differential impulse in a radial direction is found by substituting equation H5 into equation H4.

$$dI_R = 144\ BW^{\frac{F+1}{3}} \left[\frac{1}{(R_o^2 + x^2 + y^2)^{\frac{1}{2}}}\right]^F \frac{1}{\cos\ \theta}\ dxdy \qquad H6$$

The vertical component of the differential impulse is

$$dI_Z = dI_R \cos\ \theta$$

$$= 144\ BW^{\frac{F+1}{3}} \left[\frac{1}{(R_o^2 + x^2 + y^2)^{\frac{1}{2}}}\right] dxdy \qquad H7$$

The vertical component of the total impulse is

$$I_Z = 144\ BW^{\frac{F+1}{3}} \int_{-\frac{L_x}{2}}^{\frac{L_x}{2}} \int_{-\frac{L_y}{2}}^{\frac{L_y}{2}} (R_o^2 + x^2 + y^2)^{-F/2}\ dxdy \qquad H8$$

Except for a few values of F the double integration implied in equation H8 must be performed using a numerical method. For the present problem, Simpsons 1/3 Rule (22) was used and the integration of equation H8 programmed for a 24" x 24" membrane and all three sets of explosive material constants given in Table H-1. The result plotted for the form

$$\frac{I_Z}{W^{\frac{F+1}{3}}} = 144\ B \int_{-\frac{L_x}{2}}^{\frac{L_x}{2}} \int_{-\frac{L_y}{2}}^{\frac{L_y}{2}} (R_o^2 + x^2 + y^2)dxdy \qquad H9$$

is given in Figure H-2.

Once the total impulse is formed the initial velocity field is found using the following impulse-momentum equation

$$I_Z = \int_{-\frac{L_x}{2}}^{\frac{L_x}{2}} \int_{-\frac{L_y}{2}}^{\frac{L_y}{2}} m(x,y)\ V(x,y)dxdy \qquad H10$$

where

$m(x,y)$ = mass of membrane at the position (x,y).

$V(x,y)$ = velocity of membrane immediately after impact at the position (x,y).

With a uniform mass per unit surface area, equation H10 becomes

$$I_Z = m \int_{-\frac{L_x}{2}}^{\frac{L_x}{2}} \int_{-\frac{L_y}{2}}^{\frac{L_y}{2}} V(x,y)\,dxdy \qquad \text{H11}$$

Three initial velocity configurations are used; the cosine, pyramid and uniform distributions. These are shown in Figure 10. To illustrate the general approach, the cosine distribution will be used.

$$V = V_o \cos\left(\frac{\pi x}{L_x}\right)\left(\frac{\pi y}{L_y}\right) \qquad \text{H12}$$

the unknown V_o is found by using the impulse-momentum equation

$$I = \rho t \int_{-\frac{L_x}{2}}^{\frac{L_x}{2}} \int_{-\frac{L_y}{2}}^{\frac{L_y}{2}} V_o \cos\left(\frac{\pi x}{L_x}\right) \cos\left(\frac{\pi y}{L_y}\right) dxdy \qquad \text{H13}$$

where

ρ = mass per unit volume

t = thickness membrane

V_o = initial velocity at origin

I = vertical component of total impulse.

Integrating as implied in equation H13 gives

$$I = \frac{4\ tL_xL_yV_o}{\pi^2} \qquad \text{H14}$$

thus,

$$V_o = \frac{I(\pi^2)}{4\ tL_xL_y} \qquad \text{H15}$$

Using equations H12 and H15, the expression for the initial velocity field is found to be

$$V = \left\{ \frac{I(\pi^2)}{4\ tL_xL_y} \right\} \cos\left(\frac{\pi x}{L_x}\right) \cos\left(\frac{\pi y}{L_y}\right) \qquad \text{H16}$$

In a similar manner, the uniform and pyramid configurations may be used.

H-2 Transient Pressure - No Initial Velocity

Cole (2) has shown that for most practical cases, the peak pressure generated by an underwater explosion can be represented by the power law

$$P_M = k\left(\frac{W^{1/3}}{R}\right)^{\theta} \qquad \text{H17}$$

where k and $\emptyset$ are explosive material constants. Table H-1 gives some typical values. The empirical pressure-time relationship

$$P = P_M e^{-t/\theta} \qquad \text{H18}$$

is also suggested. t is the time variable and θ is another naterial constant which is represented in Table H-1. A typical plot of this exponential function is given in Figure 14. As suggested by Boyd, the following distribution of pressure is assumed

$$P(x,y) = P_M e^{-t/\theta} \cos^p \left(\frac{\pi x}{L_x}\right) \cos^q \left(\frac{\pi y}{L_y}\right) \qquad \text{H19}$$

where p and q are parameters used to vary the distribution of pressure over the membrane surface. Figure 14 illustrates such an effect on the pressure distribution.

Equation H19 is used with the initial conditions that the displacements and velocity are zero.

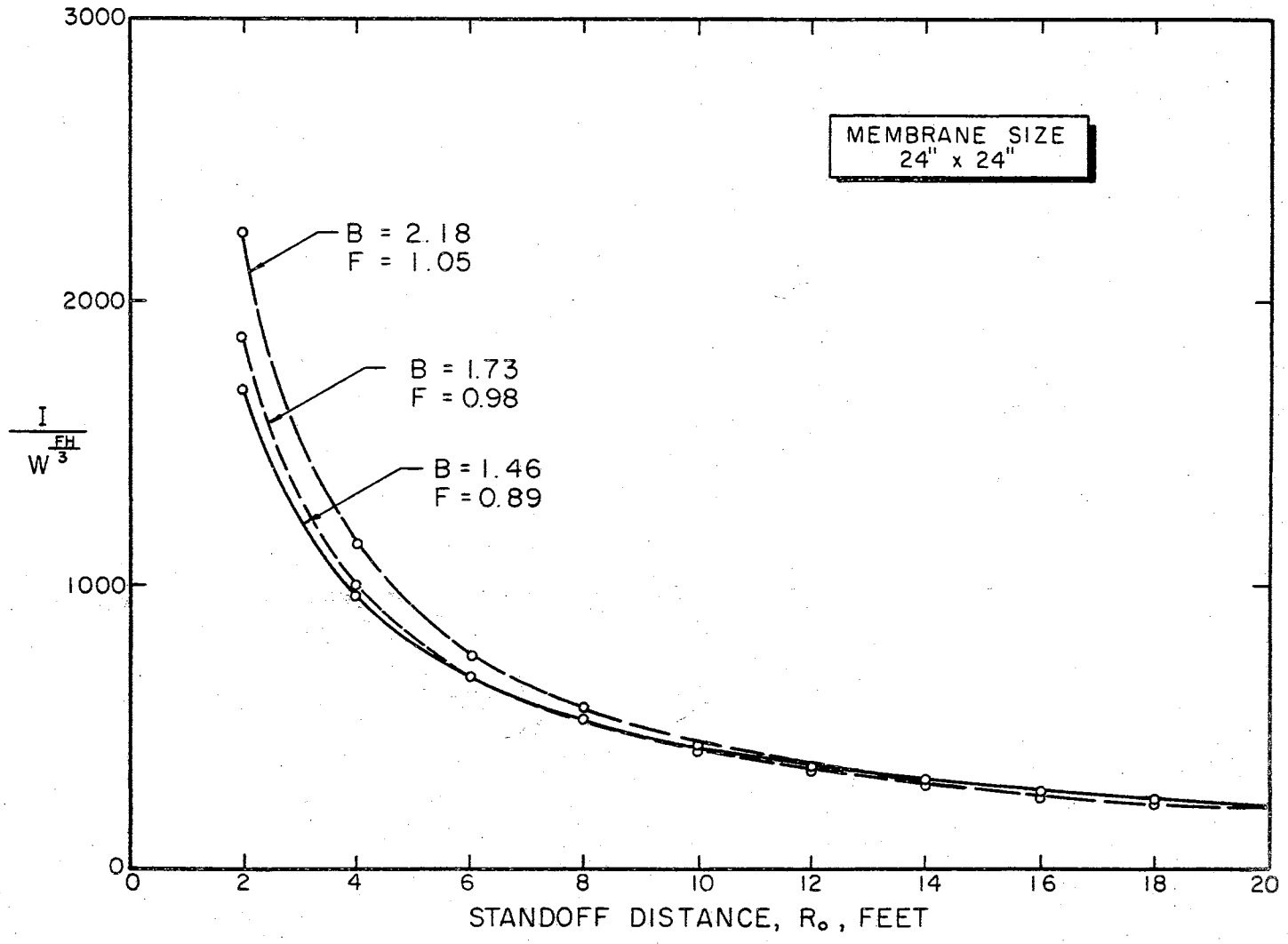

Figure H-2. Effect of Explosive Material Constants on Total Impulse

APPENDIX I

COMPUTER FLOW DIAGRAM

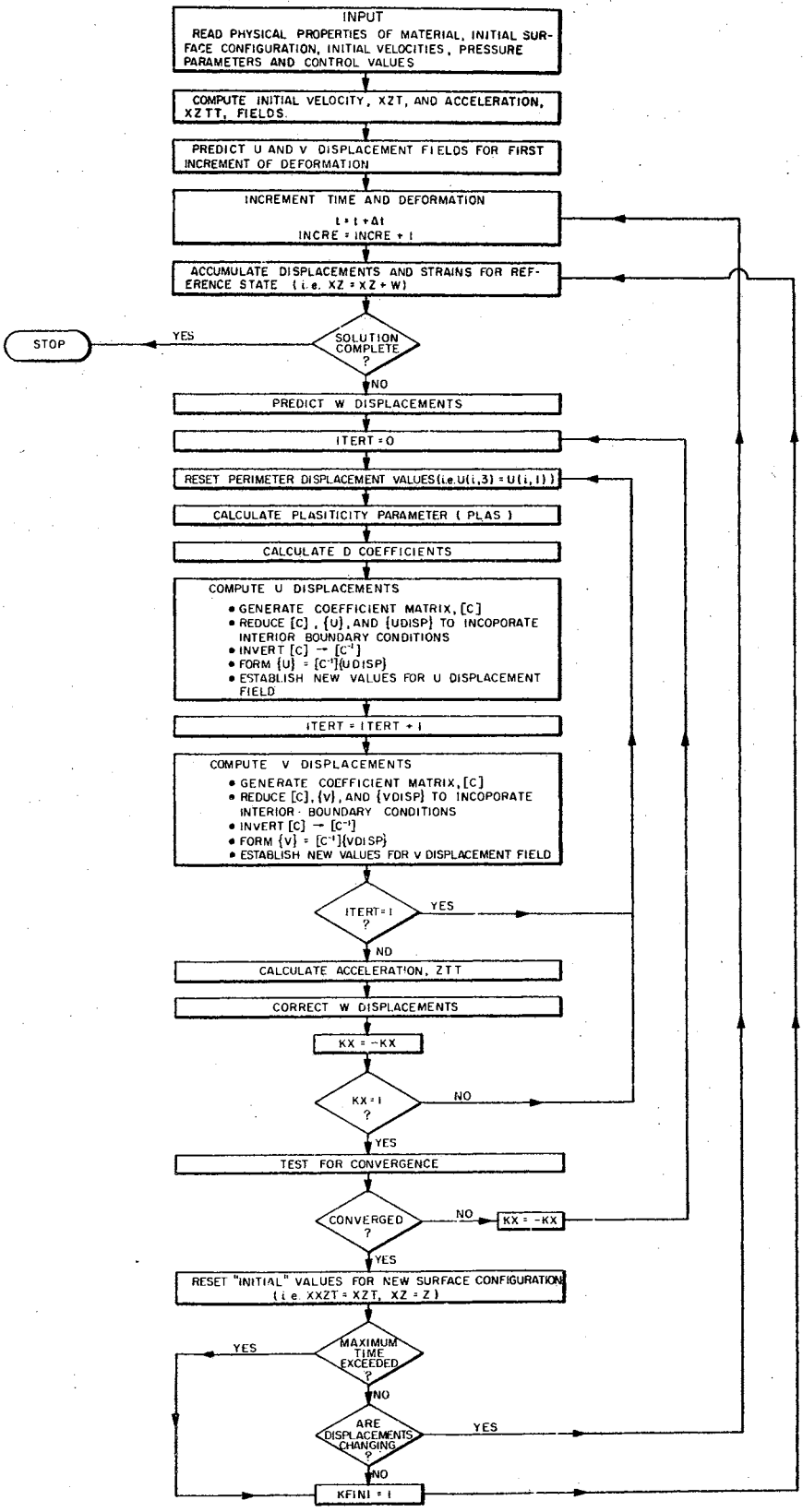

VITA

Charles Lindbergh

Candidate for the Degree of

Doctor of Philosophy

Thesis: FINITE, INELASTIC DEFORMATIONS OF CLAMPED RECTANGULAR MEMBRANES SUBJECTED TO IMPULSIVE LOADINGS

Major Field: Civil Engineering

Biographical:

Personal Data: Born at Charleston, South Carolina, November 14, 1936, the son of Elise and Carl Lindbergh.

Education: Graduated from Chicora High School, Charleston, South Carolina, in May 1954; received the Bachelor of Science degree from The Citadel, Charleston, South Carolina, in May 1958 with a major in Civil Engineering; received the Master of Science degree from Oklahoma State University, Stillwater, Oklahoma, in May 1965 with a major in Civil Engineering; completed requirements for the Doctor of Philosophy degree in May 1967.

Professional Experience: Civil Engineering Officer in the United States Air Force since 1958. Base Civil Engineer, North Charleston Air Force Station, South Carolina, 1958-1960. Planning Engineer in the Deputy for Civil Engineering, 32nd Air Division, Dobbins, AFB, Georgia, 1960-1961. Maintenance Engineer in the Deputy for Civil Engineering, 32nd Air Division, Oklahoma City Air Force Station, Oklahoma, 1961-1963. Registered Professional Engineer in Oklahoma.